2009

Development of a Ligno-Cellulosic Polymeric and Reinforced Sheet Molding Compound (SMC)

Ryan Harris Mills

DEVELOPMENT OF A LIGNO-CELLULOSIC POLYMERIC AND

REINFORCED SHEET MOLDING COMPOUND (SMC)

By

Ryan Harris Mills

B.S. Chemical Engineering, University of Maine, 1994

B.S. Biochemistry, University of Maine, 1994

M.S. Paper Science and Eng., Institute of Paper Science and Technology, 1996

A THESIS

Submitted in Partial Fulfillment of the

Requirements for the Degree of

Doctor of Philosophy

(in Forest Resources)

The Graduate School

The University of Maine

May, 2009

Advisory Committee:

Douglas J. Gardner, Professor of Wood Science and Technology, Co-Advisor

Adriaan vanHeingingen, Professor of Chemical Engineering, Co-Advisor

Raymond Fort, Professor of Chemistry

Robert Rice, Professor of Wood Science and Technology

Barry Goodell, Professor of Wood Science and Technology

LIBRARY RIGHTS STATEMENT

In presenting this thesis on partial fulfillment of the requirements for an

advanced degree and the University of Maine, I agree that the Library shall make

it freely available for inspection. I further agree that permission for "fair use"

copying of this thesis for scholarly purposes may be granted by the Librarian. It

is understood that any copying or publication of this thesis for financial gain shall

not be allowed without my written permission.

Signature:

Date:

DEVELOPMENT OF A LIGNO-CELLULOSIC POLYMERIC AND

REINFORCED SHEET MOLDING COMPOUND (SMC)

By Ryan Harris Mills

Thesis Co-Advisors: Dr. Adriaan vanHeiningen and Dr. Douglas J. Gardner

An Abstract of the Thesis Presented
in Partial Fulfillment of the Requirements for the
Degree of Doctor of Philosophy
(in Forest Resources)
May 2009

The overall objective of this dissertation was to study the surface energy and acid-base characteristics of natural fibers, glass, a wood extract, and a sheet molding compound prepreg to facilitate the fabrication of totally synthetic and partially renewable sheet molding compounds (SMCs). The water absorption and micro-mechanical performance of the totally synthetic and partially renewable SMC composites were compared through accelerated aging experiments. Reinforcing glass sized for polyester, bast kenaf fibers, hot water extract from *Acer rubrum*, and a dicyclopentadiene modified polyester prepreg were analyzed by inverse gas chromatography to evaluate and help predict how the various components may interact in a crosslinked composite SMC. Dynamic Mechanical Thermal Analysis (DMTA) was used to determine how the components in the SMC changed as a function of hygrothermal aging by analyzing the glass transitions of the individual components in the SMC.

Inverse gas chromatography (IGC) results indicated that the polyester prepreg material had an experimental dispersive surface energy value of 47 mJ/m^2 that compared well with a rule of mixture analysis of the components in the SMC giving a value of 50 mJ/m^2 both at 30°C. IGC results also indicated that the kenaf-prepreg material has a higher acid base interaction then the glass-prepreg material. The IGC results indicated that surface sizing of the kenaf fibers with styrene-maleic anhydride might improve the cohesiveness of the final kenaf based SMC. IGC results also indicated that hot water extract from *Acer rubrum* had a dispersive energy close to polystyrene and should be miscible in the prepreg material.

Hygrothermal aging was done by soaking SMC samples at 70°C for 3, 168, and 1032 hour time intervals. Standard SMC fabricated with glass reinforcement had water uptakes of less than 5 weight percent after 1032 hours. SMC fabricated with kenaf had water uptakes at 1032 hours approaching 20 weight percent indicating the kenaf based SMC is not suitable for exterior applications or applications where water contact occurs. SMC fabricated with hot water extract from *Acer rubrum* had water uptake similar to, and in some cases, better then the standard SMC references.

DMTA results indicated that thickening reactions took place without thickening agents in the SMC in the presence of excess absorbed water. The temperature range of

−50°C to 260°C during DMTA testing effectively destroyed the kenaf based SMC. The glass based synthetic SMC was the most resilient to the heat ramps followed by the extract based SMC.

Inverse gas chromatography is a useful tool for analyzing the dispersive and acid-base properties of components of a composite. Kenaf based and extract based SMC's can be fabricated and the extract based SMC's compare well with standard synthetic SMC's for water absorption and micro-mechanical properties.

ACKNOWLEDGEMENTS

I would like to take this opportunity to thank everyone on my committee. I have utilized the expertise of everyone on the committee countless times and their help and input made this dissertation the best that it could be. I would like to thank Ed Kleese of AOC resins for allowing me to visit their facility and for donating SMC prepreg's for this research work. Sara Walton and Rory Jara ran tests and gave samples that were used in my experiments. Dr. Rupert Wimmer and Dr. William Tze contributed fibers and expertise in two of the peer reviewed published works from this thesis. Many others contributed to this work through small donations of materials.

Special thanks goes to my father who raised me as a forestry apprentice and taught me a love for trees and the land; my mom who was always there to be supportive both emotionally and financially; and to my brother who was supportive of all this work. Finally, a very special thanks to Christine Leighton who helped me with the struggle of doing what is required of a Doctoral candidate and made my quality of life during this endeavor much better then it would have been without her support.

Ryan Mills

TABLE OF CONTENTS

LIST OF TABLES

LIST OF FIGURES

1. INTRODUCTION

The global forest products industry is changing at a rapid pace. The advent of the internet and information technologies, new environmental considerations, and increased global competition in the forest products industry have led to a need for new applications and technologies for wood utilization. In response to this need, research programs have been implemented by the National Science Foundation and the United States Department of Energy. This thesis work was initially supported by a grant from the Department of Energy called, "Integrated Forest Products Refinery". This project investigated removing a hot water extract from wood and converting the extract to ethanol for fuel or modified to higher value biopolymers. Dr. Adriaan vanHeiningen investigated hot water extraction of hemicelluloses from wood and their conversion to ethanol. Dr. Joseph Bozell of the National Renewable Energy Laboratory (NREL) was to investigate the synthesis of hyperbranched polyesters from hemicellulose in the extracts and Dr. Douglas Gardner was to investigate the fabrication and testing of sheet molding compound (SMC) with biobased reinforcement and extract based polymers. Because of grant budget cuts, the NREL research task was removed from the overall project, but the extraction, conversion to ethanol and biobased SMC tasks of the project were kept. This thesis presents the results of research on the utilization of kenaf bast fibers for reinforcement in SMC and the use of hot water extracts containing hemicellulose, lignin and other minor components in the SMC prepreg material.

Sheet Molding Compound (SMC) is a composite material comprised of an unsaturated crosslinked polymer, reinforcing fiber such as glass, thermoplastic processing aids, mineral fillers, and lubricant (release agent). Mechanical properties for service requirements are developed through fiber reinforcements randomly aligned in between two polymer sheets. Service requirements for the SMC material are necessary for specified amounts of time. For example, SMCs used for automotive parts have upwards of a 10 year service life; therefore, studies on how the SMC material changes with time and environmental exposure is of interest.

The research approach for making and testing the various SMC composites was to first develop an experimental protocol and demonstrate that the protocol was useful for testing a standard SMC. After developing a testing protocol, the components of the SMC composites were analyzed by inverse gas chromatography (IGC) to determine and optimize the compatibility of the blended components for maximum cohesion. Finally, SMC composites were fabricated and tested using the developed experimental protocols and results compared.

By studying the surface characteristics of the SMC components, the hypothesis was that predictions of the interactions and modifications of the components in the sheet molding compound could be made. After studying the surface characteristics and modifying the fiber surface chemistry based upon the surface analysis, the blending of the components into a SMC resin paste was done. A steel compression mold was fabricated and used to compression mold the SMC, and after compression molding, micromechanical testing samples were machined for testing.

The dispersive surface energy and acid-base characteristics of the SMC polyester pre-preg material, reinforcing glass fibers, 14 ligno-cellulosic fiber types, and hot water extract were determined by inverse gas chromatography (IGC). After completing the surface energy analysis, compression molding and micromechanical testing results from standard SMC, kenaf reinforced SMC, and hot water extract based SMCs, were determined. The micromechanical testing was done using dynamic mechanical thermal analysis (DMTA). The DMTA studies were done as a function of accelerated aging accomplished through hygrothermal aging. The water uptake of the SMC material was also analyzed as a function of hygrothermal aging.

2. BACKGROUND

There are three stages in the manufacture of sheet molding compound (SMC). An SMC is referred to as A-stage when all of the components except the reinforcement are blended and the mixture is in a liquid state. A B-stage SMC is a material with a viscosity in the millions of centipoises after the A-stage SMC is compounded with fiber reinforcement. The B-stage SMC material is flexible, with a degree of cohesion suitable for thermal processing, and the B-stage is the starting point for compression molding into the final cured C-stage SMC. To create the thermosetting material, a mold was fabricated to produce a sheet composite that can be used for mechanical and durability testing. Tests used to compare and contrast different SMCs were micromechanical testing using a DMTA MKIV-Rheometrics, and water uptake determined gravimetrically. Inverse gas chromatography (IGC) is used to help determine fiber surface properties for optimum interactions with the SMC polymer matrix. The micro-mechanical testing provides viscoelastic properties including storage modulus, loss modulus and tan delta data as a function of temperature and water uptake, [1,2]. The tan delta is the ratio of the storage and loss modulus. DMTA is used to determine glass transition temperatures and other relaxation phenomena in the material as a function of experimental parameters. Composite material relaxations may be related to chemical rearrangements and/or chemical reactions which take place in the SMC[1].

2.1 Fabrication of glass and natural fiber reinforced B- and C-stage SMC

Various papers in the literature outline processes for the fabrication of SMC hand sheets that can be used to manufacture test samples for micro-mechanics testing[3,4]. Also, at AOC resins in Valparasio, Indiana, through discussion with the technical staff, some issues related to viscosity were learned for flax based SMC. Fabrication of the B-stage SMCs were done at the Advanced Engineered Wood Composites Center at the University of Maine.

To better understand how the final SMC part is manufactured the components and their weight percentages in the material need to be known. Typical components for SMCs are as follows:

Table 2.1 Components of SMCs

Component	Weight Percent (typical ranges)	Function
Styrene	5-10	Cross-Link structure
Polyester	10-15	Cross-Link structure
Glass fiber	30.0	Reinforcement
Calcium Carbonate	40-50	Filler-reduces cost
Low Profile additive	3-15	Controls shrinkage
Initiator	1.00	Free radical initiation
Magnesium Hydroxide	<1	Viscosity enhancement
Zinc Stearate	<3	Mold release

The components used to create standard and biobased SMCs in these studies came from various locations. Kenaf fibers from Kenaf Industries, South Texas, Texas, were provided by Dr. Charles Taylor. Glass from Owens Corning surface sized for polyester resins was provided by Dr. Kevin Guigley. Thirteen other ligno-cellulosic fiber types were provided by Dr. Rupert Wimmer, University of Natural Resources and Applied Life Sciences, BOKU-Vienna. Lastly, two types of polyester pre-preg from AOC resins Valparasio, Indiana were donated for this research.

2.2 Fabrication of SMC

Because the fabrication of a B-stage SMC is fairly involved, most researchers in this field do not compound their own SMC [1,3]. For example, all the ingredients except for the reinforcement fibers need to be mixed in a high shear mixer. Then the reinforcement fibers need to be randomly and evenly distributed between two sheets of resin to create a "sandwich". The random orientation of fibers creates a material with homogeneous properties in all directions if compounded and molded correctly. After sandwiching the fibers between the resin layers, they need to be completely wetted by applying pressure using a steel roller, typically used for making paper hand sheets, to make the composite. If the fibers are sized properly, the fibers will be wetted by the resin matrix. If the surface energies are not compatible between the fiber and the matrix, wetting of the fiber will not occur and the SMC will not be structurally sound.

2.3 Inverse Gas Chromatography

Inverse gas chromatography (IGC) has been used to characterize and optimize the interaction of natural fibers and polymer composites [5]. The technique has a solid phase

packed into a column and the column is placed in an oven. The temperature is controlled as a gas mobile phase flows through the column where an inert carrier gas contains "infinitely dilute" samples of probe gases. A detector measures the time required for the probe gases to go through the packed column. The retention time is then related to thermodynamic quantities to characterize the solid phase sample. The fiber/matrix acid-base interaction can be quantified using IGC by matching the acidic parameter, (K_A), of one component with the basic component, (K_B), of the other component, and then measuring the enthalpy of adsorption of the resin onto the fibers. This will allow for the prediction of the acid-base interactions of the natural fibers with the polyester matrix. Based on this, the selection of an appropriate sizing agent for the natural fibers may be made.

2.3.1 IGC analysis

Multiple ways to analyze IGC data have been developed over the last few decades[6-10]. Because a number of different fiber types are being analyzed in this thesis a short review of the theoretical aspects of IGC analysis follows. The retention time measured by IGC, is the net retention volume (V_N, the volume of carrier gas required to elute a zone of solute vapor), per gram of adsorbent, and is determined by equation 1.

$$V_N = \frac{273.15}{T_c} * \frac{1}{w} * Q(t_r - t_i)$$

(1)

where T_c is the column temperature, w is the mass in grams of adsorbent packed into the column, Q is the corrected flow rate of the helium gas, t_r and t_i are the retention time of

probe and inert gas. Dorris and Gray [6] introduced the concept of using IGC data to determine the Gibbs free energy (G_D) of a solid as:

$$\Delta G_D = R * T * Ln(V_N) + C \qquad (2)$$

and,

$$\Delta G_D = N * a * W_A \qquad (3)$$

where N is Avogadro's number, a is the surface area of the absorbed probe molecule, W_A is the work of adhesion and R is the universal gas constant. Combining Equations 2 and 3 with the observation that only dispersive interactions are significant for non-polar interactions [7], the work of adhesion (W_A) can be written as a geometric mean of the surface energy.

$$W_A = 2 * (\gamma_S^D * \gamma_L^D)^{\frac{1}{2}} \qquad (4)$$

where γ_L^D is the London dispersive surface energy of liquid phase, γ_S^D is the London dispersion component of the surface free energy of the solid. By combining Equations 2, 3, and 4, an expression relating the eluted volume to the free surface energy is derived.

$$RTLn(V_N) = 2 * N * (\gamma_S^D)^{\frac{1}{2}} * a * (\gamma_L^D)^{\frac{1}{2}} + C \quad (5)$$

Dorris and Gray [6] proposed equations for calculating the London dispersive component of the surface free energy

$$\Delta G_D^{CH_2} = \frac{RT}{1000} \ln \frac{V_{N(C_{n+1}H_{2n+4})}}{V_{N(C_nH_{n+2})}} \qquad (6)$$

and

$$\gamma_S^D = \frac{1}{4\gamma_{(CH_2)}} \left[\frac{\Delta G_D^{CH_2}}{N * a_{CH_2}} \right]^2 *10^{12} \qquad (7)$$

where ΔG_D^{CH2} is the free energy of adsorption for a methylene group, R is the gas constant, n is the number of carbon atoms in the alkane probe molecules, $\gamma_{(CH2)}$ is the surface free energy of the methylene group, 35.6 mJ/m^2, N is Avogadro's number, a is the area of an absorbed methylene group, 6Å^2, and the factors 1000 and 10^{12} are conversion factors[7].

Schultz and Lavielle[8,9], graphed RTlnV_N versus $a(\gamma_L^D)^{1/2}$ and found a linear relationship where the slope is $2N(\gamma_S^D)^{1/2}$ and the intercept is the constant C in equation 5 when using nonpolar alkane probes. Polar probes were not found to lie on the linear line created by the alkanes and the perpendicular distance from the alkane line to the polar probe is ΔG^{AB} or ΔG^{SP}, (Figure 2.1).
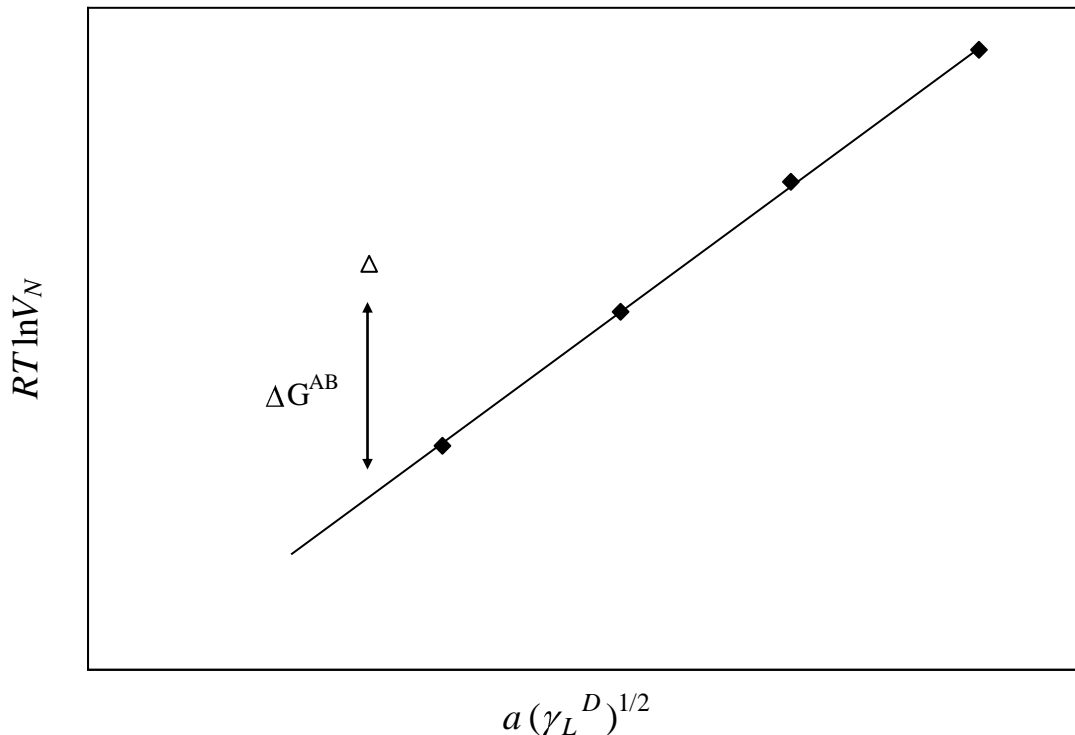
Figure 2.1 Example graph demonstrating IGC relationships where ♦ are non-polar probes and Δ is a polar probe.

   Donnet *et. al.*[10] developed an analysis where the specific interactions on solid surfaces are determined based upon the polarizability of the gas probes. The analysis started with the assumption that two non identical molecules that exchange only non dispersive forces can be described by the London equation [10]. The London equation relates the potential energy of interaction, θ_L, to the molecules deformation polarizability, $\alpha_{0,i}$, characteristic electronic frequency, v_i, distance of the absorbate to the absorbent molecules, $r_{1,2}$, permittivity in a vacuum, ε_0, and Plank's constant, h. The deformation polarizability for the molecules was calculated from the refractive index of the molecules using Debye's equation. After assuming that the harmonic mean of the molecules electronic frequency can be substituted with the geometric mean, (according to Donnet *et. al.* this introduces less then a 4% error), Equation 8 can be derived [10].

$$\theta_L = K(hv_s)^{\frac{1}{2}} \alpha_{O,S} (hv_L)^{\frac{1}{2}} \alpha_{O,L} \quad (8)$$

For the case of the alkane probes where ΔG^{SP} is zero, equation 8 may be written as equation 9 because the dispersive energy is assumed to be described by the London equation[10]:

$$RT \ln V_n + C = \theta_L = K(hv_s)^{\frac{1}{2}} \alpha_{O,S} (hv_L)^{\frac{1}{2}} \alpha_{O,L} \quad (9)$$

When polar probes are used for testing the surface characteristics, ΔG^{SP} is not zero and is added to Equation 9.

$$[-\Delta G_D] = RT \ln V_n + C = \theta_L = K(hv_s)^{\frac{1}{2}} \alpha_{O,S} (hv_L)^{\frac{1}{2}} \alpha_{O,L} + [-\Delta G^{SP}] \quad (10)$$

As was the case with the Schultz method, the perpendicular distance from the alkane line to the polar probe is the ΔG^{SP}. The polarization method was developed because of temperature, partial pressure limitations, and material limitations, of the previous methods described [10].

By running experiments at different temperatures, the free energy of absorption is measured. The Gibbs free energy of adsorption is related to the enthalpy of adsorption by the following expression:

$$\Delta G^{AB} = \Delta H^{AB} - T \Delta S^{AB} \quad (11)$$

From this equation the enthalpy of adsorption can be determined by plotting ΔG_{AB} versus T producing a straight line where the intercept is ΔH^{AB} at zero Kelvin [11, 12]. Some researchers plot $\Delta G^{AB}/T$ versus $1/T$ where the slope is ΔH^{AB} [13]. The assumption in this

11

analysis is that ΔH^{AB} and ΔS^{AB} for these systems are temperature independent as IGC experiments are typically run over a small temperature range.

Gutmann's approach[14] of using electron donors and acceptors for the enthalpy of acid-base interactions can now be applied.

$$-\Delta H^{AB} = K_A DN + K_B AN \qquad (12)$$

The DN and AN are the acceptor and donor numbers related to chemical references. The donor number, DN, was defined as the negative of the enthalpy of formation for the chemical made by the acid base reaction with antimony pentachloride. The corresponding electrophilicity of a chemical species was determined from the ^{31}P NMR shifts induced by triethylphosphine oxide, a basic probe. The K_A and the K_B are constants that show how the solid differs from the references used with the standards[14].

2.4 DMTA Testing and Analysis

After creating a B-stage SMC, a crosslinked or C-Stage SMC was fabricated. First, a mold was fabricated for making a cross linked plastic sheet. Many articles describe the engineering variables needed to make an appropriate mold [15]. Heat must transfer into the SMC to start and propagate the cross linking reaction. Also, a random orientation of the fibers in the SMC is needed to assure equal mechanical properties in all directions in the SMC. To create this random orientation, the SMC must flow in the molding process. Making plies of the B-Stage SMC creates the flow in the mold during pressing. These plies are of smaller dimensions then the mold and the plies are stacked until the correct weight of SMC is achieved.

An ideal mold is made from stainless steel; however, this is cost restrictive. Carbon steel is adequate, but care needs to be taken so that the SMC doesn't bond to the walls of the mold preventing separation of the top plunger from the receiver. A generic "rule of thumb" for molding B-Stage SMC was learned during a trip to the AOC resins pilot plant in Valparasio, Indiana (2004, Ed Kleese Technical Manager AOC Resins, Personal communication). The "rule of thumb" states: a temperature of $300^{\circ}C$ and pressure of 1000 psig should be applied to the B-Stage SMC during compression molding for x minutes per x millimeter of thickness of the final SMC part. A carbon steel mold was fabricated and all SMCs were fabricated using this "rule of thumb".

DMTA data allows determination of glass transition temperature, T_g, for the various components in the composite by taking the ratio of the storage, (elastic response), modulus and loss, (viscous response), modulus called the tan delta for the material and the T_g is affected by the following considerations:

- **Free volume** - the volume of polymer mass not occupied by the molecules themselves. If the molecules are tightly packed and have little room to move, they require more energy to move relative to a polymer mass with more void space.

- **Attractive forces between molecules** - tightly bound molecules need more thermal energy to produce motion, which in turn increases Tg.

- **Rotation about bonds** - steric hindrance prevents motion, so that more energy is needed for rotation to occur, again resulting in a higher Tg.

- **Stiffness of chain** - more or less similar to rotation about bonds, in that if a chain of molecules needs more energy to bend or twist, a higher Tg is required for the motion to occur.

- **Chain length** - the chain length of molecules affects their motion which affects the Tg. Plasticizers soften a polymer by interfering with the chain motions. Furthermore, the plasticizer forms secondary bonds with the polymer thereby reducing the bonding forces between the polymer chains.

The T_g determined by DMTA is frequency dependent and, in many cases, not the same as T_g from static tests like differential scanning calorimetry; therefore, the main "glass transition" in DMTA is called an α-transition. Other transitions can be seen below the glass transition temperatures; β-transitions arise from the motion of flexible side chains of polymers with short branches. γ-, δ-transitions, and other transitions, are generally due to main chain motion of segments containing 4 carbons or less. The magnitude of β-, γ-, δ-, etc., transitions is less than that of α-transitions since they involve smaller segments of the polymer than with the α-transition. Also, if a polymeric network is cross-linked at, or less than, every 40 carbons, a glass transition may not be achieved and a degradation of the network may result. The glass transition is a temperature range and not a finite point. Work has been done recently to define the glass transition temperature and this is how the transition was analyzed for this thesis work[16]. The start of a glass transition change can be seen within the storage modulus appearing as a decrease in the modulus. This decrease in slope continues until the glass transition is completed and the slope returns to normal. The inflection point on the tan delta corresponds to the half way point found for the glass transition for the storage modulus. Therefore, many different "glass transitions" can be reported when in actuality it is better to report a glass transition range especially because so many different factors can slightly skew the exact temperature for the glass transition.

From the factors that affect the glass transition temperatures, it becomes apparent that chemical reactions that change the configuration and/or conformation of chemicals in the polymer matrix will have a significant impact on the range and location of glass transitions in the material. By studying changes in the DMTA scans of the material as a function of aging, an understanding of what may happen to those materials in the composite develops. Work has been done using the DMTA tan delta scan to track chemical reactions in the composite matrix[1]. This was possible because much work has been done on the individual materials in the composite[17,18,19,20]. Viscosity enhancers and low profile additives have been added to the SMC for processing ease and dimensional stability of the material respectively. The viscosity enhancers typically have been metal oxides such as magnesium, calcium, or zinc oxides. These oxides can react with the carboxylic functional groups on the polyester chains and form ionic complexes[1,17,18,19]. The reaction of metal oxide with carboxylic functional groups on the polyester chains is known as 'thickening reaction''. Also, the low profile additive, typically polyvinyl acetate, can react with water to form polyvinyl alcohol and acetic acid.

The thickening reaction may not seem significant; however, the reaction of metal oxides and the carboxylic functional groups is the reaction that causes the viscosity enhancement in the SMC that is necessary to process the material. When switching to natural fibers that exhibit both capillary and chemical effects which induce absorption of solvating agents in the SMC, an understanding of the thickening reaction and the fiber interactions are critical to predict and control this enhanced thickening process in the B-Stage SMC. The thickening reaction takes place after the compounding of the fibers into the SMC as the material sits for a few days and the viscosity of the material increases to

the millions or tens of millions of centipoise. Initial work with a SMC from AOC resins indicated that water is necessary for this reaction but the data on this are unclear. The reaction of polyvinyl acetate with water may compete with the thickening reaction for water[1]. The acetate functionality of the polyvinyl acetate may react with water to change its glass transition characteristics. The tan delta peak for the polyvinyl acetate peak decreases and even disappears after prolonged accelerated aging studies[1]. However, even though this peak disappears there should be a new peak for the polyvinyl alcohol. This is not discussed in the literature and was investigated in the current study. To determine if acetate is being given off by the material, the water used for hygrothermal aging was examined by high performance liquid chromatography (HPLC).

By understanding the chemical reactions taking place in the standard SMC, a methodology for studying SMC was created. This methodology was applied to the biobased SMC to analyze the chemical reactions and optimize mechanical properties in the material.

After fabrication, samples were tested using DMTA to determine glass transition temperatures and possible chemical reactions. An evaluation was made for the biobased SMC compared to the synthetic SMC.

2.5 References

1. Mendoza-Patlan N., Martinez-Vega J., Revellino M.; "Physico-chemical effects of hydrothermal ageing of sheet molding compounds between -60 and 250°C"J. Mater. Sci., 36 1523-1529, (2001)

2. Bucknall C.B., Davies P., Partridge I.; "Phase separation in styrenated polyester resin containing a poly(vinyl acetate) low-profile additive" , Polymer 26, 109-112, (1985)

3. van Voorn B., Smit H., Sinke R., de Klerk B.; "Natural fibre reinforced sheet moulding compound" Composites: part A 32 1271-1279, (2001)

4. Hepworth D., Bruce D., Vincent J., Jeronimidis G.; "The manufacture and mechanical testing of thermosetting natural fibre composites" J. Mater. Sci. 35 293-298, (2000)

5. Tze W., Walinder M., Gardner D.; "Inverse gas chromatography for studying interactions of materials used for cellulose fiber/polymer composites" J. Adhes. Sci. Technol. 20(8), 743-759, (2006)

6. Dorris G.M., Gray D.G.," Adsorption of Normal-Alkanes at Zero Surface Coverage on Cellulose Paper and Wood Fibers; J. Colloid Inter. Sci., 77, 353-362, (1980)

7. Riedl B., Matuana L.M.; Encyclopedia of Surface and Colloid Science, 2842-2855, (2002)

8. Schultz J., Lavielle L.; ACS Symposium Series, Washington D.C., 391, 185-202, (1989)

9. Schultz J., Lavielle L.," Surface-Properties of Carbon-Fibers Determined by Inverse Gas-Chromatography - Role of Pretreatment";Langmuir, 7(5), 978-981, (1991)

10. Donnet J.B., Park S.J., Balard H.," Evaluation of Specific Interactions of Solid-Surfaces by Inverse Gas Chromatography - A New Approach Based on Polarizability of the Probes"; Chromatographia, vol. 31, No. 9/10, 434-440, (1991)

11. Tze W., Gardner D.; "Contact angle and IGC measurements for probing surface-chemical changes in the recycling of wood pulps" J. Adhes. Sci. Technol. 15(2), 223-241, (2001)

12. Gulati D., Sain M.; "Surface characteristics of untreated and modified hemp fibers" Polym. Eng. and Sci. 46:269-273 (2006)

13. Tshabalala M.A.; "Determination of the Acid-Base characteristics of lingocellulosic surfaces by inverse gas chromatography"J. Appl. Polym. Sci. 65:1013-1020 (1997)

14. V. Gutmann; The Donor Acceptor Approach to Molecular Interactions; Plenum, New York, 1978, Chapter 2

15. Castro J., Lee C.; "Thermal and cure analysis in sheet molding compound compression molds" Polymer Eng. and Sci., vol 27 no. 3, 218-224, (1987)

16. Herzog B., Gardner D., Lopez-Anido R., Goodell B.; "Glass-transition temperature based on Dynamic Mechanical Thermal Analysis Techniques as an indicator of the adhesive performance of vinyl ester resin" J. Appl. Polym. Sci.; vol 97(6), 385-394, (2005)

17. Alvey F.; "Study of the reaction of polyester resins with Magnesium Oxide" J. Polym. Sci.; A-1 vol 9, 2233-2245, (1971)

18. Vancso-Szmercsanyi I., Szilagyi A.; "Coordination polymers from polycondensates and metal oxides. II. Effect of water molecules on the reactions of polyesters with MgO and ZnO" J. Polym. Sci., vol 12, 2155-2163, (1974)

19. Laleg M., Blanchard F., Chabert B., Pascault," Contribution to the Study of the Thickening Mechanism of Unsaturated Polyester Resins in the Presence of MgO."; Eur. Polym. J. vol 21 No 6, 591-596, (1985)

20. Ghorbel I., Valentin D.; "Hydrothermal effects on the physico-chemical properties of pure and glass fiber reinforced polyester and vinyl resin" Polym. Composites, vol 14 no. 4, 324-334, (1993)

3. EQUIPMENT AND EXPERIMENTAL PROCEDURES

3.1 Introduction

As many of the same experimental procedures are used on different materials in the chapters of this thesis, a standalone chapter is presented for all the equipment and experimental details. A SMC consisting of polyester resin, polyvinyl acetate (PVAc), magnesium oxide (MgO), glass reinforcement, mold release agent, styrene, and catalyst was obtained from AOC resins, Valparaiso Indiana. A compression mold made of carbon steel was designed and fabricated to produce a Sheet Molding Compound (SMC) composite of approximately 18 cm by 18 cm. To make the molded SMC, B-stage SMC was compression molded into C-stage SMC at 1000 psi, 150°C and 3 minute cure time. Samples of 7 mm x 3 mm x 45 mm were cut from the SMC. These samples were sanded to 1.8 mm thickness and then dried to constant weight at 70°C and 103°C.

3.1.1 Aging Experiments

Hygrothermal tests were performed to simulate an accelerated exposure of the SMC to an exterior environment. The aging experiments were done according to previous work in the literature[1]. Samples were cut using a diamond cutting saw, and polished to 7 mm x 1.8 mm x 45 mm and dried at 103°C until constant mass was achieved. After drying, the samples were submersed in water using a honeycomb type network to identify the different samples being aged. The samples were hygrothermally aged at 70°C for 3, 168, and 1032 hours. After the selected aging time elapsed, a sample was removed from the water, weighed, and tested using DMTA analysis. An aliquot of aging solution was kept

for high performance liquid chromatography (HPLC) analysis. Dried references were used to compare to the aged samples and to determine repeatability.

3.1.2 Dynamic Mechanical Thermal Analysis

DMTA analysis was done to determine the storage (elastic) modulus (E') and loss (inelastic) modulus (E'') and loss tangent tan δ. The DMTA experiments were run isochronally in three point bending mode with a temperature range of -50ºC to 260°C at 1 Hz frequency and 1°C per minute ramp rate with an MKIV-Rheometrics DMTA. Strain settings were 1% to assure operation in the linear viscoelastic range. Liquid nitrogen was used to achieve the low temperature testing. All DMTA analysis was done at a frequency of 1 Hz and thermal heat ramps of 1°C per minute to compare to previous results[3].

3.1.3 HPLC Analysis

The aging solution was analyzed by high performance liquid chromatography (HPLC) to determine whether any of the SMC components leached into the water. Samples were analyzed using a Shimadzu HPLC equipped with a refractive index detector on a BioRad HPX-87H organic acid analysis column. The mobile phase was 0.5mM sulfuric acid at 0.6mL/min, run at 60°C.

3.2 IGC Materials and Methods

3.2.1 Sample preparation

Ligno-cellulosic fibers can be divided into several groups depending on the location of the fibers in the plant, i.e. grass fibers, bast fibers, leaf fibers and fruit fibers. For grass fibers wheat straw (*Triticum sp.*), bleached wheat pulp fibers, rice hulls, (*Oryza sativa*)

and reed (*Phragmites communis*) were selected. For bast fibers hemp (*Cannabis sativa),* flax (*Linum usitatissium*), jute (*Corchorus olitorius*) and kenaf (*Hibiscus cannabinus*) were selected. Sisal (*Agave sisalana*) and the banana fiber abaca (*Musa textiles*) represented the leaf fiber group. Finally, fruit fibers were obtained from unicellular seed or fruit hairs including cotton (*Gossypium*) and poplar hairs as seed hair fibers (*Populus sp.*), and finally kapok (*Ceiba pentandra*) and coir (*Cocos nucifera*) as fruit hair fibers. Most of the fiber types were obtained commercially and the fiber samples were of high quality. With the exception of wheat pulp, the fibers underwent regular processing steps such as retting, decortication, separation, cleaning and drying, with no additional modification treatment done to the fibers. The bleached wheat pulp was directly obtained from a wheat pulp mill and a small company that produces special blankets and other bedding products delivered the poplar seed fibers. All fiber types were analyzed by IGC and the results compared with fiber chemistry data obtained from the literature.

The fourteen fiber types were sheared in a Wiley Mill until passing through a 0.5 mm diameter screen. The chopped fibers were collected and screened using a 45 mesh screen then followed by a 60 mesh screen for a maximum fiber size of 60 mesh. IGC columns were packed with the fibers and the samples were conditioned at 103°C in the IGC with 15 standard cubic centimeters, (sccm), of helium until the flame ionizing detector recorded a background signal of <5 pA at 30°C. Three replicate IGC experiments were conducted using flax, cotton, and coir for analysis of variance.

SMC material used for the SMC and glass experiments comprised of 28.10% dicyclopentadiene modified polyester resin of molecular weight (MW) 12,000, 13.08% polystyrene (MW 250,000), 0.97% polyethylene powder, 6.27% styrene, 0.02% BHT (di-

tertiarybutylhydroxytoluene; as inhibitor), 0.48% compatibilizer, 0.15% of 5% pBQ (parabenzoquinone) solution, 0.05% black pigment, 2.42% zinc stearate, and 48.45% calcium carbonate, (Hubercarb w4).

The SMC was crosslinked at 150°C for 30 minutes. The 30 minute time at temperature was long enough to enable the styrene to react and crosslink with the polyester without the addition of an initiator. After crosslinking, the material was placed in double lined plastic bags and hammered into coarse particles. The coarse particles were ground to a powder with a mortar and pestle. The ground polymer was screened first by a 45 mesh screen then by a 60 mesh screen for a maximum particle size of 60 mesh. The powder sample was heated for 3 days at 150°C to drive off volatiles. IGC columns were packed and the samples were conditioned at 150°C in the GC oven with 15 standard cubic centimeters, (sccm), of helium until the flame ionizing detector recorded a background signal of <5 pA at 30°C.

Chopped strand glass fibers, Owens Corning brand 973, a conventional reinforcing system designed by Owens Corning Corporation specifically for SMC use, were also analyzed using IGC analysis. The glass fibers are commercially sized for enhancing medium-solubility resin compatibility with either polyester or vinyl ester resins. The strands were packed "as is" with lengths over 1 inch into the IGC column. The glass fibers were conditioned at 103°C for 24 hours with 10 sccm of helium until the flame ionizing detector recorded a background signal of <5pA at 30°C.

3.2.2 IGC measurements

For the SMC IGC analysis, experiments were conducted using two available IGC instruments. One IGC instrument consisted of a Hewlett-Packard HP 6850 Gas chromatograph equipped with an automatic injector and the second instrument was a fully automated Surface Measurements Systems SMS IGC with head space temperature control. For an IGC column into which the particle samples are packed, the HP 6850 uses Teflon tubing with a 2.5 mm inner diameter, while the SMS IGC uses custom silane treated glass tubes. The SMC materials were analyzed using either the HP 6850 (at 65°C, 75°C, 85°C, 100°C, 110°C, and 120°C) or the SMS IGC (at 30°C, 35°C, 40°C, 100°C, 110°C, and 120°C). The glass fibers were analyzed using the SMS IGC at temperatures of 30°C, 35°C and 65°C. For the ligno-cellulosic fibers, experiments were conducted with the Surface Measurements Systems SMS IGC at the temperatures of 30°C, 35°C, and 40°C and a flow rate of 10 sccm.

Vapors of HPLC grade polar and non-polar probes were sampled by micro syringe and an "infinitely dilute" (meaning a sample of the gas phase above a liquid phase for the probe), concentration of probe was injected into the packed column and the retention time measure by a flame ionization detector. An infinitely dilute sample of methane was injected to determine the residence or so called dead time in the column. The probe retention time and the methane retention time were entered into Equation 1 with the mass of the packed material in the column and were used for calculating the dispersive energy and K_a, K_b of the fibers. Calculations were done using an Excel spread sheet and packaged software from SMS. To calculate K_a and K_b equation 12 is written in y=mx+b form and AN^* used where AN^* is in energy/mole because AN is a unitless value:

$$\frac{-\Delta H_A^{AB}}{4.184\,AN^*} = \frac{DN}{AN^*}\,Ka + Kb \qquad (13)$$

Values of DN and AN* were taken from the literature and are reported in Table 3.1 for the probes used in IGC.

Table 3.1. Physical constants for probes used in IGC.

Probe	Polarizability Index $\alpha_0(h\nu)^{0.5}x10^{49}$ $C^{3/2}\,m^2\,V^{-1/2}$	DN Kcal/Mole	AN* Kcal/Mole	Specific Characteristic
n-Octane	11.4	-	-	Non-polar
n-Nonane	12.5	-	-	Non-polar
n-Decane	13.6	-	-	Non-polar
n-Undecane	14.7	-	-	Non-polar
Acetone	5.8	17	2.5	Amphoteric
Chloroform	7.8	-	4.8	Acidic
Tetrahydrofuran	6.8	20	0.5	Basic
Ethyl acetate	7.9	17.1	1.5	Amphoteric

3.3. Extracted Wood Materials and Methods

3.3.1 Wood material preparation

Rory Jara a graduate research assistant at the University of Maine Chemical Engineering department did the extractions and compositional analysis for the Red Maple except for

the Diffuse Reflectance IR Analysis. Red Maple (*Acer rubrum*) trees were harvested and debarked. Then, bolts were cut for stranding. The stranding was done at a thickness of 0.025".

Approximately 5 kilograms of the strands were air dried at room temperature and moisture content was determined in an oven at 105 ºC based on oven dry weight. The dried wood material was stored in double plastic bags for later extraction experiments.

3.3.2 Extraction procedure

The extractions were done using a modified ASE-100 extractor operating at pressures of 100-150 atm. The steps are summarized in Figure 1. Approximately 30 grams of dry wood were used for the extraction. Pure water was used as extraction liquid. The extraction was done at 160°C for 90 minutes.
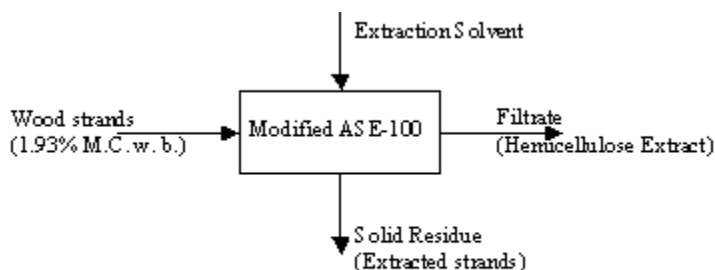
Figure 3.1. Extraction of hot water extract using a modified Dionex ASE-100.

Glass fiber filters were placed at the inlet and outlet of the extraction cell. At the end of the extraction process, the liquid phase in the extraction cell was displaced into a collection bottle using fresh water at a volume of 1.5 times that of the extraction cell (i.e.

150 ml). The wood remaining after the displacement process is removed from the extraction cell.

The liquid and solid phases are treated separately. The weight and pH of the liquid phase are recorded. Two samples of approximately 25 ml are taken, centrifuged to remove fine particles, and then freeze dried for solids content determination. Both the freeze dried solids and the remaining liquid phase are stored in a refrigerator for future analysis. The remaining wood material in the extraction cell was oven dried overnight at 105°C (±5) and its weight determined.

The gravimetric extraction yield was calculated by comparing the amount of oven dry extracted wood before and after extraction.

3.3.3 Chemical analysis procedure

The mono-sugar composition of the liquid phase (hemicellulose extract) was determined by a two step hydrolysis and high performance anion exchange chromatography (HPAEC) and pulsed amperometric detection (PAD). Chromatography of the samples was performed using a Dionex LC system coupled to an AS 50 autosampler. The high performance liquid chromatography (HPLC) system was equipped with a CarboPac PA1 column (4 X 250) in combination with a CarboPac guard column and run at 20ºC. Separation was performed at a flow rate of 0.7 ml/min in the column and 1 ml/min in the post column using a combined gradient of three eluents prepared from degassed distilled HPLC grade water: eluent A, distilled water; eluent B, 0.3 M NaOH prepared from a 50% solution NaOH to minimize the carbonate content in the final eluent; eluent C, 0.17 sodium acetate (NaAc) in 0.2M NaOH prepared accordingly. The

eluents were degassed by flushing helium and pressurized continuously with the eluent degas module of Dionex. Gradients of NaOH and NaAc were used simultaneously to elute the monosaccharides by mixing the three eluents. This resulted in the following gradient of NaOH: 0-5 min, 40%; NaAc: 0-5 min, 60%; water: 6-36.6 min. Samples (20 uL) were injected at 15.5 min. The effluent was monitored using a pulsed-electrochemical detector in the pulse-amperometric mode with a gold working electrode and a Ag/AgCl reference electrode to which potentials of E1 0.1 V, E2 -2 V, E3 0.6 V, and E4 -0.1 V were applied for duration times T1 0.4 s, T2 0.02 s, T3 0.01 s, and T4 0.07 s. Quantification of the samples was performed using the response factors calculated from the peak areas of the mixed standard solutions for five sugars (glucose, mannose, galactose, arabinose and xylose). Fucose was used as internal standard.

The total lignin content was determined as the sum of the precipitated lignin after a two step hydrolysis (Klason lignin[2]) and the soluble lignin remaining in the liquid phase. The precipitated lignin was determined gravimetrically and that in the liquid phase spectrophotometrically at 205 nm using Nicolet Evolution 100 model (Thermo Electron Corporation). The acetyl groups were determined as acetic acid after hydrolysis on a Shimadzu HPLC CTO-10A and refractive index detector (RID-10A). Protein content was determined as a function of the nitrogen content in the extract. Uronic acids were determined by methanolysis and gas chromatography[3].

3.4 Diffuse Reflectance IR Analysis

Diffuse reflectance Fourier transform infrared spectroscopy (DRIFT) was performed on freeze dried hardwood hot water extract samples. The powdered extract was mixed

with KCL to form a 3% extract in KCL mixture, according to instructions provided with the instrument, and infrared spectra were obtained after purging the water out of the infrared chamber by pumping the chamber down with nitrogen at 5 ml/min for 2 hours to minimize water in the infrared chamber.

3.5 References

1. Mendoza-Patlan N., Martinez-Vega J., Revellino M.; "Physico-chemical effects of hydrothermal ageing of sheet molding compounds between -60 and 250°C"J. Mater. Sci., 36 1523-1529, (2001)

2. Browning B.L.,"Methods of wood chemistry", Ed. John Wiley & Sons. New York (1967).

3. Scott, R.W., "Calorimetric determination of hexuronic acids in plant materials". Analytical Chemistry No. 7 (51), 936-941, (1979)

4. INVERSE GAS CHROMATORAPHY FOR STUDYING THE SURFACE ENERGY AND ACID-BASE CHARACTERISTICS OF SMC PREPREG, REINFORCING GLASS AND LIGNOCELLULOSIC FIBERS, AND WOOD HOT WATER EXTRACT MATERIAL

4.1 Chapter Summary

Sheet Molding Compound (SMC) is a material comprised of a polyester thermosetting matrix with thermoplastic, inorganic filler, metal oxides, reinforcement fibers, and material performance enhancers embedded in a cross-linked matrix. To achieve the optimum mechanical properties required for a composite material, the surface free energy of the polyester composite needs to be understood. In the present study, the composite matrix and reinforcement fibers are compared for their surface free energy and acid-base characteristics based on inverse gas chromatography (IGC) measurements. The IGC data were also used to assess the effect of chemical modifications performed on the fibers to improve fiber/matrix interactions and overall composite cohesion. Our results show that any fiber reinforcement system for the polyester composite material would have to be acid to promote good adhesion as the matrix system is very basic. A commercial glass reinforcement sized for polyester was found to have a lower interaction parameter compared to cellulosic fibers. This finding suggests that cellulosic fibers might have an advantage competing with a conventional glass-fiber reinforcement system in fiber/matrix bonding for SMC composites.

IGC has also been applied to 14 ligno-cellulosic fiber types including grass fibers, bast fibers, leaf fibers, seed fibers, and fruit fibers. This was done to provide insight into the impact of fiber composition on the surface characteristics of the different fiber types and explore possible correlations among the data. The dispersive surface energy, and K_a, K_b constants are reported for the 14 fiber types and compared to values reported in the literature. The fiber dispersive energies ranged from 35.5 mJ/m^2 to 44.2 mJ/m^2 at 20°C with K_a from 0.01 to 0.38 and K_b from 0 to 1.05. A correlation was found at 40°C for surface energy related to fiber composition and fiber type where the surface energy decreases with increasing lignin and hemicellulose composition but increased with increasing cellulose concentration.

Hardwood hot water extractives can be used as a feed stock for ethanol plants or for renewable polymer applications, such as replacing synthetic polymers in SMC composites. The hot water extraction to produce the hardwood extractives was performed at 160°C and 90 minutes using *Acer rubrum* wood strands as raw material. The weight loss of wood material after extraction was approximately 16% and the main two components in the extract were xylan (46.9%) and lignin (17.6%). The dispersive surface energy and acid-base surface characteristics for this multi-component freeze-dried mixture of hot water extracted *Acer rubrum* components was determined by inverse gas chromatography. The dispersive surface energy of the extract solids was found to be non-responsive thermally and having a magnitude of 34.6± 0.2 mJ/m^2 with a K_a of 0.13 and K_b of 0.46. The maple wood had a surface energy of 42.7 mJ/m^2 at 20°C following extraction, and the surface energy before extraction was 40.4 mJ/m^2 at 20°C confirming

that removing the lower surface energy extractives increased the surface energy of the extracted wood. Also, before extraction the K_a and K_b of the red maple were 0.19, 0.92, respectively, and after extraction the K_a and K_b were, 0.15, and 1.17. Infrared spectroscopy (IR) was used to characterize the wood surfaces and correlate the IR data to the bulk chemical composition analysis results and also, to the surface energy values. These findings indicate that the hot water extract components contribute to the overall average surface energy of maple wood by lowering the surface energy relative to other surface components. Removal of extractives may increase the adhesion possibilities for wood surfaces and the extractives may be used in composites as a substitute for petroleum-based polymers.

4.2 Background

4.2.1 Background for 14 lignocellulosic fiber type analysis

Bio-based composite materials are receiving considerable attention competing with composites derived from petroleum sources. The reinforcement of composites with natural fibers rather than commonly used glass fibers is a field of active research[1-6]. Much attention has been devoted to the study of acid-base characteristics of various pulped products[7-11]; however, relatively little work has been done to characterize other non-wood fiber types. To better understand how a matrix material interacts with a reinforcement fiber, the surface characteristics of both the fiber and matrix material need to be determined. A relatively easy technique for determining surface characteristics of ligno-cellulosic fibers is the technique of inverse gas chromatography (IGC). Therefore, in this paper the research questions asked are: (1) To what extent are surface

32

characteristics significantly different among fiber types or at least fiber categories, and

(2) Is there any coherence between the measured surface characteristics and the chemical

composition of the fibers as reported in the literature?

4.2.2 Background for polyester pre-preg analysis

Natural fiber reinforced composites have gained increasing attention over the past

decade as competitive materials for the replacement of petroleum derived materials[12].

Natural fibers have the advantages of lower weight, cost, and ease of processing as

compared to synthetic fibers[13]. However, natural fibers have a lower Young's modulus

compared to the synthetic fibers. Therefore, to compete with a completely synthetic

composite, the cohesion, solubility, and chemical bonding of a natural fiber based

composite must be maximized. One of the variables to consider when designing an

organic composite is the London dispersion component of the surface free energy (γ^D)

and acid base characteristics of both the matrix material and the reinforcing fiber. The

γ^D value of polyester[14], polystyrene[15], and the inorganic component $CaCO_3$ have been

reported[16], but the materials interacting within sheet molding compound have not been

studied.

4.2.3 Background for hot water extract analysis

Hot water extractives from wood containing significant hemicellulose content have

been studied as a possible source of biopolymers and chemicals. However most of the

previous work is focused on the purification of the different fractions in the extracts

based on their molecular size and/or chemical characteristics[17-24]. A different approach is

to use hot water extractives directly where their very particular chemical characteristics

33

are a match for specific applications. Hot water extractives from wood have both hydrophobic and hydrophilic properties and may be utilized in composites or converted to renewable polymers and fuels. This paper introduces basic properties of compounds obtained from hardwood (*Acer rubrum*) by hot water extraction to be considered for further applications. Also, the surface of wood is analyzed before and after the hot water extraction.

4.3 Experimental details and analysis

4.3.1 Experimental details for 14 ligno-cellulosic fiber types

The experimental details and procedures are presented in chapter 3 section 2 of the thesis. Flow rates for the IGC experiments were 10 sccm and the temperatures were $30°C$, $35°C$ and $40°C$. Non-parametric medians were calculated for each fiber group (Table 3.2) and these values were rank-correlated with each other by Spearman's rank correlation coefficient. The non-parametric analysis was performed as the distributions and means were not known for the individual fiber samples and non-parametric methods do not rely on the estimation of parameters such as the mean or the standard deviation describing the distribution of the variable of interest in the population or on the distribution being normal. Medians were calculated to serve as the descriptor of centrality as the distributions may be skewed and in that case the median serves as an acceptable description of centrality. Through personal communications with Dr. William Halteman Professor of Statistics at the University of Maine, Orono Maine, a statistically viable analysis using non-parametric statistics of the surface energy data is presented where the medians of the various fiber type surface energies are correlated to their

chemical composition. The statistical analysis was done in cooperation with Dr. Rupert Wimmer of the University of Natural Resources and Applied Life Sciences, Institute of Wood Science and Technology, BOKU-Vienna,Vienna, Austria, based on fiber chemical compositions found in the literature. The Spearman's analysis was done initially by Dr. Wimmer then repeated and confirmed by, myself and Dr. Halteman. The standard deviation and means for three fiber types are presented using three replicates but are not used in the non-parametric statistical analysis.   The literature values found by Dr. Wimmer are presented in Figure 4.1 A, B, and C. Since a non-parametric analysis is done on the data, the results are presented in box and whisker plots.

A
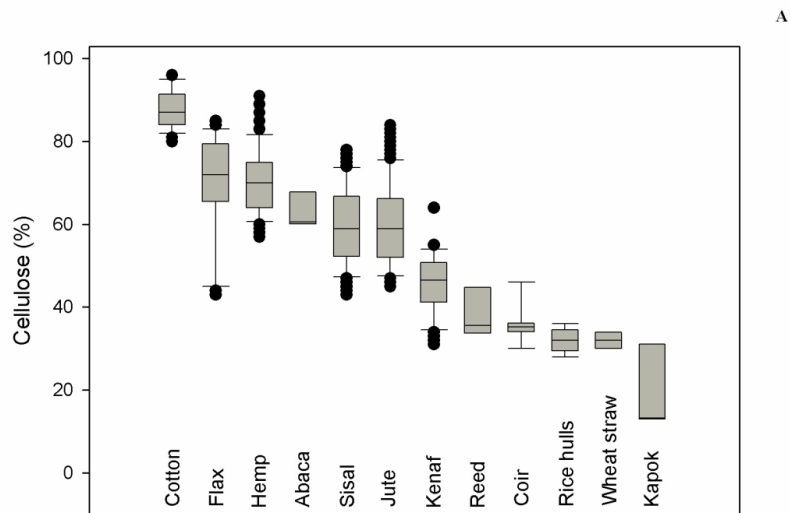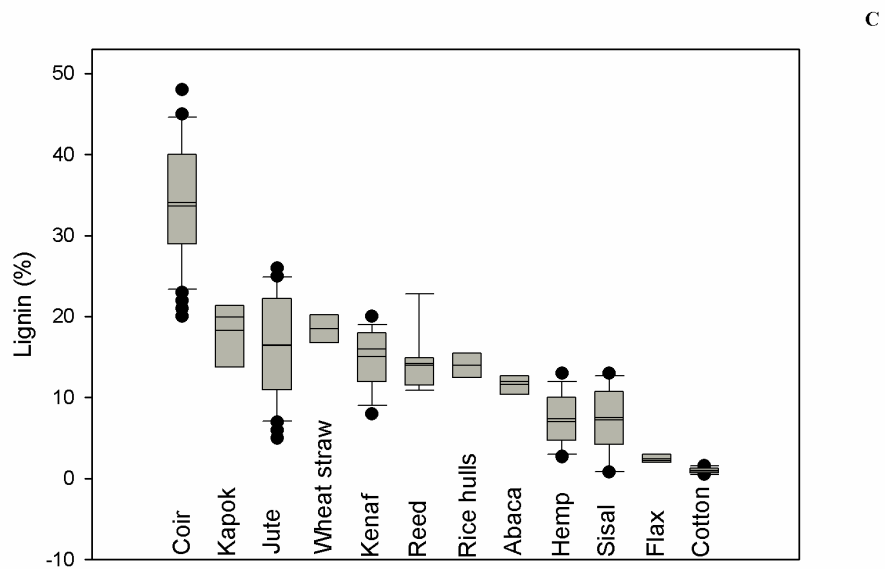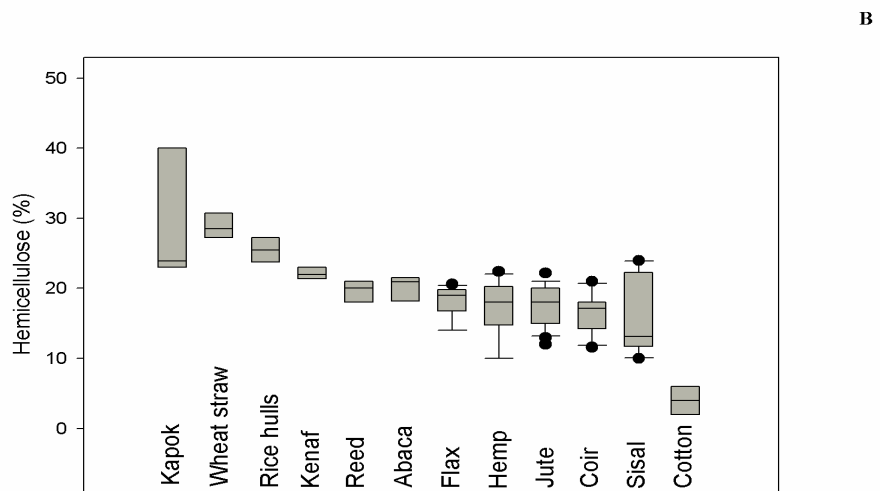
Figure 4.1. Literature values for composition of fibers, A Cellulose, B. Hemicellulose, and C. Lignin [25-52] by Dr. Rupert Wimmer, University of Natural Resources and Applied Life Sciences, BOKU-Vienna.

Box-and-whisker plots are created by ordering the data, (putting the values in numerical order), and finding the median of the data. To divide the data into quarters, the medians of the two halves are calculated. With these three points: the first middle point (the median), and the middle points of the two halves, box and whisker plots are generated where the box is defined by the 3 medians and the line known as the whisker represents 1.5 times the magnitude of the range defined by the upper and lower medians with outliers being represented by •. The box represents the data presented from the lower 25th percentile to the upper 75th percentile.

4.3.2 Experimental details for polyester pre-preg analysis

The experimental details and procedures are presented in chapter 3 section 2 of the thesis. Flow rates for the IGC experiments were 30 sccm and the temperatures were 30°C, 35°C, 40°C, 50°C, 55°C, 60°C, 100°C, 110°C, and 120°C.

Various literature sources were used for the dispersive free energy values needed for a rule of mixture analysis with the SMC matrix material and is presented in Table 4.4.

Table 4.1. Published data of the London dispersion component of the surface free energy (γ_S^d; in mJ/m^2) of materials used in the sheet molding compound matrix.

	γ_S^d at various temperatures	R^2	30°C(predicted)
Polyester resin [a]	15 (99.85^{o}C) 22 (79.85^{o}C) 32 (59.85^{o}C) 40 (39.85^{o}C)	0.99	44
Polystyrene[b]	31.6 (60°C) 33.0 (55°C) 34.1 (50°C)	0.99	39
Calcium carbonate [c]	39 (110°C) 41 (100°C) 46 (90°C) 46 (80°C) 48 (70°C)	0.91	58

Note: [a] from [14], [b] from [15], [c] from[53]; precipitated calcium carbonate, [d] the values at 30°C were obtained from linear extrapolations.

4.3.3 Experimental details for extract analysis

The experimental details and procedures for the IGC are presented in chapter 3 section 2 and for the extraction in chapter 3 section 3 of the thesis. Flow rates for the IGC experiments were 10 sccm and the temperatures were 30°C, 35°C and 40°C. Diffuse reflectance Fourier transform infrared spectroscopy (DRIFT) was performed on freeze-dried hot water extract samples. The powdered extract was mixed with KCL and infrared spectra were obtained after purging water from the infrared chamber for 2 hours.

4.4 Results and Discussion

4.4.1 Dispersive energies for 14 lignocellulosic fiber types

Results for the dispersive component of the fiber surface energy, γ_S^d, ranged from 35.5 mJ/m^2 for kenaf to 44.2 mJ/m^2 for rice hulls at 20°C. The mean and standard deviation and standard error were calculated for cotton, flax, and coir representing a large range of cellulose and lignin values. For cotton the mean is 39.4 mJ/m^2 with a standard deviation of 1.1 creating a standard error of +/-0.6, for coir the mean is 38.0 mJ/m^2 with a standard deviation of 1.6 creating a standard error of +/-0.6, and for flax the mean is 36.2 mJ/m^2 with a standard deviation of 1.1 creating a standard error of +/-0.9. The means, standard deviations, and standard errors were calculated with 3 replicates. A single factor analysis of variance was computed based upon the flax, coir, and cotton data using the data point from the non-parametric analysis; however, the means generated by the parametric analysis were not used in the non-parametric analysis. The f-factor calculated was 4.5, higher then the f-critical value of 3.4 supporting a conclusion that the variances are different and the p-value calculated was 0.06 supporting the conclusion that the mean values are different for the 3 fiber types at a 0.1 α level or 90% confidence interval.

Table 4.2. Dispersive energy as a function of temperature and regressed value at 20°C for various fiber types calculated by the Schultz and Lavielle method.

Fiber type	Dispersive energy mJ/m^2				
	40(°C)	35(°C)	30(°C)	20(°C)	R^2
Grass fibers					
wheat straw	35.4	37.5	38.0	40.9	0.90
wheat pulp bleached	38.5	39.4	40.6	42.6	0.99
Rice hulls	39.4	40.2	41.9	44.2	0.96
reed	37.2	38.3	39.6	41.9	1.00
Bast fibers					
hemp	35.9	37.8	39.5	43.1	1.00
flax	34.9	37.0	38.7	42.7	1.00
kenaf	36.9	38.3	40.0	43.1	1.00
jute	43.5	42.5	41.9	40.2	0.98
Leaf fibers					
abaca	36.2	36.2	36.0	35.8	0.90
sisal	41.2	39.8	38.4	35.5	1.00
Seed hair fibers					
cotton	38.7	38.3	39.5	40.0	0.45
poplar seed	38.9	38.7	39.9	40.6	0.66
Fruit hair fibers					
kapok	37.7	37.9	39.5	41.1	0.85
coir	36.4	37.7	39.1	41.8	1.00

Explanations for differences in the surface energies may be determined by looking at the chemical composition of the fibers. With the exception of poplar seed hairs and the wheat pulp fibers an extensive data collection was acquired from literature for all fiber types featuring cellulose, hemicellulose, and lignin percentages.

4.4.2 Statistical analysis

Table 4.3: Medians of measured dispersive energies at 40°C and composition medians with the 25th to 75th percentile group ranges for collected cellulose, lignin, and hemicellulose contents from literature sources for the five natural fiber subgroups.

Fiber group	Dispersive energy mJ/m^2 at 40°C from IGC	Cellulose % from literature review	Lignin %	Hemicellulose %	Cellulose % 25th-75th percentile	Lignin % 25th-75th percentile	Hemicellulose % 25th-75th percentile
Grass fibers	37.6	32.0	14.0	25.50	35-42	12-21	18-32
Bast fibers	37.8	64.5	11.5	18.50	41-79	4-21	17-21
Leaf fibers	38.7	59.8	9.7	17.03	55-68	8-14	14-20
Seed fibers	38.8	87.0	0.9	4.00	85-95	0-4	2-6
Fruit fibers	37.0	24.2	29.7	25.83	11-39	15-39	18-40

Significant rank correlations were found between cellulose ($r=0.9$, $p<0.1$), lignin ($r=-1.0$, $p<0.05$ and hemicellulose ($r\_-1.0$, $p<0.05$), respectively, and dispersive energy measured at 40°C. Dispersive energies at the other temperatures did not show significant rank correlations. The data found to correlate by Spearman's analysis are presented in Figure 4.1.
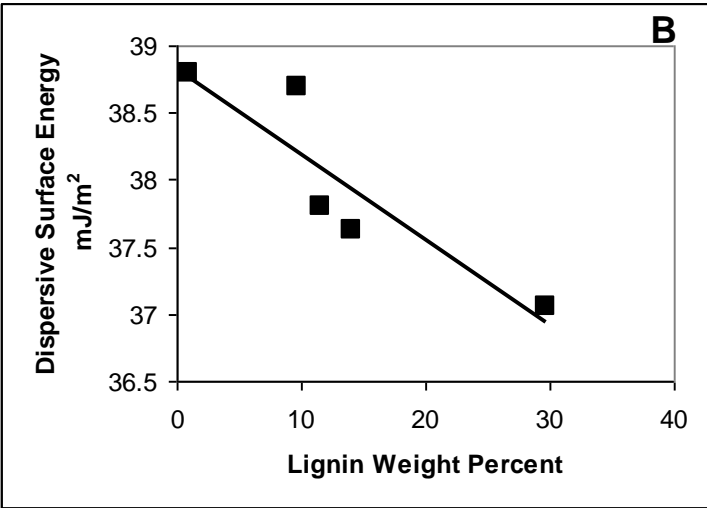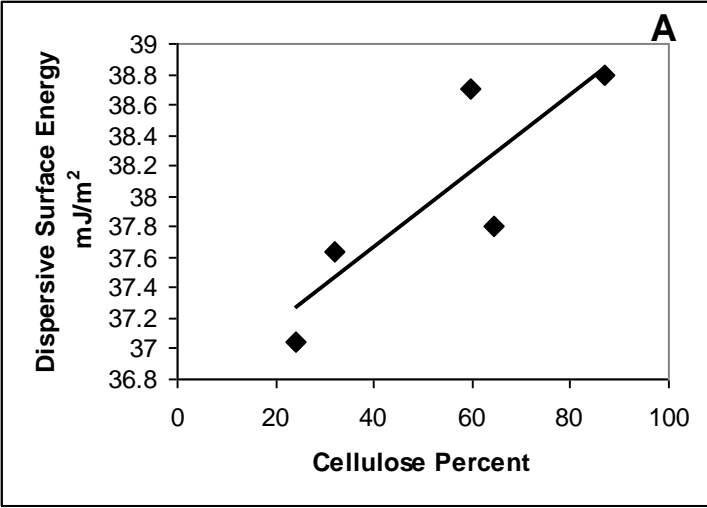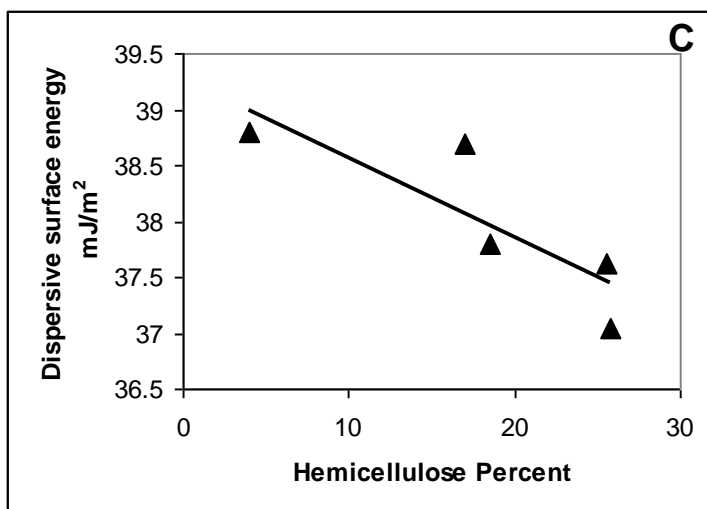
Figure 4.2. Dispersive surface energy as a function of A. percent cellulose, B. percent lignin and C. percent hemicellulose composition and dispersive surface energy values from Table 4.2 based on the non parametric Spearman's analysis.

In Figure 4.2 A, the surface energy increases as a function of cellulose as a component in the composition of the fibers, R^2=0.73. This is consistent with results found by Paredes et al[54] where hot water extract was removed from red maple and the apparent crystallinity and surface energy increased with increasing cellulose surface content. Mills et. al.[55] reported results for IGC with a hot water extract from red maple comprising of approximately 70 weight percent hemicellulose and 15 weight percent lignin of 34.7 mJ/m^2 at 40°C consistent with both part B, R^2=0.80 and C, R^2=0.70, of Figure 4.2 where as the content of lignin and hemicellulose increases the dispersive surface energy decreases.

While there was a clear association between the fiber chemistry and the measured dispersive energy levels we also hypothesize that only certain functional groups contribute to the surface energy of the fibers. In the field of adhesion it is common

knowledge that the energy of the surface is dependent upon the time lag since the material went through a surface conditioning processes. A mechanically conditioned surface should have the highest surface energy for several reasons. Reference texts such as the Wood Handbook[56] describe the best wood surfaces for bonding as being resurfaced mechanically within 24 hours of bonding to other substrates. A resurfacing using a sharp blade provides parallel and flat surfaces allowing free flowing and complete surface interactions between the bonding surfaces and outperforms the bonding created by reconditioning the wood surface by sanding as the abrasive action has been found to cause crushing of wood cells. Oxidation of the wood surface and thermal drying [57] are two other factors that decrease the surface energy of wood. Another factor is the migration of low molecular weight extractives to the surface of wood which inactivates the surface [58] and decreases the wood's surface energy. Therefore, while the differences in dispersive energy differences among fibers were found to be significant as determined by a non parametric analysis, it is also realized that other practical differences between the fibers may overshadow the noted dispersive energy differences among fibers in practical applications.

In this thesis research, fibers were sheared in a Wiley mill passing through a ½ mm screen until a 60 mesh particle size was achieved and then packed and weighed in the IGC column and conditioned. This processing will increase surface area and create a fresh surface with the lowest concentration of low molecular compounds relative to lignocellulosic surfaces that have not been through mechanical processing. In general, the highest energy values for wood, and the best bonding should occur when the material is processed, conditioned, and tested within a 1 day period[56]. Also, since IGC is a

method using infinitely dilute gas phase probes, it is generally accepted that probes preferentially select the highest energy sites of a heterogeneous surface, as the low concentration of probe molecule selects the highest energy sites on the material first for bonding. This argues that the calculated surface energy is generally greater than that which can be obtained experimentally by other techniques such as sessile drop or column wicking contact angle analysis.

The surface energy values obtained experimentally (Table 4.1) were compared to results in the literature. Gulati and Sain[59] reported a dispersive energy for hemp at 40°C being 38 mJ/m^2 (35.9 mJ/ m^2) Reutenauer and Thielmann[60] report a dispersive energy for cotton of 35.18 mJ/m^2 (39.5 mJ/m^2) at 30°C; and Tshabalala reports a value of 40 mJ/m^2 (36.9 mJ/m^2) at 40°C for Kenaf[61]. The reported kenaf and hemp values are slightly higher then found in this study and the cotton values are lower.

4.4.3 Donor acceptor analysis
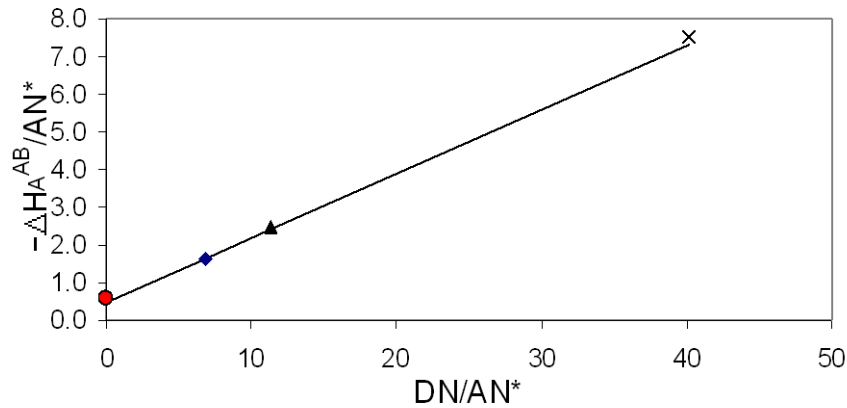
Figure 4.3. Relationship for determining K_a and K_b using data from the polarization method at 30°C, 35°C, and 40°C for the flax fiber with chloroform ●, ethyl acetate ▲, acetone◆, and tetrahydrofuran x.

45

The fourteen fiber types were analyzed to determine K_a and K_b with an example regression line for flax fiber is shown in Figure 4.3. Table 4.3 contains all the K_a and K_b values determined from the regressions with the coefficient of determination presented. From the regression and Equation 13, the values of K_a and K_b for the fibers were determined. For flax, coir, and cotton the standard deviation based on three replicates for K_a was 0.02, 0.05, and 0.05, respectively. The standard deviation of K_b for flax, coir, and cotton was 0.15, 0.23, and 0.20 respectively. The standard deviations for K_a are approximately 10 percent for flax and coir but approach 90 percent for cotton; however, the magnitude of the standard deviation is 0.02, 0.05 and 0.05, for the 3 samples and may be more indicative of experimental error then variation in the surface chemistry. Since cotton is comprised of high percentages of cellulose and the K_a appears to not be impacted by the high cellulose content, the relative experimental error may have a greater impact on the K_a for cotton due to the small value of Ka relative to the standard error. The K_b representing electron donor tendency is impacted by the hydroxyl function groups on cellulose[54] and is highest for cotton; however, standard deviations are over 30 percent and the variations may be due to surface characteristics differences related to the infinitely dilute nature of the IGC experiments as IGC probes interact with the highest energy sites on the substrate surfaces.

Table 4.4. K_a and K_b for all 14 fiber types.

Fiber type	Ka	Kb	R^2
Flax	0.17	0.49	1.00
Kenaf	0.07	0.32	0.95
Kapok	0.14	1.05	0.97
Cotton	0.06	0.50	0.98
Hemp	0.16	0.49	0.99
Rice	0.21	0.38	1.00
Poplar seed hair fibers	0.10	0.42	1.00
Wheat pulp bleached	0.10	0.47	0.92
Wheat straw	0.15	0.70	1.00
Reed	0.15	0.61	1.00
Coir	0.19	0.20	1.00
Sisal	0.38	0.74	1.00
Abaca	0.12	0.59	0.99
Jute	0.01	0.00	0.98

4.4.4 Surface scans and molecular compositions

SEM images were made from all investigated fiber types. Figures 4.4-4.8. SEM's of the different fiber types; all SEM's by Dr. Rupert Wimmer, University of Natural Resources and Applied Life Sciences, BOKU-Vienna.
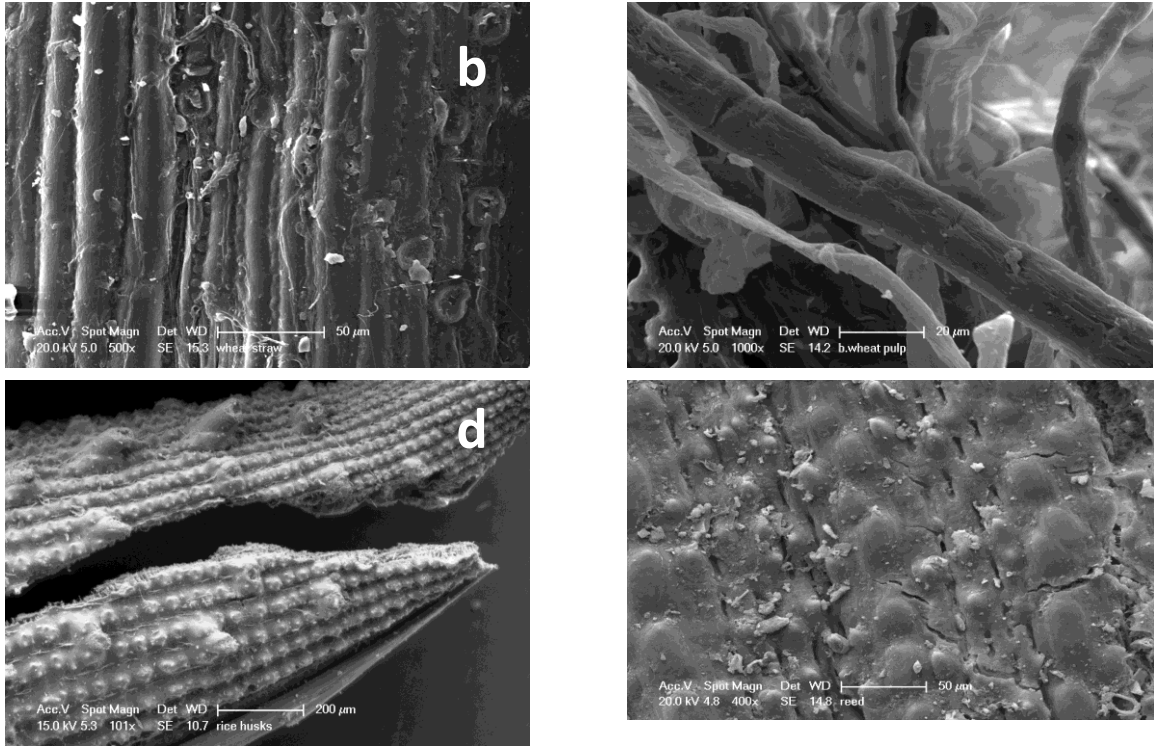
Figure 4.4. SEM images of the measured grass fibers. (a) Wheat straw fibers, (b) bleached wheat pulp fibers, (c) rice hulls, (d) reed grass.
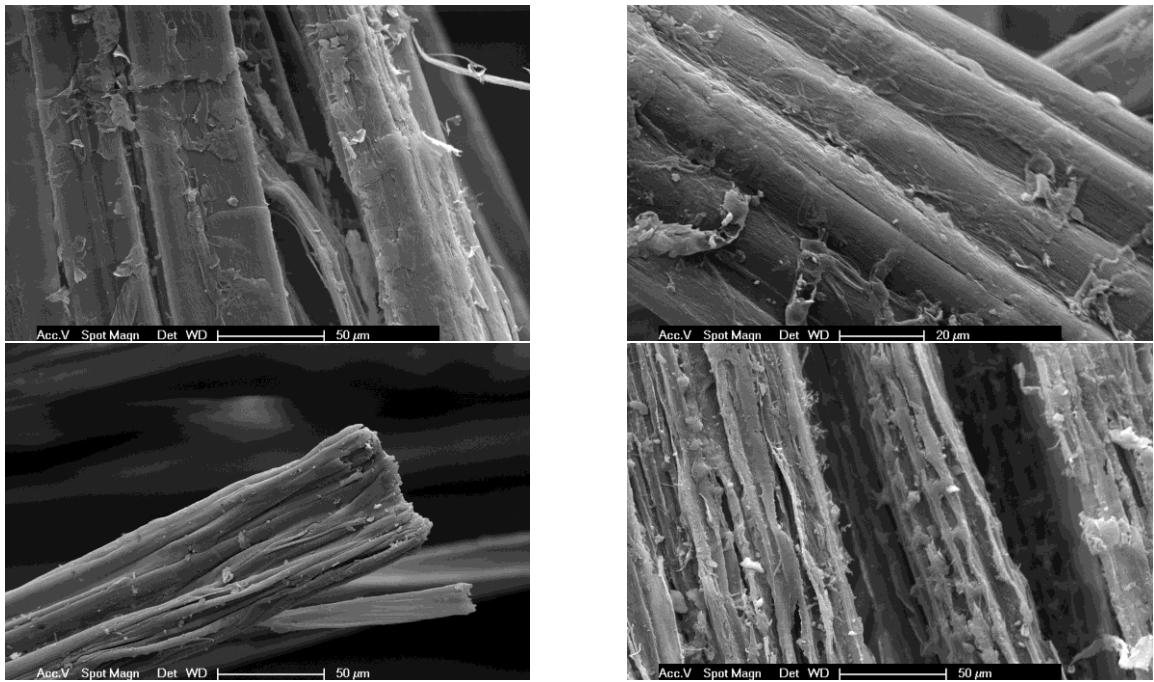
Figure 4.5. SEM image of the measured bast fibers. (a) hemp, (b) flax, (c) kenaf, (d) jute.
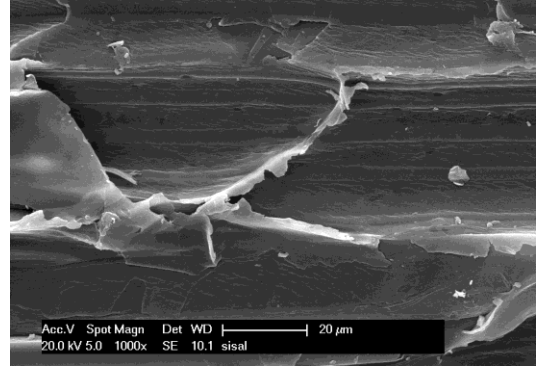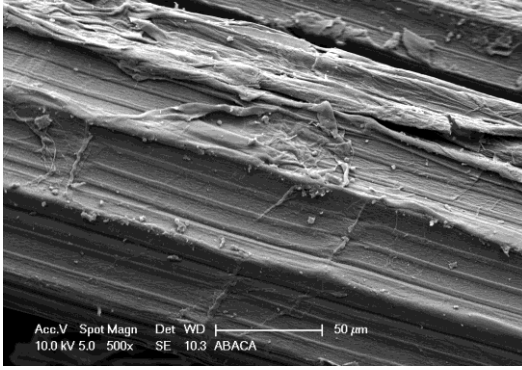
Figure 4.6. SEM image of the measured leaf fibers. (a) abaca, (b) sisal.
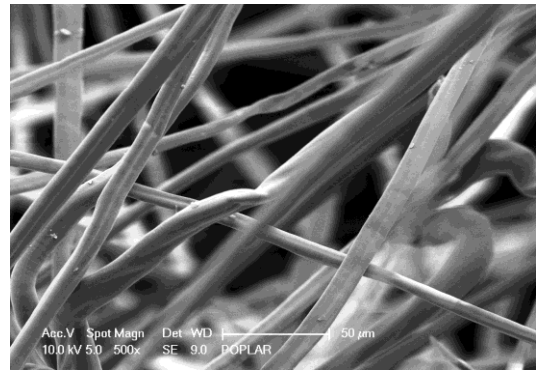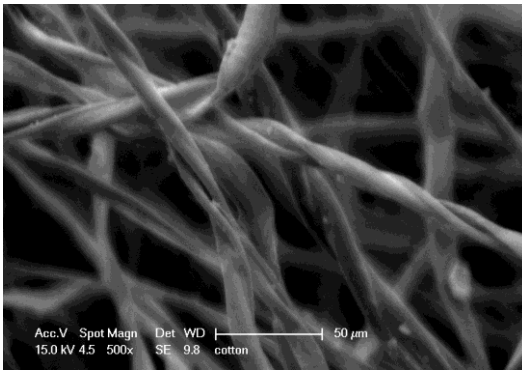
Figure 4.7. SEM image of the seed hair fibers. (a) cotton, (b) poplar.
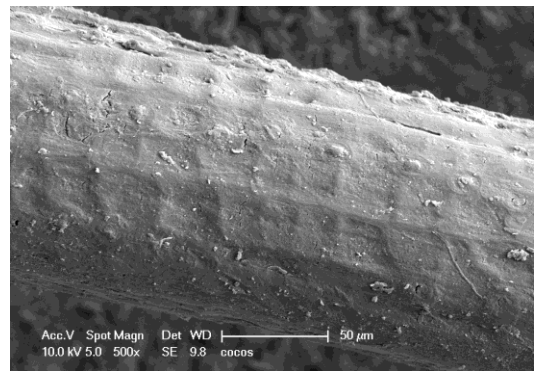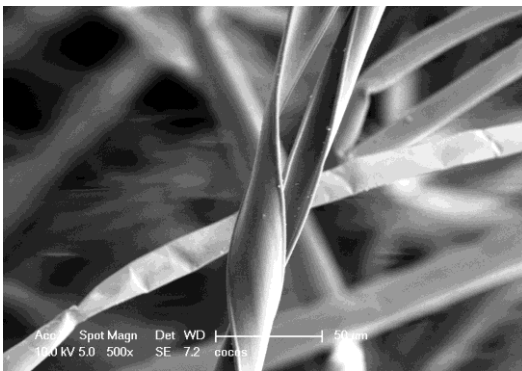
Figure 4.8. SEM image of the measured fruit hair fibers. (a) kapok, (b) coir.

The cohesion of components in a composite is dependent upon more than just secondary chemical interactions such as acid-base interactions, the surface morphology is also important as mechanical interactions contribute to adhesion interactions between components in a composite.

The grass fiber group has a strongly structured surface with thick epicuticular wax layers. These wax-cuticle layers are rather thick and might experience some mechanical removal during processing[61]. Individual wheat fibers are seen with the pulped version (Fig 4.5b) and surfaces are much smoother.

Bast fiber surfaces are generally smoother with epicuticular wax layers mostly removed during the retting process[62]. The leaf fibers abaca and sisal have very similar rippled surfaces with visible epicuticular wax and fat layers.

With the exception of coir, the two fruit fiber types exhibit thin fibers with poplar seed hairs being the thinnest (under 10μm). Surfaces are much smoother than the other natural fiber types and the extent of epicuticular wax layers are limited. Coir fiber surfaces are much thicker (>100μm) but also smooth with a slight rippled structure that include pit formations[62].

In general, most of the fibers displayed similar K_a's and K_b's; however, looking at kapok and cotton, as examples, kapok has both a higher K_a and K_b this result could be related to kapok only containing 13% cellulose and cotton having 92% cellulose. Perhaps extractives on the surface or the aromatic nature of lignin may be contributing to the large electron donor nature of the kapok versus the cotton. Jute displayed a rather non-reactive surface. This may be due in part to no pretreatment other than mechanical

shearing in a Wiley mill but leads to interesting questions about the nature of the surface of the fibers. Many fiber types are covered with waxy coatings with low surface energies. In Figures 4.1A, 4.1B, and 4.1C it is apparent that there is a wide range in lignin and cellulose composition; however, the hemicellulose concentration stays relatively constant. The only large changes in the acid-base characteristics are seen in the extreme cases of cotton and kapok. This indicates that there may be a sizable amount of surface area of the fiber comprising hemicellulose as this component changes the least amount from fiber to fiber. Also, Figures 4.4-4.8 show the topography of the fibers and it's apparent that the surfaces are very different on a micrometer scale and although this shouldn't impact interactions on a molecular scale, the interactions between a matrix material and the fibers may be significantly impacted by the surface geometries. More analytical work needs to be done to determine the exact nature of the fiber surfaces to correlate with this work.

4.4.5. Suggestions for composite fabrication

- Most of the fiber types have a waxy layer that may act as a weak boundary layer in the cohesion and adhesion interactions in a composite and as such should be either mechanically or chemically removed before use in a composite material.

- Hemicellulose and lignin tend to lower the surface energy of fiber surfaces and some chemical treatments to lower their surface concentrations may be needed.

- Mechanical treatments of the surface of fibers may create significant increases in surface area that may lead to better bonding and cohesion in a composite material.

4.4.6 Dispersive energy, acid-base, and cohesion interaction values for SMC paste

Large temperature ranges were explored for the polyester based material. In Figure 4.9, a linear response to temperature is seen for the dispersion component of the surface free energy, γ_S^d. Results for γ_S^d also demonstrated slightly higher values for the SMC material, (47 J/m^2 at 30°C; Figure 4.9) as compared to previous literature work for pure polyester, (44mJ/m^2 at 30°C; Table 4.4)[14], and polystyrene, (39 mJ/m^2 at 30°C; Table 4.4)[15]. The higher γ_S^d value of the SMC material is thought to be contributed by calcium carbonate ($CaCO_3$), a major component of the matrix material. Keller and Luner[53] reported that preconditioning of the (precipitated) $CaCO_3$ samples at different temperature levels (100-300°C) would result in a huge range of 55-250 mJ/m^2 (at 100°C column temperature) for γ_S^d values because of the influence of physi- and chemisorbed water on the surfaces within the pore structure of the sample. At a preconditioning temperature of 120°C, which approximated the temperature (150°C) used for preconditioning our samples, the γ_S^d value of (precipitated) $CaCO_3$ was 58 mJ/m^2 when extrapolated to the test (column) temperature of 30°C (Table 4.4). Using a composition of 28.1% polyester, 20% polystyrene, and 48.5% $CaCO_3$, the rule of mixture provides for the SMC matrix a γ_S^d value of 50 mJ/m^2, which closely agrees with the experimental value of 47 mJ/m^2 (at 30°C; Fig. 4.9) from this study. Three replicates were run and a standard deviation of 0.4 mJ/m^2 and standard error of 0.2 mJ/m^2 were calculated for the SMC matrix material dispersive surface energy.
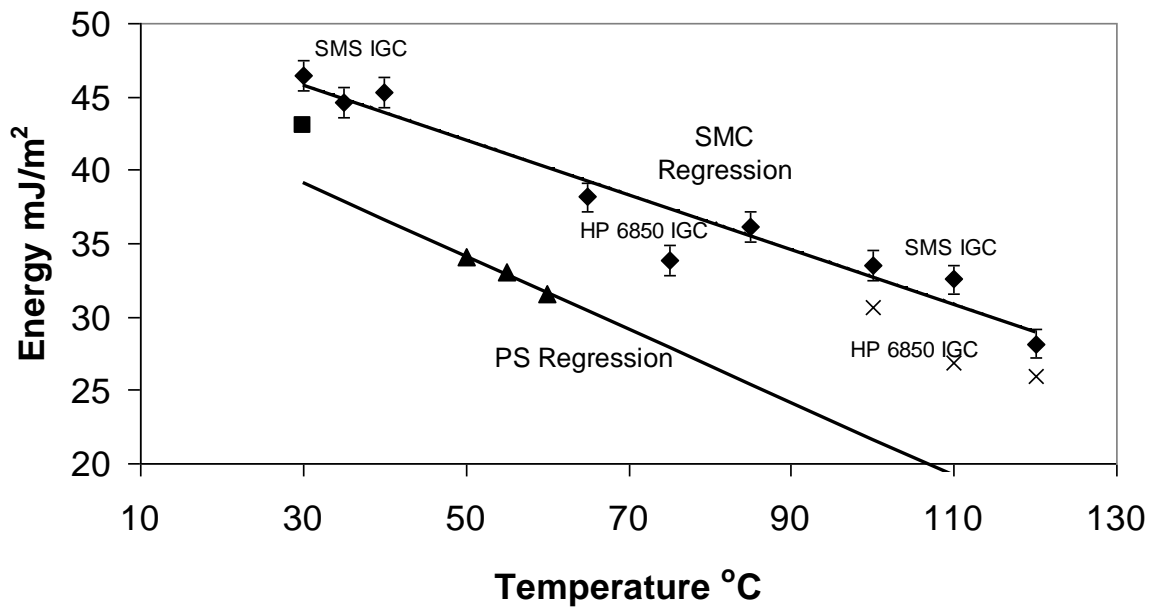
Figure 4.9. Dispersive surface energy for the SMC material ◆, polystyrene,(PS) ▲ [15], polyester ■ [14], and the SMC material repeated at higher temperatures X with a second instrument. Three temperatures were run per experiment and the instrument used for the experiment is listed by the data in the figure. The SMS IGC was used for the temperatures of 30°C, 35°C, 40°C, 100°C, 110°C, 120°C and the HP 6850 IGC was used for the temperatures of 65°C, 75°C, 85°C, and repeated temperatures of 100°C, 110°C, and 120°C marked as X. SMC regression R^2=0.94, PS regression R^2=0.99.
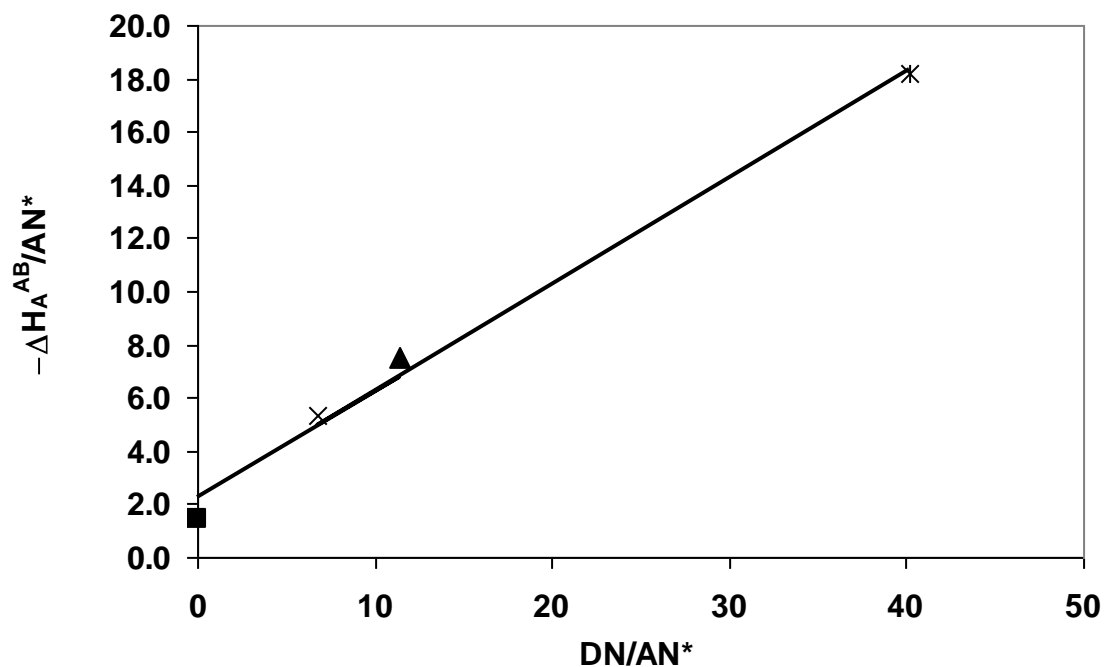
Figure 4.10. Relationship for determining K_a and K_b using data from the polarization method at $100°C$, $110°C$, and $120°C$ for the SMC material with chloroform ■, ethyl acetate ▲, acetone ✕, and tetrahydrofuran ✳.

From the slope and intercept of the data in Figure 4.10, K_a and K_b are determined. In the current investigation, the determination of the polar characteristics of the solid material could only be determined at higher temperatures because of the irreversible adsorption of the probes into the polymer matrix. These higher temperature levels ($100°C$, $110°C$, and $120°C$), together with a higher flow rate of 30 ml/min for the carrier gas, were required to facilitate movement of the probes through the column[63,64] so that meaningful K_a and K_b values could be calculated. However, at higher temperatures Santangelo *et. al.*[65], report a glass transition of approximately $100°C$ for polystyrene, and this may lead to some bulk adsorption phenomena beyond what is expected with IGC. Keller et. al.[54], who worked with $CaCO_3$ using inverse gas chromatography, also found

that the basic characteristic of the $CaCO_3$ was so strong that acidic probes could not be used because of the reaction, (irreversible adsorption), with the $CaCO_3$. Despite the potential impact of bulk adsorption on our findings, the high coefficient of determination for the regression is an indication that the IGC theory is valid under the protocol (e.g. temperatures of $100°C$, $110°C$, and $120°C$) that were adopted.

The K_a of the SMC material was found to be 0.40 and K_b is 2.23. Previously, polystyrene has been reported to have a K_a of 0.06, and a K_b of $0.35^{[15]}$, or 0.28 and $0.46^{[66]}$. The very high K_b for the composite material is thought to be due to the high density of electron donating oxygen's with unshared pairs of electrons available for donor interactions resulting in high basicity[53] in the CaCO3 and because polystyrene with high *pi* bonding character only has a K_b of 0.35-0.46.

The IGC analysis was repeated with chopped strand glass reinforcement fibers. The London dispersion component of surface free energy (γ_S^d) changed over the temperature range of 40-65°C with values of 39.8, 41.1, 41.2, mJ/m^2 at 65°C, 35°C, 30°C, extrapolating to $41.5mJ/m^2$ at 25°C with a 1.00 coefficient of determination. Glass has been studied extensively by Dutschk *et* al [67] and their findings indicated that the technique of IGC is "too sensitive to give an unambiguous description of the complex character of heterogeneous fibers"; however, since a rule of mixtures worked with the complicated polyester system and since this glass is sized for polyester, the technique may apply. Park *et. al.*[68] determined the total surface energy of polyester sized glass fibers to be approximately 38 mJ/m^2. The value found using IGC is somewhat higher than the value found by Park *et. al.* but is consistent with IGC values being higher than contact angle analysis values. In Table 4.4, polyester has been reported as having a value of 44 mJ/m^2

and the SMC has a value of 47 mJ/m^2 for the dispersive surface energy. A glass

dispersive surface energy of 41.5mJ/m^2 at 25°C should be compatible with the SMC

assuming the acid-base surface energies are not too large. The K_a and K_b values

calculated were 0.20 and 0.35 with a coefficient of determination of 0.99.

If the K_a and K_b for the multi component polyester SMC material are known together

with the K_a and K_b for the fiber reinforcement, a reinforced composite can designed. Tze

et. al.[69] reviewed how the acid-base interactions in a composite can be maximized to

enhance the mechanical strength of a composite.

$$I_{a-b} = K_{a,f} K_{b,m} + K_{b,f} K_{a,m} \qquad (4)$$

I_{a-b} is known as the interaction parameter the subscripts a,b,f, and m refer to acid, base,

fiber, and the matrix, respectively. K_a and K_b have been determined for various sizing

agents with Lyocell fiber reinforcement[69] and are used to determine the interaction

parameter with the SMC material.

Table 4.5. Sized and untreated cellulose fiber K_a and K_b values for calculating the interaction parameter with the SMC material

	Ka	Kb	Ia-b
SMC material	0.4	2.23	
Polyester sized glass	0.20	0.35	0.59
Sized cellulose			
untreated cellulose, (lyocell) *	0.36	0.39	0.96
Amino-silanated *	0.33	0.52	0.94
Phenylamino-silanated *	0.32	0.42	0.88
Phenyl-silanated *	0.34	0.43	0.93
Octadecyl-silanated *	0.33	0.27	0.84
SMA-Grafted *	0.42	0.57	1.16

Note * from [58].

From Table 4.5, it is apparent that the only sizing agent that gives a higher interaction parameter as compared to the untreated fiber is styrene-maleic anhydride, (SMA-Grafted) for the cellulosic fibers. The reason is apparent considering that SMA-Grafted is the only sizing agent listed that increases the acidic character of the fiber. Because of the high K_b for the SMC material, any fiber reinforcement in the material will need to have a high acidic character to promote a good interaction. The polyester sized glass has a lower interaction parameter compared to the biobased fibers indicating that the biobased fibers might have an advantage for surface interactions competing with glass for overall cohesion within a SMC matrix. The glass fibers are sized to promote surface-free energy compatibility (like-like affinity) for polyester and polystyrene matrices, but cellulosic fibers sized to favorable interaction parameter values are likely to bond to SMC materials

through enhanced acid-base interactions. The improved fiber/matrix bonding for sized cellulosic fibers is analyzed further in Chapter 5 of this thesis.

4.4.7 Dispersive energy, acid-base, and molecular composition values for extract

4.4.7.1 Chemical analysis of the extract

The calculated extraction yield was about 16% based on the original wood. The final pH of the extract was 3.5. Table 4.6 shows the chemical composition for the freeze dried hot water extract.

Table 4.6. Chemical analysis of freeze dried hot water extract (all values in g/100g of dried extract)

Component	Weight percentage g/100 g
Cellulose	3.94
Xylan	46.88
Mannan	2.89
Galactan	4.55
Acetyl groups	7.63
Uronic acids	9.41
Proteins	1.54
Total lignin	17.59
Ash	1.97
Total	**96.40**

4.4.7.2 IGC analysis

Table 4.7. Dispersive surface energy of the extract, maple before and after extraction at 20°C, 30°C, 35°C, and 40°C

T (°C)	γ_s^d (mJ/m^2)				
	40	35	30	20(regressed)	R^2
Hot Water Extract	34.7	34.4	34.7	34.6	0.00
Maple before extraction	36.3	36.9	38.5	40.4	0.93
Maple after extraction	38.3	39.1	40.6	42.7	0.97

In Table 4.7 the dispersive surface energy is shown at 30, 35 and 40 °C. Typically the dispersive surface energies calculated by IGC tend to decrease with increasing temperature due to an increase in the entropy contribution to the Gibbs free energy. However, with the hot water extract the dispersive surface energy seems to be unresponsive to temperature change based upon 3 replicates with a standard deviation of 0.4mJ/m^2. This may be due to the amorphous nature of the extractives being non-reactive to thermal changes and in a lowest energetic state. The maple wood after extraction had the highest surface energy, 42.7 mJ/m^2 at 20°C and the maple wood before extraction was 40.4 mJ/m^2 at 20°C. These results compare well with results found by Paredes et.

al.[54], who found that as the extraction time was increased the surface energy of the extracted wood increased.
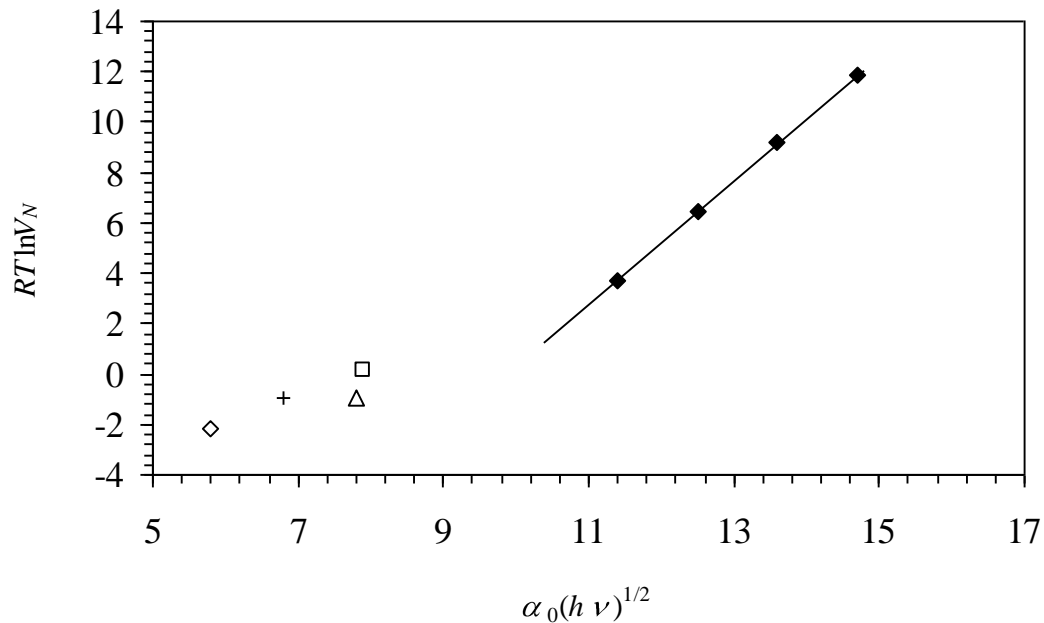
Figure 4.11. Example polarization plot at $30°C$ to determine acid base characteristics of the hot water extracted material with n-alkanes◆, ethyl acetate□, tetrahydrofuran +, chloroform Δ, acetone ◇, similar plots generated for Maple before and after extraction.

In Figure 4.11, the n-alkanes exhibit a linear relationship representing the apolar characteristic of the hot water extracted material, and this relationship is used to determine γ_S^d by the Schultz and Lavielle method.
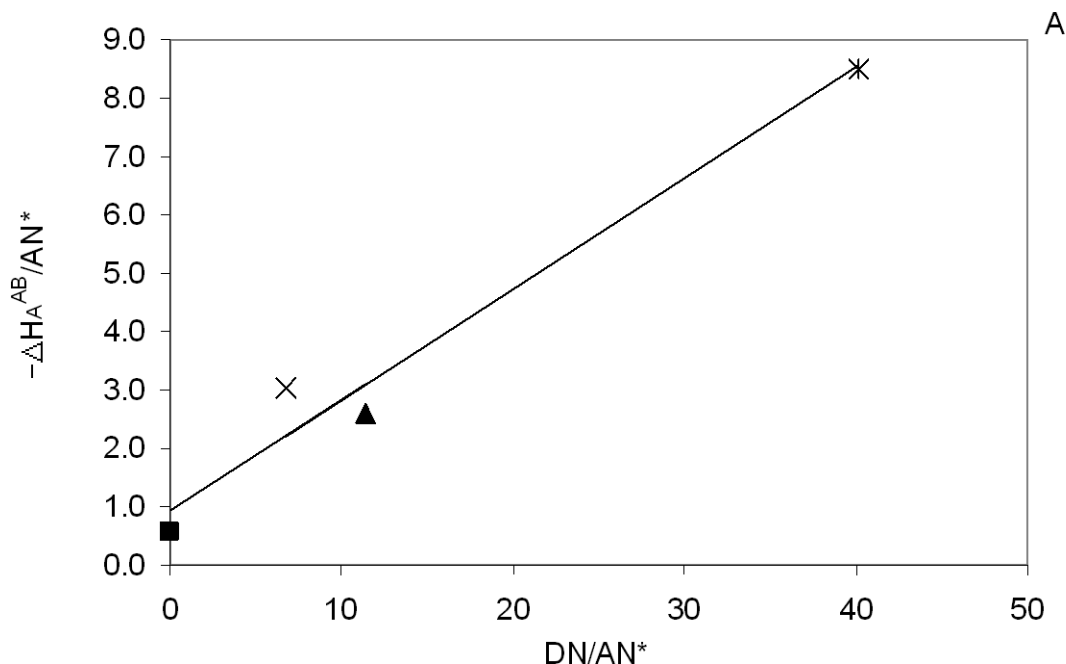
Figure 4.12. Example relationship for determining K_a and K_b using data from the polarization method at 30°C, 35°C, and 40°C for the maple wood before extraction with chloroform ■, ethyl acetate ▲, acetone ✕, and tetrahydrofuran ✳.

From the slope and intercept of the data in Figure 4.13, K_a and K_b are determined. The K_a of the extractive material was found to be 0.13 and K_b is 0.46 with R^2=0.97; for the maple before extraction the K_a and K_b are 0.19, 0.92 with R^2=0.97and after extraction the K_a and K_b are, 0.15, 1.17 with R^2=0.90. The standard deviation in the K_a values for three replicates was 0.05 and for the K_b values was 0.13 for the extract. To the author's knowledge, no other papers have reported K_a and K_b values for hot water extract from maple wood. In Table 4.8, the surface energies are reported and agree with the results found by Parades et. al.[54], both in trend and in magnitude where for maple wood a surface energy of 39.4 mJ/m^2 and extracted maple wood of 43.8 mJ/m^2 was reported.

Table 4.8. γ_d, K_b, and K_a for the wood materials. Standard deviation values for hot water extract: for three replicates, K_a was 0.05, K_b was 0.13 and 0.11mJ/m^2 for the surface energy. Replicates were not generated for the red maple wood samples.

	γ_d(mJ/m^2)	K_b	K_a
Hot water extract	34.6	0.46	0.13
Red maple	40.4	0.92	0.19
Extracted red maple	42.7	1.17	0.15

The surface energy trend of increase in surface energy as extract is removed corresponds well with literature results found by Gardner et. al.[70], where results indicate that low molecular weight compounds lower the surface energy of wood materials. Conversely, the result that the surface energy increases as these low molecular weight compounds are removed from the surface is to be expected. An increase in surface energy values as extract is removed correlates well with an increase in the K_b of the wood material, and this corresponds with the surface energy trend (Figure 4.13).
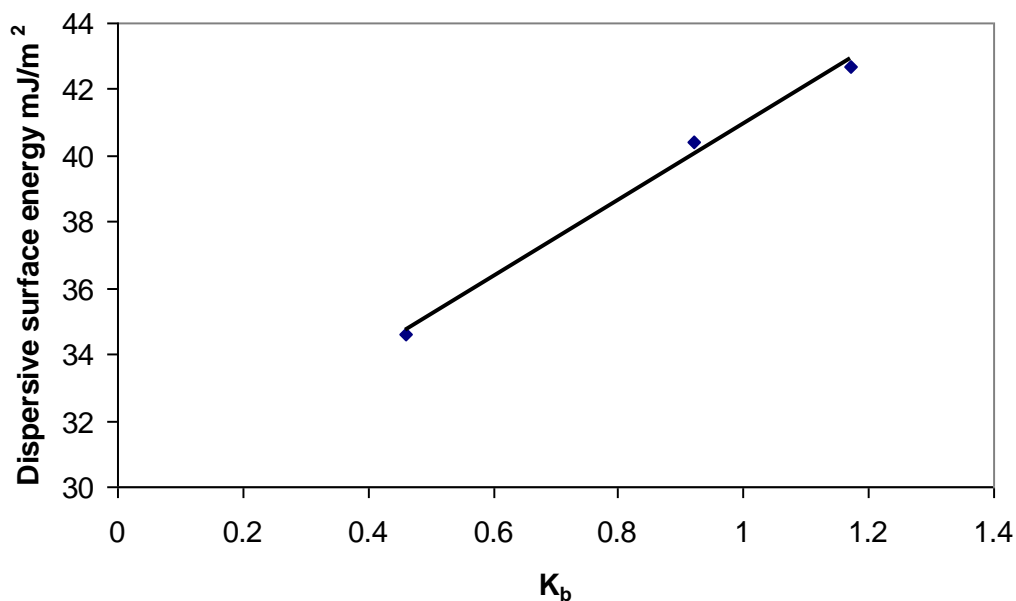
Figure 4.13. Dispersive surface energy as a function K_b of the extract, maple wood, and extracted maple wood R^2=0.99.

The difference in the electron acceptor surface character is not significant. A further analysis of the surface properties may give more insight into the nature of the wood and extract surface.

4.4.7.3 Diffuse Reflectance IR Analysis

Diffuse reflectance Fourier transform infrared spectroscopy (DRIFT) was performed on freeze-dried hot water extract samples. The powdered extract was mixed with KCL and infrared spectra were obtained after purging water from the infrared chamber for 2 hours.
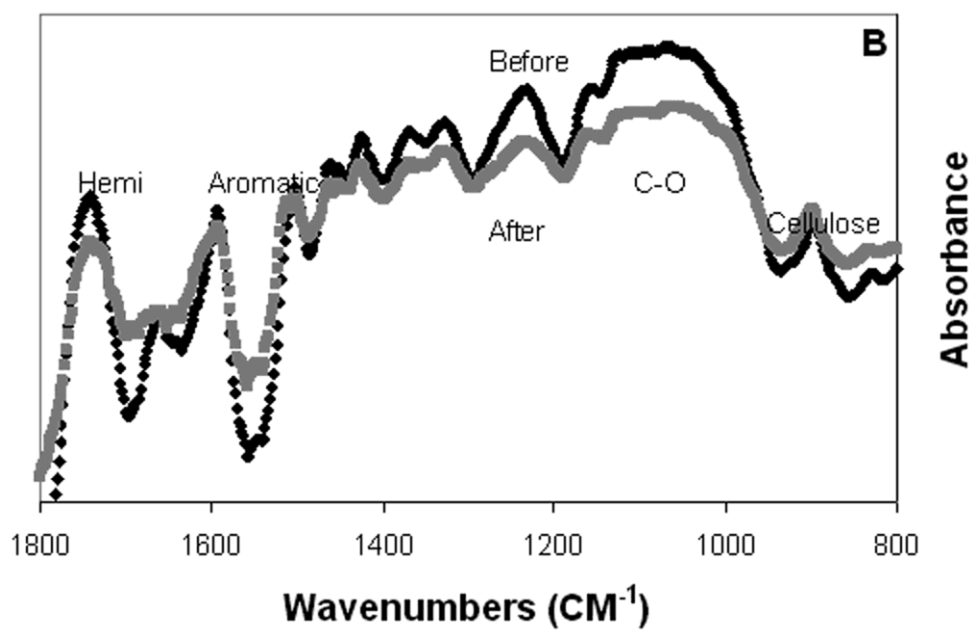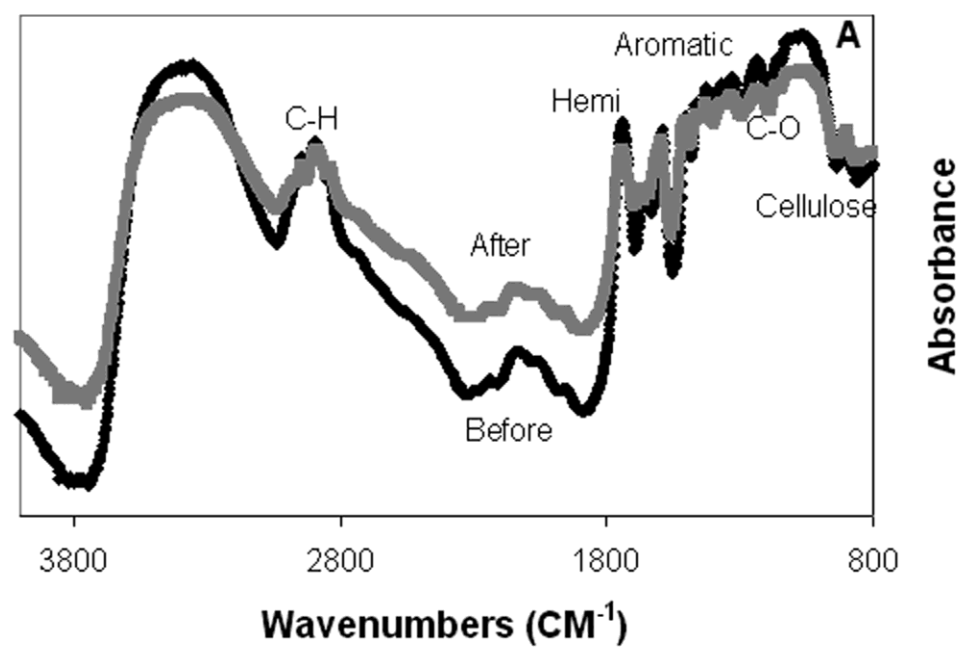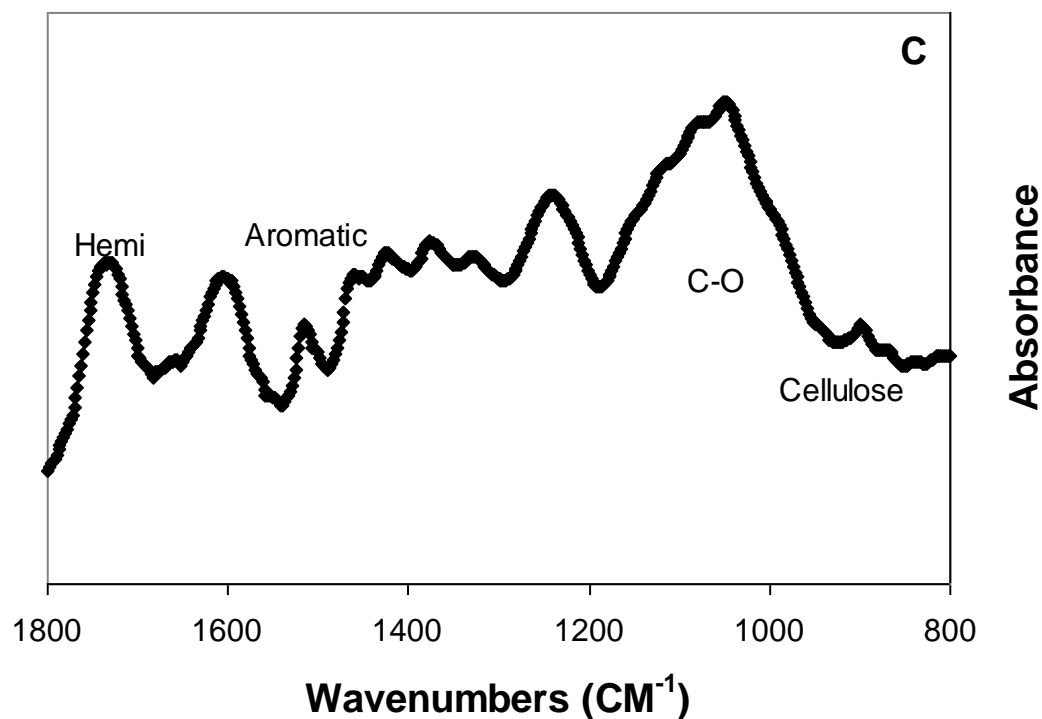
Figure 4.14. Drift spectra for A. maple before and after extraction 800 to 4000 cm^{-1}, B. wood before extraction and after extraction 800 to 1800 cm[-1,] C. hot water extract from 800 to 1800 cm^{-1}. All spectra are labeled "after" for after extraction, "before" for before extraction spectra, "Hemi" for hemicellulose, "C-H" for aliphatic C-H stretching, "Cellulose" for cellulose, "Aromatic" for lignin aromatic compounds in the wavenumber ranges corresponding to peaks due to those functional groups and compounds.

Grandmaison et. al.[71] used DRIFT spectroscopy with extracts of *Populus tremuloides* and in those spectra identify the IR ranges on wood surfaces due to various functional groups and chemical species. The IR ranges for the functional groups and chemical species on the surface are used here to analyze the maple wood before and after extraction. Figure 4.14A is an example of the overall spectrum seen for the maple wood before and after extraction. The rest of the analysis is focused on Figures 4.14B and 4.14C because the wavenumber range is most appropriate for analysis. From Table 4.4,

the composition of the extract contains hemicellulose, lignin and cellulose and these components should be seen in the DRIFT scans. The spectral region of 1450-1595 cm^{-1} has peaks that are attributed to the aromatic lignin. The large peak at 1505 cm^{-1} is due to the lignin aromatic ring vibration. The peak attributed to cellulose is at 895 cm^{-1} and for this peak the relative peak area in Figure 4.14B is larger for the maple wood after extraction then before extraction indicating that the surface concentration of cellulose for the maple increases with the removal of the extract. These findings should be compared to the results found by Paredes et. al.[54] who determined that extraction time increased the apparent crystallinity of the cellulose microfibrils. The peak attributed to hemicellulose is found at 1740 cm^{-1} and is seen before and after extraction of the wood, and in the extract. The 1740 cm^{-1} peak is the second largest peak after the peak at 1035 cm^{-1} attributed to the C-O bonds in all the polysaccharides, lignin alcohols and lignin ethers showing that hemicellulose is a macromolecule found in the extract and on the surface of the wood in large quantities. Schultz et. al.[72] developed DRIFT spectra regression equations for sweetgum, *Liquidambar styraciflua*, and white oak, *Quercus alba*, for percent glucose, percent xylose, and percent lignin as a function of absorbance peak ratios. These empirical relationships were used with the maple in this study to give a pseudo quantitative analysis of the wood surface before and after extraction.

Table 4.9. Calculation of surface concentration of xylan, glucose, and lignin using empirical relationships developed by Schultz et. al.[72]

	% xylan		% glucose		% lignin
Before extraction	17		61		27
After extraction	14		75		37

The concentrations calculated using the relationships developed by Schultz et. al.[72] show that there is a decrease in xylan concentration as glucose and lignin concentrations increase. A mass balance indicates that the concentrations add to more then 100 percent; however, considering these relationships were developed for sweetgum and white oak with an ability to rapidly determine lignocellulosic concentrations using DRIFT spectroscopy, the values may still be interpreted as giving an indication of the magnitude for the concentrations and the change in concentration on the surface due to extraction. The hot water extract itself has concentration values out of the range of the correlations found by Schultz et. al.[72] and no meaningful values were found analyzing the extract with the relationships.

Paredes et. al.[54] found that as extraction times increased, the surface energy of the wood increased and the apparent percent cellulose crystallinity of the surface increased. These findings would be consistent with removal of hemicellulose from the surface of wood due to extraction, consistent with both the quantitative and qualitative DRIFT analysis findings.

4.5 Conclusions

Fourteen different fiber types were tested using inverse gas chromatography. From these data, dispersive surface energies were calculated and compared and found to be between 35.5 mJ/m^2 and 44.2 mJ/m^2 for all the fiber types at 20°C. There is a clear association between the fiber composition and the measured dispersive energy levels at 40°C as was found by Spearman's rank correlation coefficient and is displayed in Figures 4.1 A, B, and C. The only large changes in the acid-base characteristics are seen in the extreme cases of cotton and kapok. This indicates that there may be a sizable amount of surface area of the fiber comprising hemicellulose as this component changes the least amount from fiber to fiber. The SEM micrographs show that the grass fiber group has a strongly structured surface with thick epicuticular wax layers on the surface. Bast fiber surfaces are generally smoother than the other fiber types. Fruit fiber types exhibit thin fibers. The leaf fibers abaca and sisal have very similar rippled surfaces with visible epicuticular wax and fat layers. The fibers with wax layers may need treatments to remove the surface wax for good cohesion in materials as the wax layers reduce the overall surface energy of the fiber and may act as a weak boundary layer. Mechanical interlocking being an important mechanism for adhesion is dependent on rough surfaces and may be an advantage for the fiber types that are not smooth. Fiber types with rippled surfaces may have an advantage for cohesion in materials both from mechanical interactions and chemical interactions as there is more surface area for both mechanisms of adhesion to contribute to the fiber matrix interactions.

Individual components of a material create a weighted average London dispersion component of the surface free energy characteristic for the material. This weighted

average includes the interactions of the individual components in the material with each other and follows a simple rule of mixtures. Since the last component to go into a SMC are the reinforcing fibers and the interactions between the fibers with the matrix are critical for proper mechanical reinforcement, the surface free energy for the composite after compounding is needed. The K_a and K_b for the SMC material is used to calculate the interaction parameter for fiber and sizing agents. Any fiber reinforcement to be used with the SMC material should have a high acidic character to maximize the matrix fiber interaction. The commercially available polyester sized glass reinforcement has the lowest interaction parameter as compared to the sized and unsized cellulosic fibers used in this analysis. Therefore, cellulosic fibers may have an advantage compared to glass for surface interactions with the matrix material.

The extraction yield using hot water at 160 ºC and 90 minutes was approximately 16%. The two major components in the extract were xylan (46.88%) and lignin (17.59%). The IGC technique determined a thermally stable dispersive surface energy of 34.6± 0.2 mJ/m^2 within one standard deviation of 0.4mJ/m^2.with a K_a of 0.13 and K_b of 0.46 for the hemicellulose-extract material. Red maple wood exhibited a surface energy of 42.7mJ/m^2 at 20°C after extraction and 40.4 mJ/m^2 before extraction at 20°C. Also, for the maple wood before extraction the K_a and K_b are 0.19, 0.92 and after extraction the K_a and K_b are 0.15, and1.17. The DRIFT scans of the extract, wood before, and wood after extraction closely resembled DRIFT scans of other wood samples found in the literature. The DRIFT scans before and after extraction reveals that there is a higher concentration of cellulose on the wood surface after extraction. The peaks found from the infrared analysis are consistent with the chemical analysis of the extract presented in Table 4.6.

4.6 References

1. Matuana L.M., Park C.B., Balatinecz J.J.," Cell morphology and property relationships of microcellular foamed PVC/wood-fiber composites" ; Polym. Eng. Sci., 38(5), 765-773, 1998

2. Woodhams R.T., Thomas G.," Wood Fibers as Reinforcing Fillers for Polyorefins"; Polym. Eng. Sci. 24, 1166-1171, (1984)

3. Kazayawoko M., Balatinecz J.J., Matuana L.M.," Surface modification and adhesion mechanisms in woodfiber-polypropylene composites"; J. Mater. Sci., 34, 6189-6199, (1999)

4. Matuana L.M., Woodhams R.T., Balatinecz J.J., Park C.B., "Influence of interfacial interactions on the properties of PVC cellulosic fiber composites"; Polym. Compos., 19(4), 446-455, (1998)

5. Tze W.T.Y., Wålinder M.E.P., Gardner D.J.," Inverse gas chromatography for studying interaction of materials used for cellulose fiber/polymer composites; J. Adhesion Sci. Technol. 20(8), 743-759, (2006)

6. Clemons C.M., Giacomin A.J., Koutsky J.A.," Dynamic fracture toughness of polypropylene reinforced with cellulose fiber"; Polym. Eng. Sci., 37(6), 1012-1018, (1997)

7. Lundqvist Å, Ödberg L.; "The Fundamentals of Papermaking Materials" vol 2, 1997

8. Jacob P.N., Berg J.C.," Acid-Base Surface-Energy Characterizatoin of Microcrystalline Cellulose and 2 Wood Pulp Fiber Types Using Inverse Gas Chromatography"; Langmuir, 10, 3086-3093, (1994)

9. Carvalho M.G., Santos J.M.R.C.A., Martins A.A., Figueiredo M.M," The effects of beating, web forming and sizing on the surface energy of Eucalyptus globulus kraft fibres evaluated by inverse gas chromatography."; Cellulose, 12, 371-383, (2005)

10. Boras L., Sjostrom, J.; International Symposium on Wood and Pulping Chemistry, Proceedings, ISWPC, v 2, p 9-1/9-4, (1997)

11. Chtourou, H.; Riedl, B.; Kokta, B.V." Surface Characterizations of Modified Polyethylene Pulp and Wood Pulp Fibers Using XPS and Inverse Gas Chromatography"; J. of Adhesion Sci. Tech., 9(5), p 551-574, (1995)

12. Holbery J., Houston D., "Natural-fiber-reinforced polymer composites in automotive. applications".; JOM, 58 (11), 80-86, (2006)

13. Bledzki A.K., Gassan J., " Composites reinforced with cellulose based fibres"; Prog. Polym. Sci. 24, 221-274, (1999)

14. Gulati D., Sain M., "Surface characteristics of untreated and modified hemp fibers"; Polym. Eng. Sci. 46, 269-273, (2006)

15. Simonsen J., Hong Z., Rials T.G., "The properties of the wood-polystyrene interphase determined by inverse gas chromatography"; Wood Fiber Sci. 29, 75-84 (1997)

16. Keller D.S., Luner P.; The fundamentals of Papermaking Materials; vol. 2, 911-954, (1997),

17. Nabarlatz D., Torras C., Garcia-Valls R., Montané D. Purification of xylo-oligosaccharides from almond shells by ultrafiltration, Separation and Purification Technology 53, 235-243 (2007)

18. A. Ebringerová Structural diversity and application potential of hemicelluloses, Macromol. Symp. 232, 1-12 (2006)

19. Ebringerová A., Heinze T. Xylan and xylan derivatives – biopolymers with valuable properties, 1, Macromol. Rapid Commun. 21, 542-556 (2000)

20. Yuan Q.P., Zhang H., Qian Z.M., Yang X.J. Pilot-plant production of xylo-oligosaccharides from corncob by steaming, enzymatic hydrolysis and nanofiltration, J. Chem. Technol. Biotechnol. 79, 1073-1079 (2004)

21. Garrote G., Cruz JM., Domínguez H., Parajó JC Valorisation of waste fractions from autohydrolysis of selected lignocellulosic materials, J. Chem. Technol. Biotechnol. 78, 392-398 (2003)

22. Vázquez M.J., Garrote G., Alonso J.L., Domínguez H., Parajó J.C. Refining of autohydrolysis liquors for manufacturing xylooligosaccharides: evaluation of operational strategies, Bioresource Technology 96, 889-896 (2005)

23. Montané D., Nabarlatz D., Martorell A., Torné-Fernández V., Fierro V. Removal of lignin and associated impurities from xylo-oligosaccharides by activated carbon adsorption, Ind. Eng. Chem. Res. 45, 2294-2302 (2006)

24. Browning B.L.,"Methods of wood chemistry", Ed. John Wiley & Sons. New York (1967).

25. Ass B.A.P.,. Ciacco G.T., Frollini E.," Cellulose acetates from linters and sisal: Correlation between synthesis conditions in DMAc/LiCl and product properties"; Bioresource Technology 97, 1696–1702, (2006)

26. Mazumdera B.B., Akiko Nakgawa-izumi b, Kuroda K., Ohtani a Y., Sameshima K.," Evaluation of harvesting time effects on kenaf bast lignin by pyrolysis-gas chromatography; Industrial Crops and Products 21, 17–24, (2005)

27. Bismarck, A., Mohanty, A.K., Aranberri-Askargorta, I., Czapla, S, Misra, M., Hinrichsen, G., Springer, "Surface characterization of natural fibers; surface properties and the water up-take behavior of modified sisal and coir fibers J. Green Chemistry, 3, 100–107, (2001)

28. Clemons, C. M.; Caulfield, D.F., "Natural Fibers", Chapter 11 of Functional Fillers for Thermoplastics, M. Xanthos, ed., Wiley-VCH Verlag GmbH & Co. KGaA, 195-206, (2005)

29. Dien B.S., Jung, H.G., Vogel K.P., Casler M.D., Lamb J.F.S., Weimer P.J., Iten L., Mitchell R.B., Sarath G.," Chemical composition and response to dilute-acid pretreatment and enzymatic saccharification of alfalfa, reed canarygrass, and switchgrass Biomass Bioenergy, 30(10), 880-891, (2006)

30. Franck, R.R. Overview. In: Franck, R.R. (ed.): "Bast and other plant fibres." Boca Raton, Boston, New York, Washington DC, CRC: 1-23. (2005).

31. Han, J.S. Properties of nonwood fibers. In: Proceedings of the Korean Society of Wood Science and Technology Annual Meeting, Seoul, Korea. The Korean Society of Wood Science and Technology, 3–12, (1998)

32. Hori, K., Flavier, M.E., Kuga, S., Lam T.B.K., Iiyama K.," Excellent oil absorbent kapok [Ceiba pentandra (L.) Gaertn.] fiber: fiber structure, chemical characteristics, and application "; J Wood Sci 46:401-404, (2000)

33. Hurter, A.M: Proceedings of TAPPI Pulping Conference 1988. New Orleans, LA, USA, Book 1: 139-160, (1988)

34. del Rıó, J. C.; Gutiérrez, A.," Chemical composition of abaca(*Musa textilis*) leaf fibers used for manufacturing of high quality paper pulps."; J. Agric. Food Chem. 54: 4600-4610 (2006)

35. Lam, T.B.T. Hori, K., Iiyama, K.," Structural characteristics of cell walls of kenaf (Hibiscus cannabinus L.) and fixation of carbon dioxide"; J Wood Sci 49:255–261 (2003)

36. Mwaikambo, L. Y.,” Review of the History, Properties and Application of Plant Fibers” African J.of Sci. and Tech. 7 (2): 120-133 (2006)

37. Mwaikambo, L. Y. Ansell , M. P.,” The determination of porosity and cellulose content of plant fibers by density methods”; 2001: J Mat Sci Letters 20, 2095 – 2096 (2001)

38. Nilsson, T.,” Microscopic studies on the degradation of cellophane and various cellulosic fibres by wood-attacking microfungi : Mikroskopiska undersökningar av vedangripande mikrosvampars nedbrytning av cellofan och olika cellulosahaltiga fibrer”; Studia Forestalia Suecica *117*, 1–32, (1974)

39. Rahman M.M., Khan, M.A., “Surface treatment of coir (Cocos nucifera) fibers and its influence on the fibers' physico-mechanical properties“ Composites Sci. and Tech. 67, 2369–2376, (2007)

40. Reddy N., Yang, Y., “Biofibers from agricultural byproducts for industrial applications”; Trends in Biotech. Vol.23 No.1: 22-27, (1999)

41. Reddy; N., Salam, A., Yang, Y., “Effect of lignin on the heat and light resistance of lignocellulosic fibers”; Macromol. Mater. Eng., 292, 458–466, (2007)

42. Rowell R.M., “A new generation of composite materials from agro-based fiber”; Proceedings of 3rd international conference on frontiers of polymers and advanced materials**;** January 16-20**;** Kuala Lumpur**,** Malaysia New York: Plenum Press; 1995.

43. Rowell, R.M., “Composite materials from agricultural resources.” In: Oleson, O., Rexen, F., Larsen, J. (eds.): Research in industria application of non food corps, I: plant fibres. Proceedings of a seminar; Copenhagen, Denmark, Lyngby, Denmark, Academy of Technical Science 27-41, (1995)

44. Rowell, R.M., Han1, J.S., Rowell, J.S., Characterization and Factors Effecting Fiber Properties. In: E. Frollini, A.L. Leão and L.H.C. Mattoso (eds). Natural Polymers and Agrofibers Composites, Sãn Carlos - Brazil - São Carlos: USP-IQSC / Embrapa Instrumentação Agropecuária / Botucatu: UNESP: 115-134, (2000)

45. Silva G.G., De Souza, D.A., Machado, J.C., Hourston, D.J.,” Mechanical and thermal characterization of native Brazilian coir fiber”; Journal of Appl. Polym. Sci., Vol. 76, 1197–1206 (2000)

46. Sun R.C., Fang J.M., Goodwin A., Lawther, J.M., Bolton A.J., ”Fractionation and characterization of polysaccharides from abaca fibre”; Carbohydrate Polymers 37, 351–359, (1998)

47. Thygesen A., Oddershede, J., Lilholt H. Thomsen A.B., Stahl K," On the determination of crystallinity and cellulose content in plant fibres" Cellulose; 12(6), 563–576, (2005)

48. Thygesen A., Daniel G., Lilholt H., Thomsen A.B.,"Hemp Fiber Microstructure and Use of Fungal Defibration to Obtain Fibers for Composite Materials"; Journal of Natural Fibers, 2(4), 19-37, (2006)

49. van Dam JEG, van den Oever MJA, Keijser, ERP, van der Putten J.C., Anayron C., Josol F., Peralta A.," Process for production of high density/high performance binderless boards from whole coconut husk - Part 2: Coconut husk morphology, composition and properties"; Ind. Crop Products 24, 96–104, (2006)

50. Ververis C, Georghiou K, Christodoulakis N, Santas P, Santas R., "Fiber dimensions, lignin and cellulose content of various plant materials and their suitability for paper production"; Ind Crop Product 19, 245–254, (2004)

51. Jeffree C.E., Baker E.A., Holloway P.J., "Ultrastructure and Recrystallization of Plant Epicuticular Waxes"; New Phytologist, 75(3), 539-563, (1975)

52. Ouajai S, Shanks RA, "Composition, structure and thermal degradation of hemp cellulose after chemical treatments"; Polymer degradation and stability, 89(2), 327-335: (2005)

53. Keller D.S., Luner P., "Surface energetics of calcium carbonates using inverse gas chromatography"; Colloids Surface A 161, 401–415, (2000)

54. Parades J., Mills R, Gardner D., Shaler S.," Surface Characterization of Red Maple Strands After Hot Water Pre-Extraction"; Wood and Fiber Sci. 41(1), 28-50, (2009)

55. Mills R., Jara R., Gardner D., van Heiningen A.," Inverse gas chromatography for determining the surface free energy and acid-base chemical characteristics of a water extracted hardwood (*Acer rubrum*)" ;J. Wood Chem. and Tech. 29: 11–22, (2009)

56. Forest Products Laboratory; "Wood Handbook, Wood as an Engineered Material"; Forest Products Society, pp. 9-1-9-5, (1999)

57. Christiansen A.W.," How Over-drying Wood Reduces its Bonding to Phenol-Formaldehyde Adhesives - A Critical Review of the Literature .1. Physical Responses; Wood Fiber Sci., 22, 441-459, (1990)

58. Back E.L.," Oxidative Activation of Wood Surfaces for Glue Bonding"; Forest Prod. J. 41(2) 30-36, (1991)

59. Gulati D., Sain M.," Surface characteristics of untreated and modified hemp fibers"; Polymer Eng. and Sci. 46, 269-273, (2006)

60. Reutenauer S., Thielmann F., "The characterisation of cotton fabrics and the interaction with perfume molecules by inverse gas chromatography (IGC)"; J. Mater. Sci., 38, 2205-2208, (2003)

61. Tshabalala M.A., " Determination of the acid-base characteristics of lignocellulosic surfaces by inverse gas chromatography; J. Appl. Polym. Sci., 65, 1013-1020 (1997)

62. Bismarck A, Mohanty AK, Aranberri-Askargorta I, Czapla S, Misra M, Hinrichsen G, Springer J, " Surface characterization of natural fibers; surface properties and the water up-take behavior of modified sisal and coir fibers"; Green Chemistry, 3(2), 100-107, (2001)

63. Price G.J., Ansari D.M., "Surface modification of calcium carbonates studied by inverse gas chromatography and the effect on mechanical properties of filled polypropylene"; Polym. Int. 53, 430–438 (2004)

64. Qin R.Y., Schreiber H.P., "Application of Invese Gas Chromatography to Molecular-Diffusion in Polymers"; Langmuir, vol 10, No. 11, 4153-4156, (1994)

65. Santangelo P.G. , Roland C.M., Chang T., Cho D., Roovers J., "Dynamics near the glass temperature of low molecular weight cyclic polystyrene"; Macromolecules, 34, 9002-9005, (2001)

66. Tze W.T.Y; "Effects of fiber/matrix interactions on the interfacial deformation micromechanics of cellulose-fiber/polymer composites"; PhD Thesis, University of Maine, August 2003

67. Dutschk V., Mäder E., Rudoy V., "Determination of polarity parameters for glass fibres by inverse gas chromatography: Some results and remarks"; J. Adhes. Sci. Technol., Vol. 15, No. 11, 1373–1389 (2001)

68. Park S.J., Kim T.J., "Studies on surface energetics of class fabrics in an unsaturated polyester matrix system: Effect of sizing treatment on glass fabrics"; J. Appl. Polym. Sci., 80, 1439–1445 (2001)

69. Tze, W.T.Y, Wålinder M.E.P., Gardner D.J., "Inverse gas chromatography for studying interaction of materials used for cellulose fiber/polymer composites"; J. Adhes. Sci. Technol., 20(8), 743-759, (2006)

70. Gardner, D. J., M. P. Wolcott, L. Wilson, Y. Huang, and M. Carpenter. "Our understanding of wood surface chemistry in 1995." In: Wood Adhesives Proceedings No. 7296, Forest Products Society, CityplaceMadison, StateWI., 29-36 (1995)

71. Grandmaison J.L., Thibault J., Kaliaguine S., Chantal P.D. Fourier-transform infrared spectroscopy and thermogravimetry of partially converted lignocellulosic materials; Anal. Chem. 59, 2153-2157 (1987)

72. Schultz T.P., Templeton M.C., McGinnis G.D. Rapid determination of lignocellulose by diffuse reflectance fourier transform infrared spectroscopy; Anal. Chem. 67, 2867-2869 (1985)

5. DMTA STUDIES OF SYNTHETIC, KENAF, AND HOT WATER EXTRACT BASED SHEET MOLDING COMPOUND

5.1 Chapter Summary

SMCs used for automotive parts have upwards of a 10 year service life; therefore, studies on SMC material changes with time and environmental exposure are of interest. In the current study, hygrothermal aging is used to accelerate normal environmental aging and dynamic mechanical thermal analysis (DMTA) is used to study the mechanical and chemical changes as a function of temperature and aging time. Results from the current study show through high performance liquid chromatography (HPLC) analysis that polyvinyl acetate (PVAc) does not appear to chemically react with water in the SMC material. DMTA data demonstrate that water has two functions in what is referred to as the "thickening reaction" for SMC. Kenaf and hot water extract-based SMC's were made without addition of a thickening reagent and DMTA data for the kenaf-based SMC indicates that the thickening reaction for SMC may occur without a metal oxide thickening agent. Water uptake for kenaf-based SMC was much greater, approaching 20 weight percent, compared to standard SMC in the range of 1 to 2 weight percent gain. Hot water extract-based SMC exhibited water uptake comparable to standard SMC in the 1 to 2 weight percent range and the extract appears to have a viscoelastic relaxation in the SMC from -10°C to 5°C.

5.2 Introduction

To obtain a better understanding and develop experience with the material properties of standard glass reinforced SMC, initial work was performed which replicated studies reported in the literature. Then the research work was extended to compare the properties and performance characteristics of SMC fabricated using biobased fiber reinforcement with glass reinforced SMC. Hygrothermal aging analysis was previously done using a class A SMC and, in the current work, the experimental protocols followed in prior research were used in the analysis of the various SMC formulations.

SMC in the initial study was a material comprised of an unsaturated polyester resin, PVAc low profile additive, MgO thickening agent, $CaCO_3$ filler, peroxide catalyst, and zinc stearate mold release agent. SMC has been used for some time in the automotive and building product industries. The mechanical properties of the composite may be engineered through changes in the relative percentages of the components. However, since most service applications for SMC are external and the material is exposed to heat and moisture variations over long periods of time, the aging properties are highly relevant.

After making and testing a standard SMC composite, an experimental protocol, based on previous research, was developed and applied to a standard glass SMC, a kenaf reinforced SMC, and a glass reinforced SMC with a hot water extract additive to replace some low profile additive and filler. Subsequently, the different SMC formulations were subjected to the hygrothermal aging tests followed by DMTA testing and comparisons were made among the standard and biobased SMCs .

Kenaf, glass, and glass with hot water wood extract SMCs in this study have a polymer matrix comprised of an unsaturated polyester resin, poly styrene low profile additive, $CaCO_3$ filler, peroxide catalyst, and zinc stearate mold release agent.

The kenaf-based SMC contained 15 weight percent bast kenaf fibers as reinforcement and the extract-based SMCs replaced the low profile additive and filler components in a SMC composite with a hot water extract from hardwood that is described in Chapter 4. The DMTA and hygrothermal aging results are used to compare the SMC fabricated with a kenaf fiber reinforcement to a 15%, 30% glass-based SMC and to a 30% glass-based SMC with 1.5% or 8.5% hot water extract in the matrix material. Kenaf- and glass-based SMC were compounded and hand made at the University of Maine Advanced Engineered Wood Composites Center (AEWC) by adding glass to prepreg polyester with varying concentrations of extract in the SMC prepreg, and then cross-linked by heat and pressure treatment.

SMC composites are known to develop microvoids when exposed to humidity and can deteriorate over time in humid environments[1, 2]. Previously, DMTA analysis was used to study class A SMC that had been exposed to hygrothermal aging[3]. Results from the previous studies indicated that PVAc was hydrolyzed to poly(vinyl alcohol) (PVOH) and water is necessary for the reaction of carboxylic acid functional groups and MgO. These findings are evaluated in the current study and new findings are presented.

5.3 Experimental Procedures

Experimental procedures were presented in Chapter 3 section 1. Briefly, synthetic and biobased SMCs were aged by soaking in water at 70°C for 3 hours, 168 hours, and 1032

hours.   After aging, the water absorption and micromechanical properties were determined.   For synthetic SMC, HPLC was performed on the aging solution to determine if components of the SMC leached into solution during aging.

5.4. Results and Discussion

5.4.1 Water uptake as a function of time

After polishing, the samples were aged and water uptake was gravimetrically determined as a function of time.
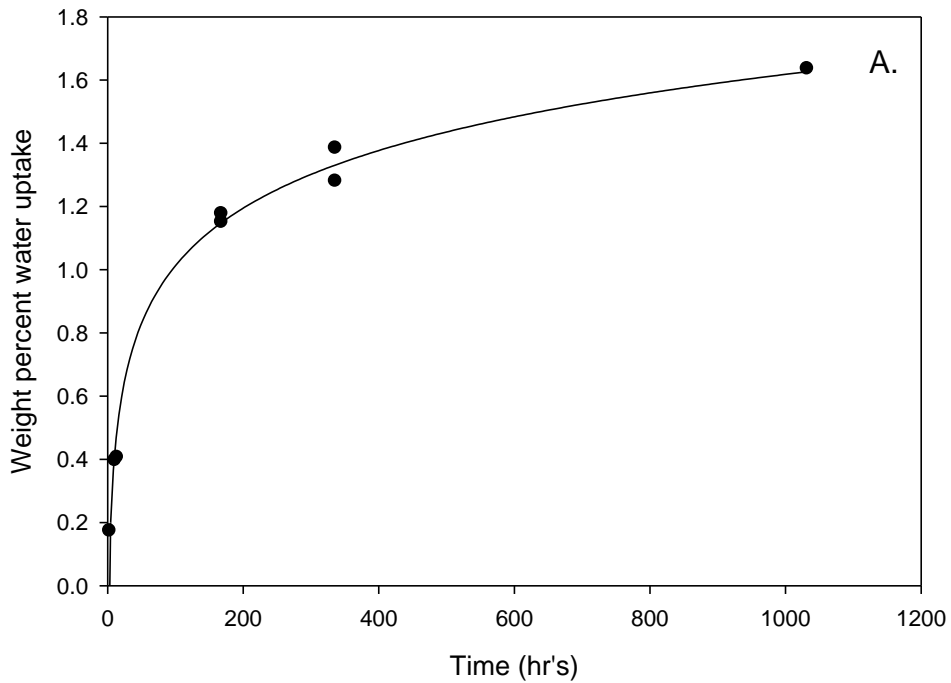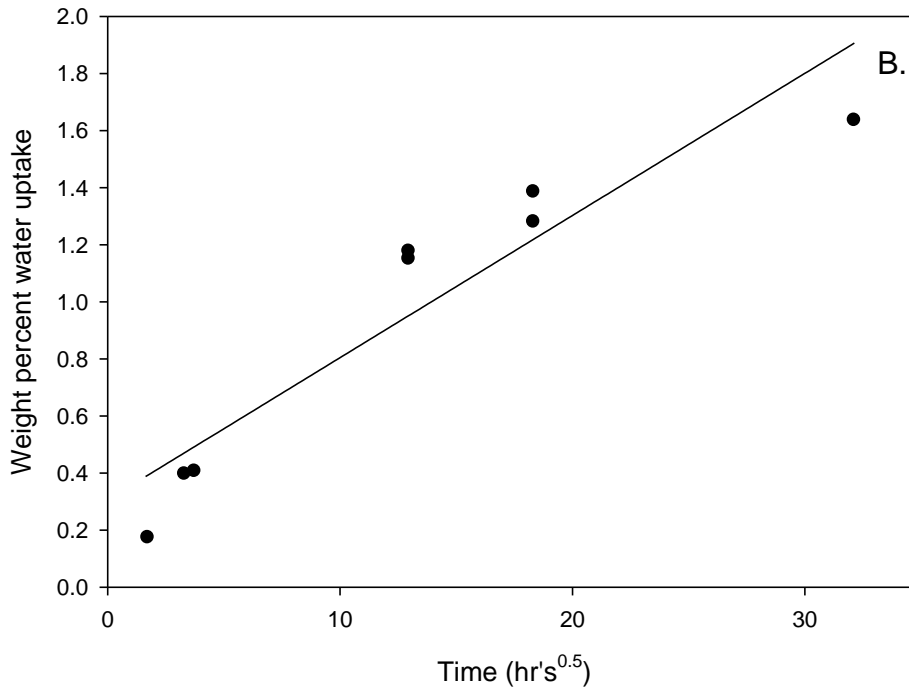
Figure 5.1. Dry weight percent water uptake during aging, A. as a function
of time, and B. as a function of the square root of time.

Water sorption for the material approaches saturation at 1032 hours of aging and the

sorption has a behavior agreeing with previous diffusion studies of SMC material (Fig

5.1.). Equation 1 is used to determine the diffusion coefficient for the SMC [4].

$$M = M_m \left[\frac{4}{\pi} \sqrt{\frac{Dt}{e^2}} \right] \qquad (1)$$

Where M is the mass of water absorbed, M_m is the mass at saturation, D is the diffusion

coefficient and e is the thickness of the material. The diffusion coefficient was calculated

to be 8.64×10^{-13} m^2/s and is within reasonable agreement with the diffusion coefficient of

9.44×10^{-13} m^2/s reported for a glass reinforced polyester composite[4].

5.4.2 Material storage modulus response
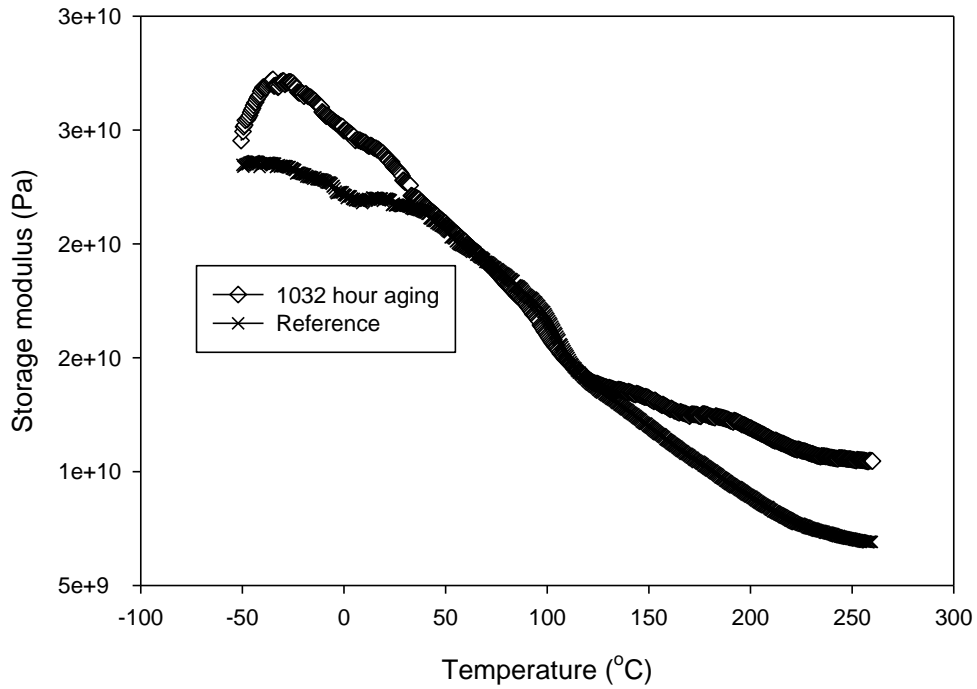
Figure 5.2. Storage modulus for reference ✕ and 1032 hr aged sample ◊

Patlan et. al. reported that the storage modulus of the SMC material doesn't change with aging in magnitude, but the glass transition peaks change. Thus, the changes in the tan δ peaks are determined to understand the changes occurring in the material as a function of aging time.

5.4.3 DMTA repeatability
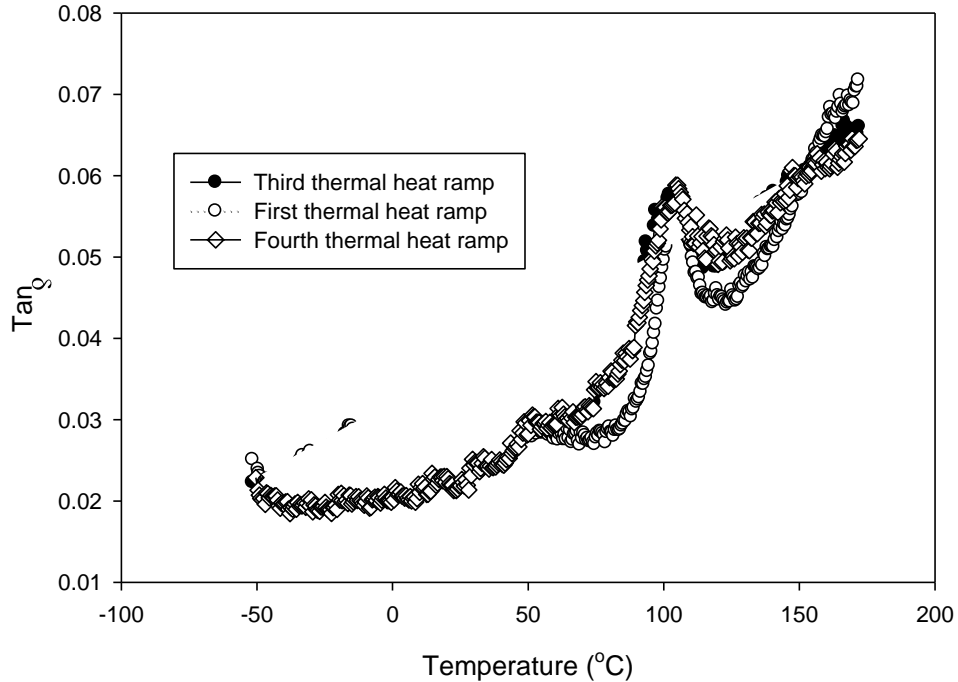
Figure 5.3. Multiple DMTA thermal ramps on the same SMC sample, Initial heat ramp, O third heat ramp,■, fourth heat ramp, ◊.

Multiple heat ramps with the DMTA were performed on the same SMC sample to establish the reproducibility of the DTMA data (see Fig 5.3). Each DMTA temperature ramp and scan has a slightly different tan δ in magnitude, but show the same glass transition peaks for the individual components in the composite. By running a series of temperature ramps on one sample, presumably all the water and volatiles in the sample should have volatilized out of the material producing a reproducible DMTA scan. In Figure 5.3 the third and fourth DMTA scans performed on the sample are nearly identical and lack some of the tan δ peaks seen in the first scan. This behavior has been seen in wood materials before[5], and the exact mechanism for the disappearance of the tan δ peaks

is not known. However, for the purposes of determining reproducibility, the third and fourth temperature ramps on the sample have nearly identical tan δ scans and demonstrate the reproducibility of DMTA.

5.4.4 DMTA glass transition analysis

Table 5.1. Glass transition peak temperatures and temperature ranges for metal oxide complex, low profile additive PVAc and PVOH, unsaturated polyester resin, and the crosslinked polyester network comprising the basis of the DMTA analysis.

Temperature °C	Temperature Range °C	Chemical pertaining to Tan Delta peak
25	15-35	$RCOOH-Mg^{2+}-HOOCR$, [3]
50	45-55	Poly(vinyl acetate), [3]
85	80-90	Poly(vinyl alcohol), [10]
110	100-120	Unsaturated polyester, (UPE), [6]
150-250	140-260	Cross linked polyester network, (PE), [3]

Table 5.1 shows the glass transition temperatures identified for different components in the SMC based on results from the literature. As was described in section 2.4, the T_g determined from DMTA is a range and not a single value; therefore, the temperature ranges for the peaks in the DMTA analysis are listed in Table 5.1.
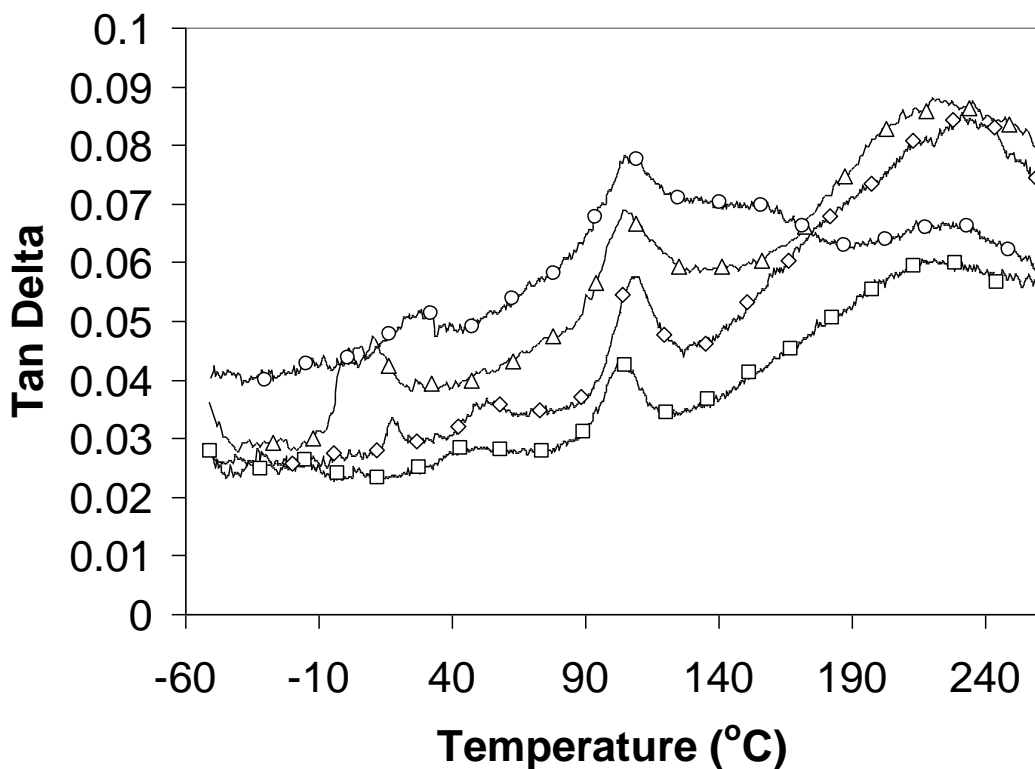
Figure 5.4.   Tan δ for initial synthetic reference and aged samples used to develop experimental protocol, reference ◊, 3hour age □, 168 hour age Δ, and 1032 hour age o for glass transition comparison.

In Figure 5.4, tan δ scans are presented for the standard synthetic reference SMC. Previously, Mendoza-Patlan *et al.* proposed that the new peak formed in the range of 15-35°C represented a metal carboxylic acid functional complex formed by the interaction of the metal oxide with the carboxylic functional groups of the polyester[3]. This peak is also observed with the SMC material in this study (Figure 5.4).   However, where the previous researchers saw only the peak after aging, in this study the peak was found for samples that experienced no accelerated aging.   In Figure 5.4, the 15-35°C peak is obvious for the reference and 168 hour aged sample.   The 15-35°C peak is seen for the 1032 hour aged

peak with the peak maximum slightly shifted up in temperature compared to the reference and 168 hour aged sample. This behavior of peaks moving upwards in temperature has been seen and reported during hygrothermal aging[4] and is caused by hydrolysis and plasticization of the matrix over long aging times. There may be a peak for the 3 hour aged sample, but this is very difficult to discern in the DMTA scan. The peaks for the reference and 3 hour aged samples are much smaller compared to the 168 and 1032 hour aged samples. Even though DMTA is not being used quantitatively for this analysis, the much larger peaks for the longer aged samples may be indicative of a larger concentration of the metal oxide species. The proposed mechanism for metal oxide coordination with the polymers reported by Mendoza-Patlan *et al.* was first presented by Vansco-Szmercsanyi *et al.* [,7,8,9,10]. This mechanism requires water to initiate the formation of the metal carboxylate and they report only minute traces of water are necessary to initiate the reaction. Mendoza-Patlan *et. al*. dried their sample in the range of 68°C to 72°C[3] and in the present study the samples were dried at 103°C to achieve constant weight to the one thousandth of a gram as Mendoza-Patlan *et. al*[3] did using a calibrated analytical balance capable of measurements to the one ten thousandth of a gram. The increased drying temperature was used to drive off all the water to inhibit the thickening reaction. Even with all the samples dried to constant weight at 103°C the peak at 25°C is still apparent as is seen in the reference scan in Figure 5.4. The peak present in the reference scan may indicate that some water may still be bound in the material. One difference between the samples used in the work of Mendoza-Patlan *et al.*[3] and the samples in the present study is the presence of unsaturated polyester after cross-linking indicating that there is more mobility in our samples. Vansco-Szmercsanyi

86

et al. [7,8,9,10] reported that only trace amounts of water were necessary to initiate the metal carboxylate reaction and the thickening reaction should take place unless the metal carboxylate complex isn't mobile enough to form the proper geometry for the reaction to occur. By aging the SMC in solution, the polymers may orient with the metal oxide over time in such a way so that the thickening reaction takes place. As the samples in this study have more mobility, less water would be necessary to allow the proper geometry to be formed for the functional groups to react with the metal oxide. This may explain the difference between the results of Mendoza-Patlan *et al.*[3] and the results presented here. Therefore, water is necessary for both the reaction to take place and also contributes to increased molecular mobility in the SMC material allowing for proper molecular orientations.

Mendoza-Patlan *et al.* also reported that PVAc was hydrolyzed to PVOH and acetate during aging. To investigate this further, the SMC aging solution was analyzed by HPLC analysis. One aging solution was used to age all samples to maximize the concentration of chemicals leached from the SMC during aging to maximize the probability of detection by HPLC.

5.4.5 HPLC analysis
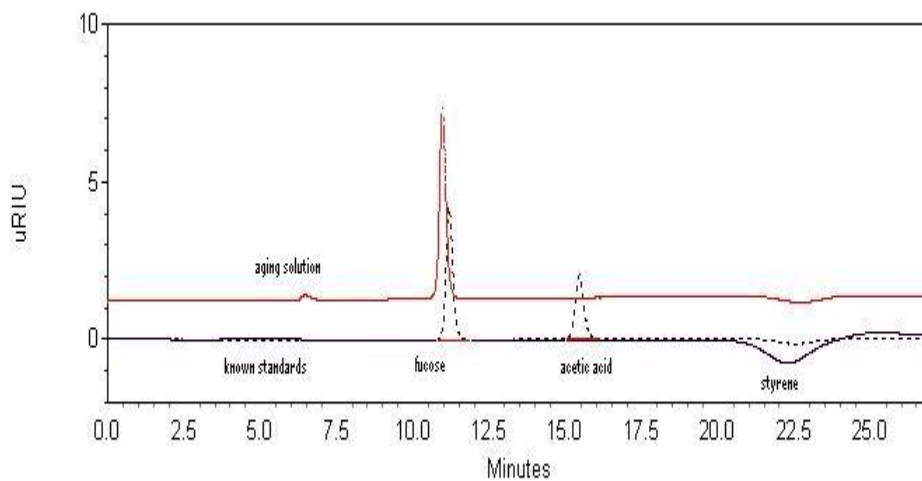
Figure 5.5. HPLC scan of aging solution for SMC, fucose and acetic acid, and styrene (Analysis by Sara Walton, graduate research assistant, Chemical Engineering, University of Maine).

In Figure 5.5, two HPLC scans are presented with the top scan being the aging solution and the bottom scan showing known references for comparison. In the scan labeled "aging solution", in Figure 5.5, three peaks are seen at 6.5 minutes, 10.8 minutes, and an inverted peak at 22.5 minutes. The standard samples are in the lower scan labeled, "known standards", in Figure 5.5 to compare with the aging solution. If polyvinyl acetate is converted to polyvinyl alcohol, acetic acid should be produced. Two peaks are seen with fucose at 10.9 minutes and acetic acid at 15.2 minutes. The acetic acid peak at 15.2 minutes doesn't correspond to any of the peaks in the aging solution indicating that acetic acid is not present in the aging solution. Based upon the composition of the SMC, styrene was hypothesized to be one of the chemicals leaching from the SMC during

aging. An inverted peak at 22.5 minutes is seen for the styrene. Comparison with the chromatograph of the aging solution therefore suggests that styrene is one of the molecules being leached out of the SMC. The other two peaks in the aging solution are still unidentified but are thought to be PVAc and residual or unreacted polyester, as these molecules may have a retention time similar to fucose. A HPLC chromatograph was not generated for PVAc because the exact PVAc used in the composite was not available. However, the decrease in intensity for the PVAc glass transition peak from DMTA analysis seen in both Mendoza-Patlan *et al.*[3] and the current investigation during aging would be consistent with PVAc being leaching from the SMC during aging. Further analysis of the DMTA curves shows no glass transition peak for PVOH, the product of the hydrolysis of PVAc. Glass transition peaks for PVOH in DMTA analysis have been determined to be in the range of $85°C$[11]. Analysis of Mendoza-Patlan *et al*[3]. DMTA curves also show no glass transition peaks for PVOH.

5.4.6 Kenaf-based SMC

The kenaf-based SMC experimental procedures followed the synthetic SMC procedures developed for the hygrothermal aging of SMC composites and are presented in Chapter 3 section 1.

5.4.6.1 Kenaf-based SMC water uptake as a function of time
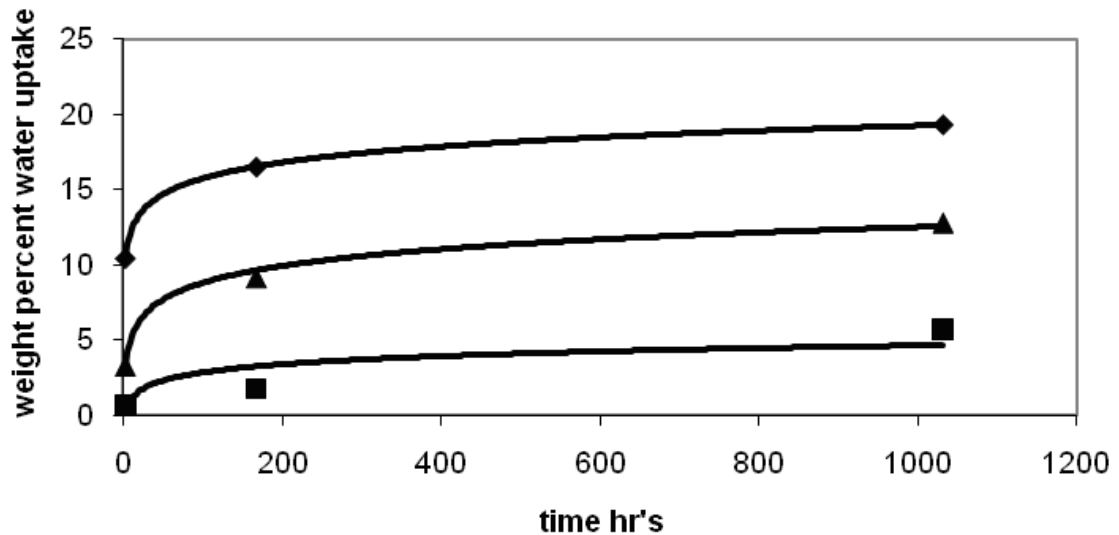
Figure 5.6. Dry weight percent water uptake during aging; ■ is 15 wt percent glass SMC, ▲ is 15 wt percent SMA treated Kenaf SMC, and ◆ 15 wt percent untreated Kenaf SMC.

In Figure 5.6 the water uptake of 15 weight percent glass, kenaf-based and SMA kenaf reinforced SMC's are compared. Only single experiments were performed for the kenaf-based SMC samples as experimental difficulties made it problematic to fabricate multiple test samples where duplicates were run for some samples with the standard SMC, see Figure 5.1. The kenaf-based SMC's absorbed an order of magnitude more water, 10% to 20%, compared to the standard reference SMC with a 1% to 2% water uptake (see Figure 5.1) and the 15 wt% glass standard SMC approaching 5% water uptake. The un-sized kenaf-based SMC had the greatest uptake of water approaching 20 weight percent of the

material. The SMA-sized kenaf-based SMC approached 15 weight percent water uptake in the same amount of time indicating that the SMA sizing may promote better bonding in the network and/or make the material more hydrophobic. The hollow structure of the bast fiber likely introduces a conduit by which the water may directly access the inner polymeric network of the composite. The 15 weight percent glass also absorbed more water, approaching 5 weight percent of the material. On visual inspection, there appeared to be more voids in the 15 wt% glass SMC and this may be due to the lower content of reinforcement in the SMC.

5.4.6.2 Kenaf-based SMC DMTA glass transition analysis

The DMTA analyses of the samples subjected to different aging times for the 15-weight percent glass reinforcement SMC is shown in Figure 5.7.
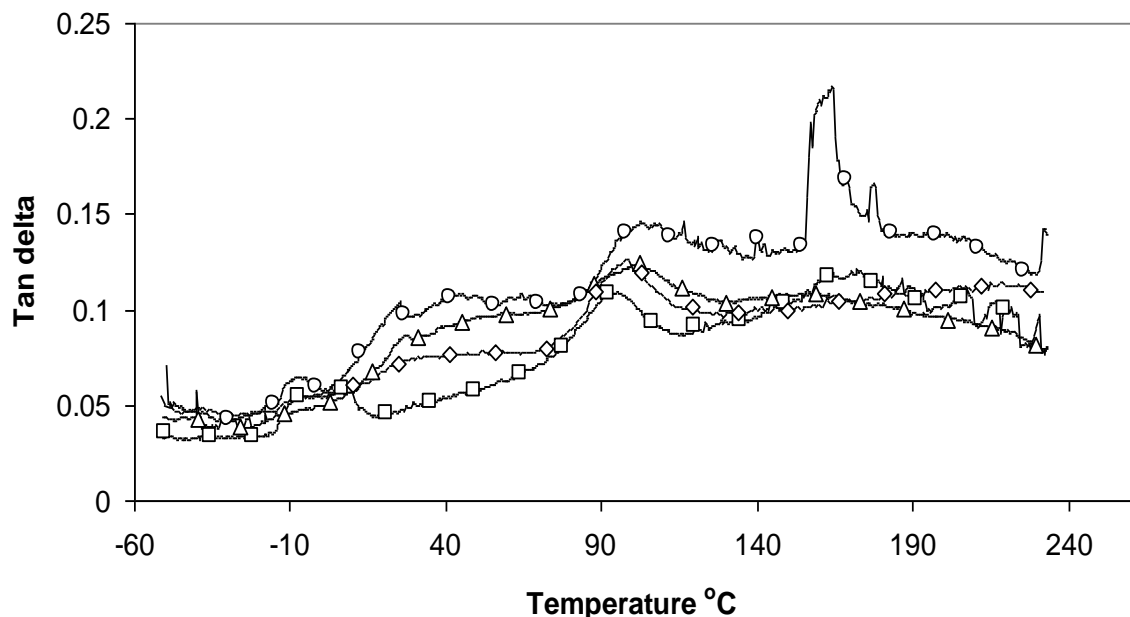
Figure 5.7. Tan δ for reference and aged samples, reference □, 3 hour age Δ, 168 hour age ◊ and 1032 hour age o for glass-based SMC at 15-weight percent glass reinforcement.

In Figure 5.7, tan δ for a 15 weight percent SMC is presented to be used as a reference for comparison with a 15 weight percent kenaf reinforced SMC. The scans show a T_g peak in the 100-120°C temperature range as one peak where the polystyrene[12] and unsaturated polyester T_g overlap. The peak for the cross-linked matrix at 140-260°C shows an increase with aging time and this increase in peak intensity may be due to water creating a more viscous response for the cross-linked network corresponding to an increase in the loss modulus and the tan δ as the tan δ is the ratio of the loss modulus to the storage modulus[3] and as the loss modulus increases and the storage modulus decreases the tan δ increases. Interestingly, peaks start to appear in the 1032 hour age sample in 15-35°C range where Mendoza-Patlan et al.[3] proposed a peak is formed for the thickening reaction described in section 2.4 and also at 0°C.
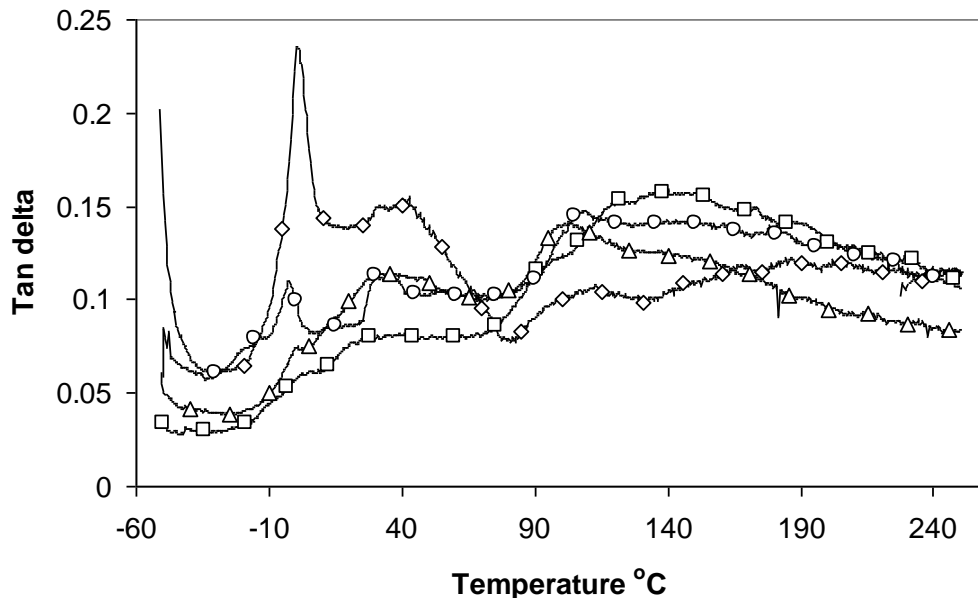
Figure 5.8. Tan δ for reference and aged samples, reference □, 3 hr Δ, 168 hr o and 1032 hr ◊ for kenaf-based SMC at 15 weight percent kenaf reinforcement.

In Figure 5.8, T_g peaks are seen as described in Table 5.1. However, a new sharp peak at 0°C is also apparent. The metal carboxylic acid functional complex produces a peak in the range of 25°C[3] as was observed for the standard SMC. This peak is also observed with the SMC material in this study. However, there is no thickening agent in this polyester prepreg material. The proposed mechanism for the metal oxide coordination mechanism requires a minute amount of water to initiate the formation of the metal carboxylate. Since there is no thickening agent in this material and there is a large uptake of water into the material with the proposed mechanism being a complexation reaction, a reasonable conclusion is that water by itself, in large enough concentration, can cause the thickening reaction in SMC. Also, a new peak appears at 0°C. Considering the large amount of water that is being absorbed by the material, a reasonable conclusion would be that there is free water in the material that freezes and melts at 0°C creating a sharp peak.
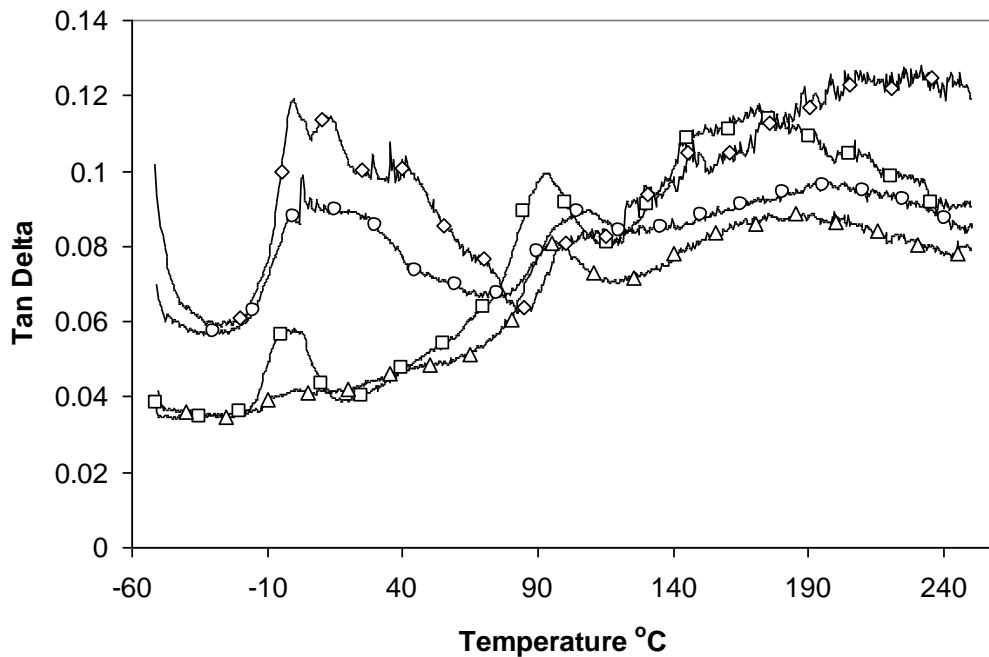
Figure 5.9. Tan δ for reference and aged samples, reference □, 3 hr △, 168 hr o and 1032 hr ◊ for 2% SMA sized kenaf-based SMC at 15 weight percent SMA sized kenaf reinforcement.

In Figure 5.9, T_g peaks are seen as described in Table 5.1. As with Figure 5.8, the peak at 25°C is present and a peak at 0°C that dramatically increases in intensity is seen. The overall intensities are lower in magnitude for Figure 5.9 compared to Figure 5.8 hypothesized to be due to a smaller amount of water absorbed as a result of SMA sizing as seen in Figure 5.6. Figures 5.7, 5.8, and 5.9 demonstrate the dominating impact water has on the micro-mechanical properties of kenaf-based SMC.

5.4.7 Extract-Based SMC

5.4.7.1 Extract SMC Water uptake as a function of time
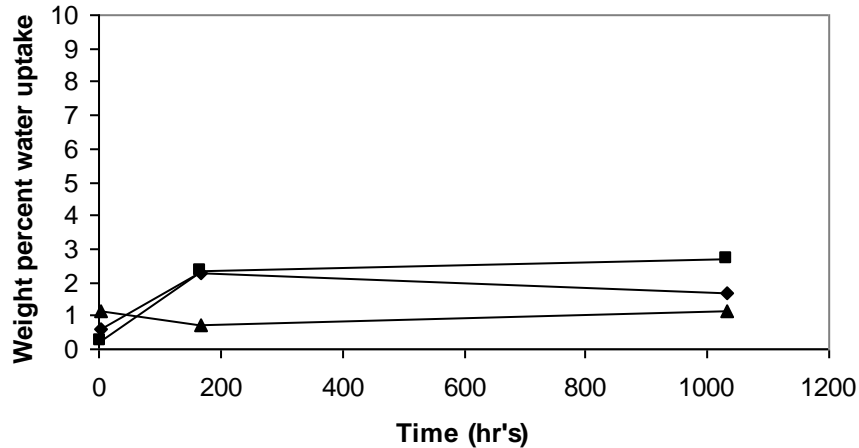
Figure 5.10. Dry weight percent water uptake during aging; ◆ is 30 wt percent glass SMC, ▲ is 30 wt percent glass with 8.5% wood extract-based SMC, and ■ 30 wt percent glass with 1.5% wood extract-based SMC.

In Figure 5.10 the water uptake for the hot water maple wood extract-based SMC is presented. For the extract-based SMCs, one sample was used to generate the water uptake data as material quantity limitations made it problematic to fabricate multiple test samples.   The 1.5%, 8.5% hot water maple wood extract SMC's, and standard SMC absorbed the similar amounts of water in a close range around 1 to 2 weight percent water after 1032 hours of aging corresponding to the values found in section 5.1 for the B-stage SMC supplied by AOC resins, see Figure 5.10. Compared to the kenaf-based SMC where water uptake approaches 20 weight percent after 1032 hours of aging, there appears to be no impact on the water absorption of the SMC by substituting components in the SMC with hot water maple wood extract.

All of the DMTA peaks for the wood extract-based SMCs are the same as the peaks presented in Table 5.1 except that one new peak was apparent in the scan. A wide peak in the range of -10°C to 5°C is seen for all the SMC samples and may be attributed to a hemicellulose relaxation in the material that isn't seen with the standard glass samples.

5.4.7.2 DMTA Analysis for hot-water extract and 30% glass reference SMC.
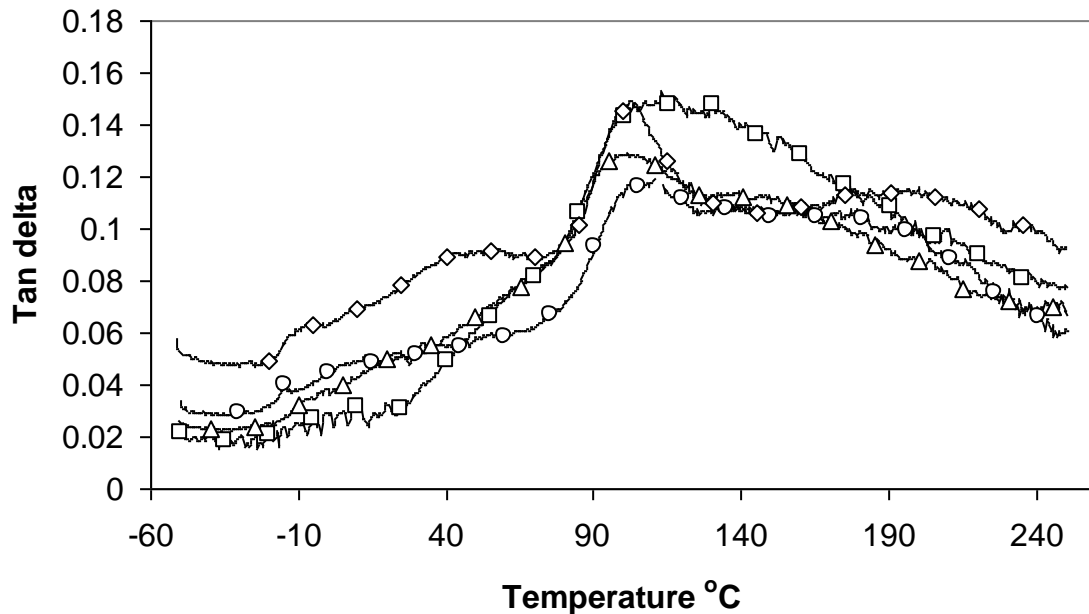
Figure 5.11. Tan δ for reference and aged samples with standard 30% glass reinforced SMC with polyester pre-preg matrix used for the hot water extract and kenaf-based SMCs, reference □, 3 hr Δ, 168 hr o and 1032 hr ◊.

In Figure 5.11, the DMTA scans are presented for a 30% glass-based SMC reference. In all of the scans there were no apparent tan delta peaks from the complexed species attributed to the thickening reaction as there is no thickening agent in this material and there is an uptake of water by the SMC, and that result is consistent with the SMC presented in sections 5.1-5.4. This result supports the proposed water dependent

mechanism for the complexation reaction. The peaks for the polystyrene, unsaturated polyester, and cross-linked matrix are again the same as Table 5.1.
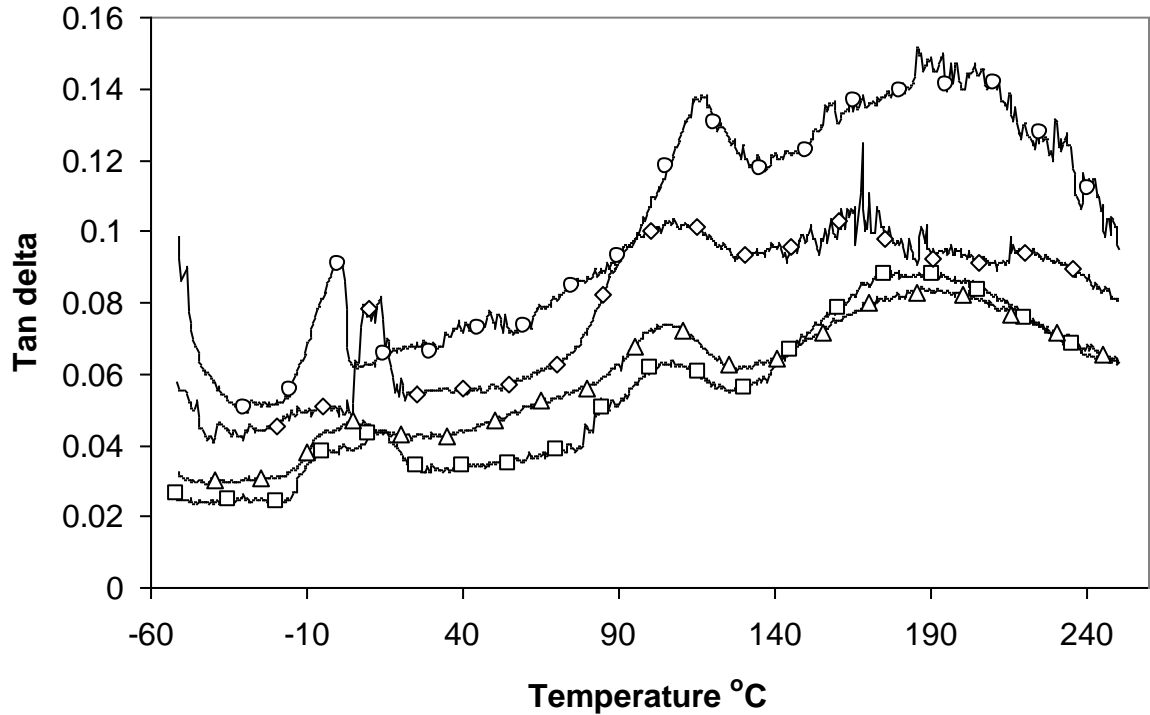
Figure 5.12. Tan δ for reference and aged samples, reference □, 3hr Δ, 168 hr ◊ and 1032 hr o; for 1.5 weight percent hot water extract based SMC at 30 weight percent glass reinforcement.

In Figure 5.12, the tan δ scans for 1.5 weight percent hot water extract SMC is presented. DMTA analysis of the 1.5 weight percent hot water extract based SMC indicates that a new peak is formed in the range from -10°C to 5°C. Considering that the only difference between the reference SMC in Figure 5.11 and the SMC in Figure 5.12 is the hemicellulose extract, and having similar water uptake as the standard reference, see Figure 5.10, a reasonable conclusion would be that the extract might have a relaxation in

that temperature range.   The viscoelastic peak response for the polystyrene, unsaturated

polyester, and cross-linked matrix are in accordance with literature values.
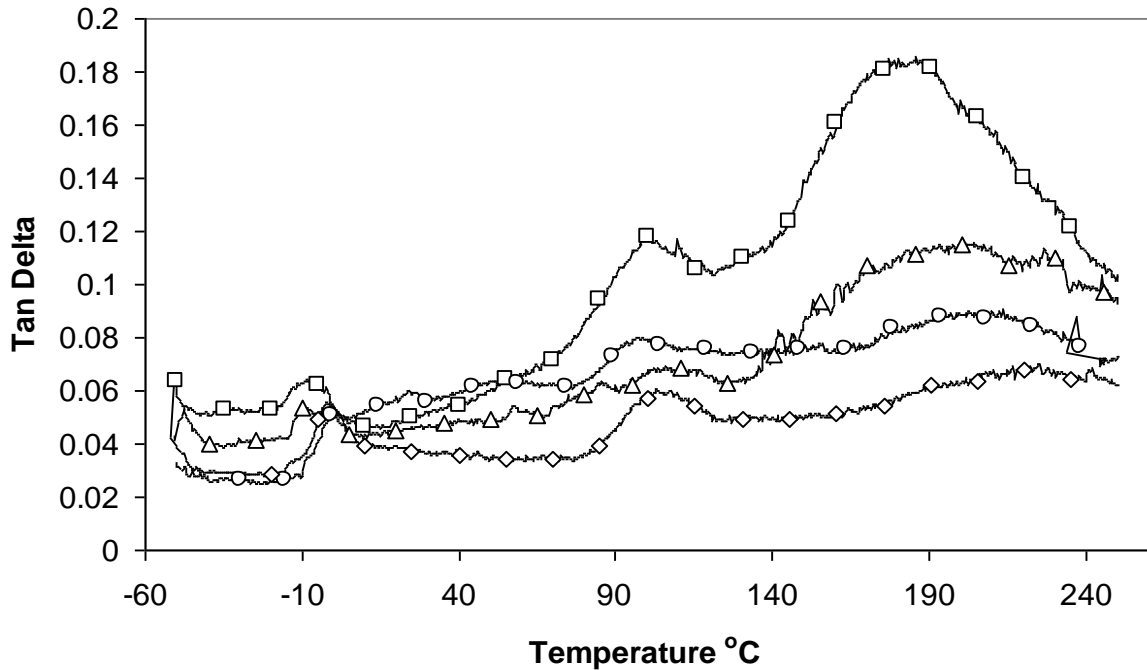
Figure 5.13. Tan δ for reference and aged samples, reference □, 3 hour aged Δ, 168 hr o
and 1032 hr ◊; for 8.5 weight percent hot water extractive-based SMC at 30 weight
percent glass reinforcement.

In Figure 5.13 tan δ scans for 8.5 weight percent hot water extract-based SMC are

presented. As with the 1.5% hot water extract-based SMC, a new peak appears from -

10°C to 5°C. The hypothesis that the hot water extract might have a relaxation in that

temperature range is supported by the tan δ scans for 1.5% and 8.5% weight percentages

for the extract in the SMC, see Figures 5.12 and 5.13.   Again, the peaks for the

polystyrene, unsaturated polyester, and cross-linked matrix are in accordance with

literature values described in Table 5.1. Because water has a physical state change in the

-10°C to 5°C temperature range and these samples absorb water, perhaps even though the

dry reference has a peak from -10°C to 5°C, water may be responsible for the peak. To determine if this is the case multiple heat ramps were run on a 168 hour aged sample.
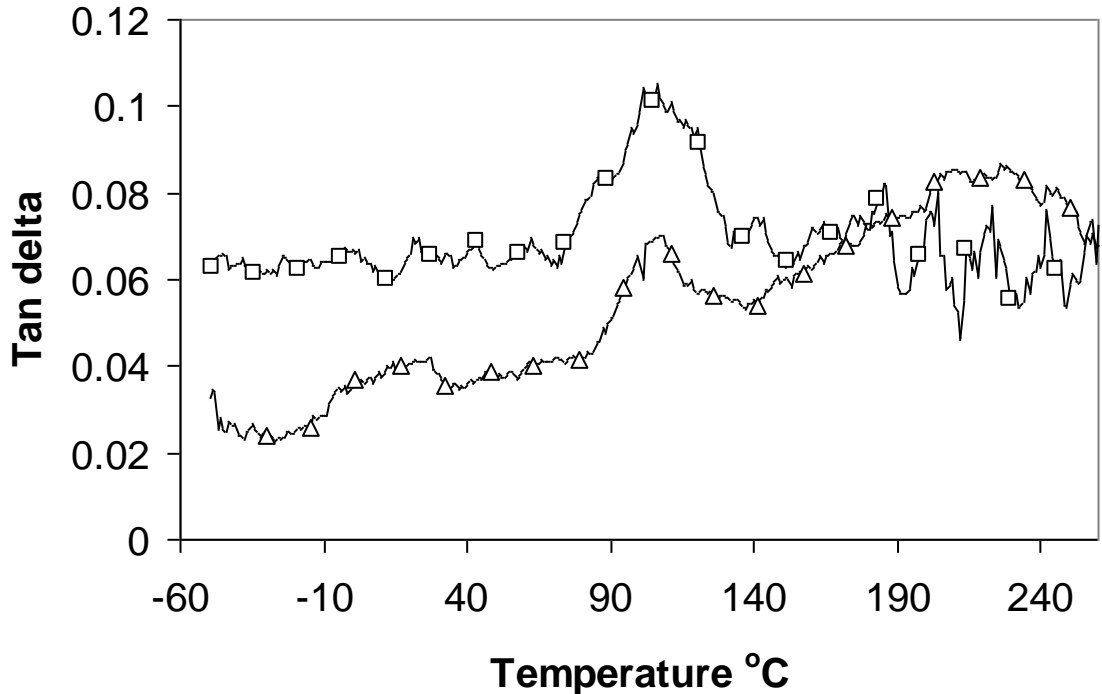
Figure 5.14. Tan δ for 168 hr aged samples, for 8.5 weight percent hot water extractive based SMC at 30 weight percent glass reinforcement with 2 heat ramps; first ramp Δ, second ramp □.

In Figure 5.14 two heat ramps are presented on the same 8.5 weight percent hot water extract-based SMC sample that has been aged for 168 hours. The motivation for doing this was to determine if the peak in the -10°C to 5°C range were due to hot water extract or water. The hypothesis presented here is that a 1°C/min heat ramp up to 260°C and maintained above 100°C for over 160 minutes should drive off most of the water in the material. This material failed on the second heat ramp and began to break down at approximately 140°C as is evident by the scatter in the Tan Delta scan for the second

ramp. Even though the SMC failed, the peak at -10°C to 5°C is seen for the second heat ramp providing an indication that it may be due to the hemicellulose extract fraction and not water.

5.5 Conclusions

Hygrothermal aging has impacts on the chemical composition and mechanical properties of SMC. The accelerated aging of SMC by hygrothermally soaking at 70°C provides insight into material changes over longer periods of time, when the material is exposed to heating and drying combined with humidity cycles. One of the most significant impacts is the plasticization of the material allowing for the molecular motion of polymeric chains resulting in the proper orientation for a complexation reaction[4]. This is shown by the presence of the MgO thickening reaction even after drying to constant weight at 103°C hypothesized to be the result of a lower degree of cross-linking compared to previous studies[3]. In addition, the presence of the SMC thickening reaction without metal oxide in the material may indicate that only water is needed for the reaction. The low profile additive not covalently linked to the polyester matrix may leach into the aging solution over time and explains the decrease in the PVAc peak for the standard SMC. The PVAC doesn't react with water to form PVOH because there was no peak for PVOH in the DMTA scans and no acetic acid found in the SMC aging solution. An excess amount of unbound water was found in the kenaf-based SMC as demonstrated by a narrow state change peak at 0°C. The high water weight gains may restrict the use of kenaf as a reinforcing material in SMC.   The hot water extract mixture is readily incorporated into a SMC material. This allows for the fabrication of an industry standard 30 weight percent SMC with 1.5 and 8.5 weight percent extract in the pre-preg material.

The accelerated aging of SMC by hygrothermally soaking at 70°C provides insight into how the material may change over longer periods of time when exposed to heating and drying combined with humidity cycles. The hot water extract-based SMC's water uptake was similar to standard SMC. A new peak is seen from -10°C to 5°C and is attributed to the hot water extract because the peak is seen in the dried reference, in both weight percent SMC's, and is apparent after 2 heat ramps to 260°C. Since water uptake is in the same range as standard SMC and the extracted SMC has 30% glass, the ability of using the hot water extract in the SMC pre-preg material appears promising.

5.6. References

1. Chan-Park M.B. and McGarry F.J., "Tough low profile additives in sheet molding compound", Polym. Composite 17, 537-547, (1996).

2. R. Saito , W.M.J. Kan and L.J. Lee," Thickening behaviour and shrinkage control of low profile unsaturated polyester resins", Polymer 37, 3567-3576, (1996).

3. Mendoza-Patlan N., Martinez-Vega J., Revellino M.; "Physico-chemical effects of hydrothermal ageing of sheet molding compounds between -60 and 250°C"J. Material Science, 36, 1523-1529, (2001)

4. Ghorbel I., Valentin D.; "Hydrothermal effects on the physico-chemical properties of pure and glass fiber reinforced polyester and vinyl resin" Polymer Composites, vol 14 no. 4, 324-334, (1993)

5. Frazier C.E.; "Hydroxymethylated resorcinolcoupling agent: A review and recent results" Forest Products Society 62nd International Convention, June 22-24, Union Station St. Louis Missouri (2008).

6. Saratomer Corporation, "Saratomer Composites Concepts, vol. 1" http://www.sartomer.com/TechLit/3025.pdf, as on 1 March 2007

7. Vancso-Szmercsanyi I., Szilagyi A.; "Coordination polymers from polycondensates and metal oxides. II. Effect of water molecules on the reactions of polyesters with MgO and ZnO" J. Polymer Sci., vol 12, 2155-2163, (1974)

8. A. Szilagya, V. Izvekov and I. Vancso-Szmercsanyi,"Coordination Polymers .8. IR Spectroscopic Studies on the Mechanism of the Reaction Between Polyester and Zinc-Oxide", J. Polym. Sci. Pol. Chem. Ed. 18, 2803-2810, (1980)

9. I. Vancso-Szmercsanyi and Z.S. Szekely-Pecsi," Metal-Containing Coordination Polymers .14. Relations Between the Structure and the Melt Viscosity of Polyesters Containing MG Ions", J. Polym. Sci. Pol. Chem. Ed. 21, 1901-1911, (1983)

10. Alvey F.; "Study of the reaction of polyester resins with Magnesium Oxide" J. Polymer Sci.; A-1 vol 9, 2233-2245, (1971)

11. I. Cendoya, D. Lopez, A. Alegria and C. Mijangos," Dynamic mechanical and dielectrical properties of poly(vinyl alcohol) and poly(vinyl alcohol)-based nanocomposites J. Polym. Sci. Pol. Phys. 39, 1968-1975, (2001)

12. Santangelo P.G. , Roland C.M., Chang T., Cho D., Roovers J., "Dynamics near the glass temperature of low molecular weight cyclic polystyrene"; Macromolecules**,** 34, 9002-9005, (2001)

6. CONCLUSIONS AND RECOMMENDATIONS

6.1 Conclusions

The overall objective of this dissertation research was to fabricate bio-based SMC materials and compare their material properties with a standard glass-based SMC. Kenaf bast fibers were selected and used to replace the glass fibers in SMC. Styrene maleic anhydride sizing was used to treat one set of kenaf-based SMC. In addition, hot water wood extract was added to the polyester prepreg to produced samples containing 1.5 and 8.5 weight percent extract in the SMC matrix at a 30-weight percent glass reinforcement.

6.1.1 Inverse Gas Chromatography

Inverse gas chromatography studies were conducted on the polyester prepreg matrix material, 14 ligno-cellulosic fiber types, and a hot water maple wood extract. The dispersive surface energy (γ_S^d) of the SMC material was 47 mJ/m^2 at 30°C, approximating a weighted average for the dispersive surface energies of the individual components in the composites. The acid-base components (K_a and K_b) of the prepreg material were 0.4 and 2.23, respectively. Inverse Gas Chromatography was also used to characterize the surface properties of 14 ligno-cellulosic fiber types. The dispersive component of the fiber surface energy, γ_S^d, ranged from 35.5 mJ/m^2 for kenaf to 44.2 mJ/m^2 for rice hulls at 20°C. The fibers acidic and basic components were also determined. In general, most of the fibers displayed similar K_a's and K_b's. However, kapok and cotton both had higher K_a and K_b values. This result could be attributed to kapok only containing 13% cellulose and cotton, 92% cellulose. Perhaps extractives on the surface or the aromatic nature of lignin

may be contributing to the large electron donor nature of the kapok versus the cotton. Jute exhibited a non-reactive surface. This may be due in part to no pretreatment other then mechanical shearing in a Wiley mill, but leads to interesting questions about the surface of the fibers.

Kenaf was selected as a ligno-cellulosic fiber type that was used as reinforcement in the SMC material. The γ_S^d of the kenaf was 40.0 mJ/m2 at 30°C with K_a and K_b values of 0.07 and 0.32, respectively. An interaction parameter was determined for the interaction of a sized and un-sized ligno-cellulosic fiber with the pre-preg polymeric matrix. Findings indicated that a cellulosic fiber sized with styrene- maleic anhydride provided an optimum interaction parameter between the polyester pre-preg and kenaf fibers; therefore, the kenaf fibers were treated with a 2 weight percent SMA sizing agent.

Finally, IGC studies were conducted on a hot water wood extract from red maple wood samples. The dispersive surface energy of the extract was non-responsive thermally, having a magnitude of 34.6 ± 0.2 mJ/m^2 with a K_a of 0.13 and K_b of 0.46. A surface energy of 39 mJ/m^2 at 30°C has been reported for polystyrene and this is close to the value of the hot water extract. The similar values of surface energy for the hot water extract and polystyrene coupled with the high K_b value for the hot water extract indicates that the extract should be miscible in the polyester pre-preg.

6.1.2 Hygrothermal Aging

SMC composites made with 15 and 30 weight percent glass, 2 weight percent SMA sized and un-sized kenaf at 15 weight percent in the SMC, and 1.5 and 8.5 weight percent hot water extract in a 30 weight percent glass SMC were fabricated. The samples were

hygrothermal aged by soaking the samples at 70°C for 3, 168, and 1032 hours. In Figure 8.1, the water uptake by all the different SMC formulations are compared.
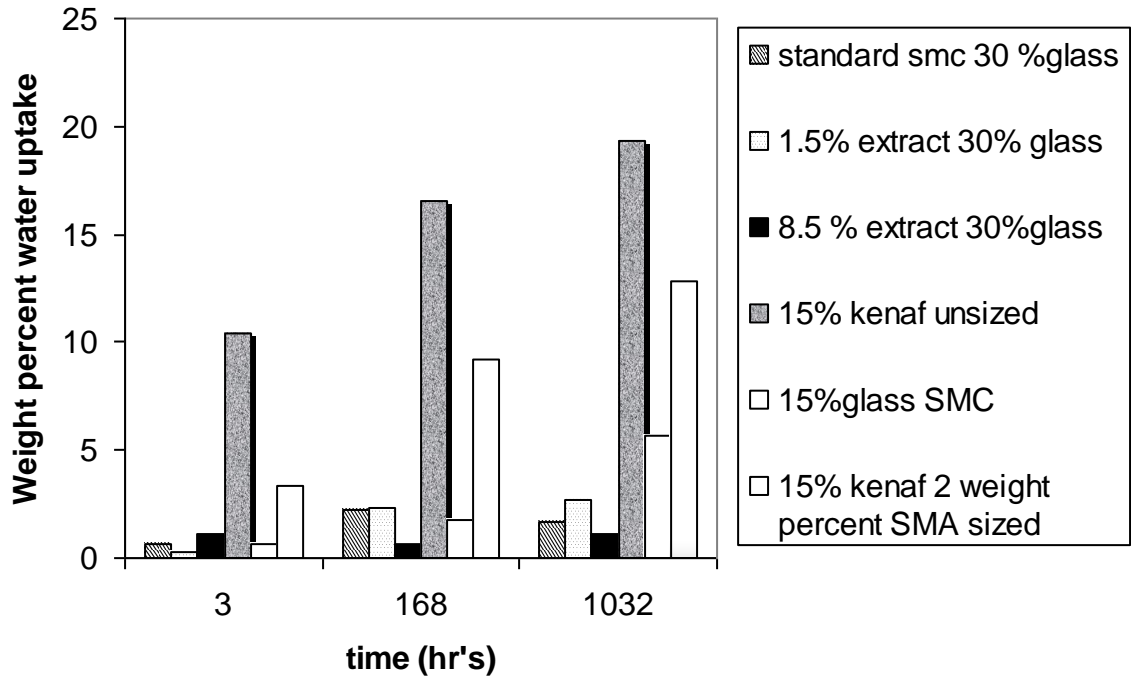
Figure 6.1. SMC composite water uptake by time and type.

In general, all the SMC's manufactured with 30 weight percent glass absorbed less than 3 weight percent water. The 15 weight percent fiber SMCs all absorbed over 5 weight percent water with un-sized kenaf-based SMC attaining nearly 20 percent weight gain. The SMA fiber sizing reduced the water uptake by approximately 40%. However, the water uptake was much larger then glass-based SMCs and would not be appropriate for exterior applications where water would rapidly deteriorate the material. The SMC's made with hot water extract absorbed water in a similar amount to the standard SMC's indicating that those SMC's might be good candidates for automotive parts.

6.1.3 DMTA studies

DMTA studies examining the viscoelastic properties of the various SMCs were also conducted. Most composite glass transitions agreed with the temperature ranges reported in the published literature. A new tan delta peak was discovered in the DMTA scans in the -10°C to 5°C range for the SMC's made containing wood hot water extract. Two heat ramps from -50°C to 260°C were done on the same 8.5 weight percent hot water extract based SMC after 168 hours of hygrothermal aging. The peak from -10°C to 5°C was seen in both ramps indicating that the peak was not caused by water. Because the extract was the only new component in the SMC composite, the peak was attributed to a relaxation by the extract components, presumably hemicellulose.

The DMTA studies done with the kenaf-based SMC displayed a narrow peak at 0°C. This peak was attributed to the large amount of water uptake by the kenaf-based SMC. With upwards of 20 weight percent water in the material, the hypothesis is that much of the water is in a free form and able to go through a physical state change (melting) at 0°C. Also, a peak in the 25°C range observed in the kenaf-based SMC has been hypothesized to be due to the relaxation of the complexation of carboxylic acid functional groups previously thought to be initiated by water then completed with a metal thickening agent. Because there is no metal thickening agent in the SMC, and no peaks were observed in the hot water extract or the reference glass fiber samples, the peak at 25°C is hypothesized to be attributed to water interacting with the carboxylic acid functional groups on the polyester chains.

6.2 Recommendations

Much of the work in this dissertation was done:

1) To study interfacial interactions to evaluate the cohesiveness within traditional and bio-based SMC composite materials.

2) To determine water uptake in the SMC by accelerated aging through hygrothermal treatment

3) To analyze how the various components of the SMC react to hygrothermal aging to provide information necessary to aid in determining proper component recipes for SMC composites made with renewable components that are capable of competing with standard industrial SMC for service applications.

Now that the materials have been made and the individual components analyzed for surface properties using inverse gas chromatography and the micromechanics analyzed using dynamic mechanical thermal analysis, a logical next step would be to conduct macro mechanical testing of the materials using appropriate testing standards such as prescribed by American Society for Testing and Materials (ASTM). Izod impact testing by ASTM D256-00[1] would be an appropriate test to determine how well the material would perform in a severe impact and tensile testing by ASTM D638-01[2] would be appropriate to test the tensile properties of the various SMC's. More research on bio-based SMC's should be done to determine mechanical properties as a function of hot water wood extract content. Also, mechanical testing should be done as a function of hygrothermal aging to correlate the micro mechanical results to the macro mechanical results.

The high water uptake for the kenaf-based SMC's is problematic. Higher sizing contents for styrene-maleic anhydride may be examined in an attempt to reduce the water uptake of the kenaf.

6.3. References

1. ASTM standard, "Standard Test Methods for Determining the Izod Penulum Impact Resistance of Plastics" D 256-00 Annual book of ASTM Standards, 2002

2. ASTM standard, "Standard Test Method for Tensile Properties of Plastics" D 638-01 Annual book of ASTM Standards, 2002

REFERENCES

A. Ebringerová Structural diversity and application potential of hemicelluloses, Macromol. Symp. 232, 1-12, (2006)

A. Szilagya, V. Izvekov and I. Vancso-Szmercsanyi,"Coordination Polymers .8. IR Spectroscopic Studies on the Mechanism of the Reaction Between Polyester and Zinc-Oxide", J. Polym. Sci. Pol. Chem. Ed. 18(1980)2803

Alvey F.; "Study of the reaction of polyester resins with Magnesium Oxide" J. Polymer Sci.; A-1 vol 9, (1971) 2233-2245

Ass B.A.P.,. Ciacco G.T., Frollini E.," Cellulose acetates from linters and sisal: Correlation between synthesis conditions in DMAc/LiCl and product properties"; Bioresource Technology 97 (2006) 1696–1702

ASTM stardard, "Standard Test Methods for Determining the Izod Penulum Impact Resistance of Plastics" D 256-00 Annual book of ASTM Standards, 2002

ASTM stardard, "Standard Test Method for Tensile Properties of Plastics" D 638-01 Annual book of ASTM Standards, 2002

Back E.L.," Oxidative Activation of Wood Surfaces for Glue Bonding"; Forest Prod. J. 41(2) 30-36, 1991

Bismarck, A., Mohanty, A.K., Aranberri-Askargorta, I., Czapla, S, Misra, M., Hinrichsen, G., Springer, "Surface characterization of natural fibers; surface properties and the water up-take behavior of modified sisal and coir fibers J. Green Chemistry, 2001, 3, 100–107

Bledzki A.K., Gassan J., " Composites reinforced with cellulose based fibres"; Prog. Polym. Sci. 24(1999) 221-274

Browning B.L.,"Methods of wood chemistry", Ed. John Wiley & Sons. New York (1967).

Boras L., Sjostrom, J.; International Symposium on Wood and Pulping Chemistry, Proceedings, ISWPC, v 2, 1997, p 9-1/9-4

Bucknall C., Davies P., Partridge I.; "Phase separation in styrenated polyester resin containing a poly(vinyl acetate) low-profile additive" , Polymer 26, (1985) 109

Carvalho M.G., Santos J.M.R.C.A., Martins A.A., Figueiredo M.M," The effects of beating, web forming and sizing on the surface energy of Eucalyptus globulus kraft fibres evaluated by inverse gas chromatography."; Cellulose, 12, 2005, 371-383

Castro J., Lee C.; "Thermal and cure analysis in sheet molding compound compression molds" Polymer eng. and sci., vol 27 no. 3 (1987) 218-224

Chan-Park M.B. and McGarry F.J., "Tough low profile additives in sheet molding compound", Polym. Composite 17(1996) 537.

Christiansen A.W.," How Over-drying Wood Reduces its Bonding to Phenol-Formaldehyde Adhesives - A Critical Review of the Literature .1. Physical Responses; Wood Fiber Sci., 22, 441-459, (1990)

Chtourou, H.; Riedl, B.; Kokta, B.V." Surface Characterizations of Modified Polyethylene Pulp and Wood Pulp Fibers Using XPS and Inverse Gas Chromatography"; J. of Adhesion Sci. Tech., 9(5), 1995, p 551

Clemons, C. M.; Caulfield, D.F., "Natural Fibers", Chapter 11 of Functional Fillers for Thermoplastics, M. Xanthos, ed., Wiley-VCH Verlag GmbH & Co. KGaA, 2005, 195-206

Clemons C.M., Giacomin A.J., Koutsky J.A.," Dynamic fracture toughness of polypropylene reinforced with cellulose fiber"; Polym. Eng. Sci., 37(6), 1997, 1012-1018

del Rıó, J. C.; Gutiérrez, A.," Chemical composition of abaca(*Musa textilis*) leaf fibers used for manufacturing of high quality paper pulps."; J. Agric. Food Chem. 54: (2006) 4600-4610

Dien B.S., Jung, H.G., Vogel K.P., Casler M.D., Lamb J.F.S., Weimer P.J., Iten L., Mitchell R.B., Sarath G.," Chemical composition and response to dilute-acid pretreatment and enzymatic saccharification of alfalfa, reed canarygrass, and switchgrass Biomass Bioenergy, 30(10): (2006) 880-891

Donnet J.B., Park S.J., Balard H.," Evaluation of Specific Interactions of Solid-Surfaces by Inverse Gas Chromatography - A New Approach Based on Polarizability of the Probes"; Chromatographia, vol. 31, No. 9/10, (1991) 434-440

Dorris G.M., Gray D.G.," Adsorption of Normal-Alkanes at Zero Surface Coverage on Cellulose Paper and Wood Fibers; J. Colloid Interface Sci., 77, (1980), 353-362

Dutschk V., Mäder E., Rudoy V., "Determination of polarity parameters for glass fibres by inverse gas chromatography: Some results and remarks"; J. Adhes. Sci. Technol., Vol. 15, No. 11, pp. 1373–1389 (2001)

Ebringerová A., Heinze T. Xylan and xylan derivatives – biopolymers with valuable properties, 1, Macromol. Rapid Commun. 21, 542-556 (2000)

Franck, R.R. 2005. Overview. In: Franck, R.R. (ed.): Bast and other plant fibres. Boca Raton, Boston, New York, Washington DC, CRC: 1-23.

Gardner, D. J., M. P. Wolcott, L. Wilson, Y. Huang, and M. Carpenter. 1996. Our understanding of wood surface chemistry in 1995. In: Wood Adhesives 1995, Proceedings No. 7296, Forest Products Society, CityplaceMadison, StateWI. pp. 29-36.

Garrote G., Cruz JM., Domínguez H., Parajó JC Valorisation of waste fractions from autohydrolysis of selected lignocellulosic materials, J. Chem. Technol. Biotechnol. 78, 392-398 (2003)

Ghorbel I., Valentin D.; "Hydrothermal effects on the physico-chemical properties of pure and glass fiber reinforced polyester and vinyl resin" Polymer Composites, vol 14 no. 4, (1993) 324-334

Grandmaison J.L., Thibault J., kaliaguine S., Chantal P.D. Fourier-transform infrared spectroscopy and thermogravimetry of partially converted lignocellulosic materials; Anal. Chem. 59, (1987) 2153-2157

Gulati D., Sain M., "Surface characteristics of untreated and modified hemp fibers"; Polym. Eng. Sci. 46(2006) 269-273

Han, J.S. (1998) Properties of nonwood fibers. In: Proceedings of the Korean Society of Wood Science and Technology Annual Meeting, Seoul, Korea. The Korean Society of Wood Science and Technology, 3–12

Hepworth D., Bruce D., Vincent J., Jeronimidis G.; "The manufacture and mechanical testing of thermosetting natural fibre composites" J. Material Science 35 (2000) 293-298

Herzog B., Gardner D., Lopez-Anido R., Goodell B.; "Glass-transition temperature based on Dynamic Mechanical Thermal Analysis Techniques as an indicator of the adhesive performance of vinyl ester resin" J. Applied Polymer Sci.; vol 97(6) (2005) 385-394

Holbery J., Houston D., "Natural-fiber-reinforced polymer composites in automotive. applications".; JOM, Volume 58; Issue 11; ISSN: 10474838

Hori, K., Flavier, M.E., Kuga, S., Lam T.B.K., Iiyama K.," Excellent oil absorbent kapok [Ceiba pentandra (L.) Gaertn.] fiber: fiber structure, chemical characteristics, and application "; J Wood Sci (2000) 46:401-404.

Hurter, A.M. 1988: Proceedings of TAPPI Pulping Conference 1988. New Orleans, LA, USA, Book 1: 139-160.

I. Cendoya, D. Lopez, A. Alegria and C. Mijangos," Dynamic mechanical and dielectrical properties of poly(vinyl alcohol) and poly(vinyl alcohol)-based nanocomposites J. Polym. Sci. Pol. Phys. 39(2001) 1968

I. Vancso-Szmercsanyi and Z.S. Szekely-Pecsi," Metal-Containing Coordination Polymers .14. Relations Between the Structure and the Melt Viscosity of Polyesters Containing MG Ions", J. Polym. Sci. Pol. Chem. Ed. 21(1983)1901

Jacob P.N., Berg J.C.," Acid-Base Surface-Energy Characterizatoin of Microcrystalline Cellulose and 2 Wood Pulp Fiber Types Using Inverse Gas Chromatography"; Langmuir, 10, 1994, 3086-3093

Jeffree CE, Baker EA, Holloway PJ, "Ultrastructure and Recrystallization of Plant Epicuticular Waxes"; New Phytologist, 75:3(1975) 539

Kazayawoko M., Balatinecz J.J., Matuana L.M.," Surface modification and adhesion mechanisms in woodfiber-polypropylene composites"; J. Mater. Sci., 34, 1999, 6189-6199

Keller D.S., Luner P., "Surface energetics of calcium carbonates using inverse gas chromatography"; Colloids Surface A 161 (2000) 401–415

Keller D.S., Luner P.; The fundamentals of Papermaking Materials; vol. 2, (1997), 911-954

Laleg M., Blanchard F., Chabert B., Pascault," Contribution to the Study of the Thickening Mechanism of Unsaturated Polyester Resins in the Presence of MgO."; Eur polym J. vol 21 No 6 (1985) 591-596

Lam, T.B.T. Hori, K., Iiyama, K.," Structural characteristics of cell walls of kenaf (Hibiscus cannabinus L.) and fixation of carbon dioxide"; J Wood Sci (2003) 49:255–261

Lundqvist Å, Ödberg L.; The Fundamentals of Papermaking Materials vol 2, 1997, 751

Matuana L.M., Woodhams R.T., Balatinecz J.J., Park C.B., "Influence of interfacial interactions on the properties of PVC cellulosic fiber composites"; Polym. Compos., 19(4), 1998, 446-455

Matuana L.M., Park C.B., Balatinecz J.J.," Cell morphology and property relationships of microcellular foamed PVC/wood-fiber composites" ; Polym. Eng. Sci., 38(5), 1998, 765-773

Mazumdera B.B., Akiko Nakgawa-izumi b, Kuroda K., Ohtani a Y., Sameshima K.," Evaluation of harvesting time effects on kenaf bast lignin by pyrolysis-gas chromatography; Industrial Crops and Products 21 (2005) 17–24

Mendoza-Patlan N., Martinez-Vega J., Revellino M.; "Physico-chemical effects of hydrothermal ageing of sheet molding compounds between -60 and 250°C"J. Material Science, 36 (2001) 1523-1529

Mills R., Jara R., Gardner D., vanHeiningen A.," Inverse gas chromatography for determining the surface free energy and acid-base chemical characteristics of a water extracted hardwood (*Acer rubrum*)" ; J. Wood Chem. and Tech. 29: 1–13, 2009

Montané D., Nabarlatz D., Martorell A., Torné-Fernández V., Fierro V. Removal of lignin and associated impurities from xylo-oligosaccharides by activated carbon adsorption, Ind. Eng. Chem. Res. 45, 2294-2302 (2006)

Mwaikambo, L. Y.," Review of the History, Properties and Application of Plant Fibers" African Journal of Science and Technology 7 (2): (2006) 120-133.

Mwaikambo, L. Y. Ansell , M. P.," The determination of porosity and cellulose content of plant fibers by density methods"; 2001: J Mat Sci Letters 20, 2001, 2095 – 2096

Mwaikambo L.Y., Ansell M.P.,"Chemical modification of hemp, sisal, jute, and kapok fibers by alkalization; J. App. Polym. Sci., 84, 2002, 2222-2234

Nabarlatz D., Torras C., Garcia-Valls R., Montané D. Purification of xylo-oligosaccharides from almond shells by ultrafiltration, Separation and Purification Technology 53, 235-243 (2007)

Nilsson, T.," Microscopic studies on the degradation of cellophane and various cellulosic fibres by wood-attacking microfungi : Mikroskopiska undersökningar av vedangripande mikrosvampars nedbrytning av cellofan och olika cellulosahaltiga fibrer"; Studia Forestalia Suecica *117*, (1974) 1–32.

Ouajai S, Shanks RA, "Composition, structure and thermal degradation of hemp cellulose after chemical treatments"; Polymer degradation and stability, 89:2(2005) 327-335

Parades J., Mills R, Gardner D., Shaler S.," Surface Characterization of Red Maple Strands After Hot Water Pre-Extraction"; Wood and Fiber Sci. 41(1) 2009, 1-13

Park S.J., Donnet J.B., "Anodic surface treatment on carbon fibers: Determination of acid-base interaction parameter between two unidentical solid surfaces in a composite system; J. Colloid Interface Sci. 206, (1998)29-32

Park S.J., Kim T.J., "Studies on surface energetics of class fabrics in an unsaturated polyester matrix system: Effect of sizing treatment on glass fabrics"; J. Appl. Polym. Sci., 80, (2001)1439–1445

Price G.J., Ansari D.M., "Surface modification of calcium carbonates studied by inverse gas chromatography and the effect on mechanical properties of filled polypropylene"; Polym. Int. **53**: (2004)430–438

Qin R.Y., Schreiber H.P., "Application of Inverse Gas Chromatography to Molecular-Diffusion in Polymers"; Langmuir, vol 10, No. 11, (1994) 4153-4156

R. Saito , W.M.J. Kan and L.J. Lee," Thickening behaviour and shrinkage control of low profile unsaturated polyester resins", Polymer 37(1996) 3567.

Rahman M.M., Khan, M.A., "Surface treatment of coir (Cocos nucifera) fibers and its influence on the fibers' physico-mechanical properties" Composites Science and Technology 67 (2007) 2369–2376

Reddy N., Yang, Y., "Biofibers from agricultural byproducts for industrial applications"; Trends in Biotech. Vol.23 No.1: 22-27.

Reddy; N., Salam, A., Yang, Y., "Effect of lignin on the heat and light resistance of lignocellulosic fibers"; Macromol. Mater. Eng. (2007), 292, 458–466

Reutenauer S., Thielmann F., "The characterisation of cotton fabrics and the interaction with perfume molecules by inverse gas chromatography (IGC)"; J. Mater. Sci., 38, (2003) 2205-2208

Riedl B., Matuana L.M.; Encyclopedia of Surface and Colloid Science, (2002), 2842-2855

Rowell RM., A new generation of composite materials from agro-based fiber"; Proceedings of 3rd international conference on frontiers of polymers and advanced materials**;** 1995**,** January 16-20**;** Kuala Lumpur**,** Malaysia New York: Plenum Press; 1995.

Rowell, R.M.,: Composite materials from agricultural resources. In: Oleson, O., Rexen, F., Larsen, J. (eds.): Research in industria application of non food corps, I: plant fibres. Proceedings of a seminar; May 1995, Copenhagen, Denmark, Lyngby, Denmark, Academy of Technical Science (1995)27-41.

Rowell, R.M., Han1, J.S., Rowell, J.S.,. Characterization and Factors Effecting Fiber Properties. In: E. Frollini, A.L. Leão and L.H.C. Mattoso (eds). Natural Polymers and Agrofibers Composites, Sãn Carlos - Brazil - São Carlos: USP-IQSC / Embrapa Instrumentação Agropecuária / Botucatu: UNESP: (2000)115-134.

Santangelo P.G. , Roland C.M., Chang T., Cho D., Roovers J., "Dynamics near the glass temperature of low molecular weight cyclic polystyrene"; Macromolecules (2001), 34, 9002-9005

Saratomer Corporation, "Saratomer Composites Concepts, vol. 1" http://www.sartomer.com/TechLit/3025.pdf, as on 1 March 2007

Schultz J., Lavielle L.," Surface-Properties of Carbon-Fibers Determined by Inverse Gas-Chromatography - Role of Pretreatment";Langmuir, (1991), 7(5), 978.981

Schultz J., Lavielle L.; ACS Symposium Series, Washington D.C., (1989), 391, 185- 202

Schultz T.P., Templeton M.C., McGinnis G.D. Rapid determination of lignocellulose by diffuse reflectance fourier transform infrared spectroscopy; Anal. Chem. 67, (1985) 2867-2869

Scott, R.W., Calorimetric determination of hexuronic acids in plant materials. Anal. Chem. No 7 (51), 1979.

Silva G.G., De Souza, D.A., Machado, J.C., Hourston, D.J.," Mechanical and thermal characterization of native Brazilian coir fiber"; Journal of Appl. Polym. Sci., Vol. 76, (2000) 1197–1206

Simonsen J., Hong Z., Rials T.G., "The properties of the wood-polystyrene interphase determined by inverse gas chromatography"; Wood Fiber Sci. 29, (1997)75-84

Sun RC, Fang J.M., Goodwin A., Lawther, J.M., Bolton A.J., "Fractionation and characterization of polysaccharides from abaca fibre"; Carbohydrate Polymers 37(1998) 351–359

Thygesen A., Oddershede, J., Lilholt H. Thomsen A.B., Stahl K," On the determination of crystallinity and cellulose content in plant fibres Cellulose"; 12:563–576

Thygesen A., Daniel G., Lilholt H., Thomsen A.B.," Hemp Fiber Microstructure and Use of Fungal Defibration to Obtain Fibers for Composite Materials"; Journal of Natural Fibers, Vol. 2(4): (2006) 19-37

Tshabalala M.A., " Determination of the acid-base characteristics of lignocellulosic surfaces by inverse gas chromatography; J. Appl. Polym. Sci., 65, (1997), 1013-1020

Tze W.T.Y., Wålinder M.E.P., Gardner D.J.," Inverse gas chromatography for studying interaction of materials used for cellulose fiber/polymer composites; J. Adhesion Sci. Technol. 20(8), 2006 743-759

Tze W.T.Y; "Effects of fiber/matrix interactions on the interfacial deformation micromechanics of cellulose-fiber/polymer composites"; PhD Thesis, University of Maine, August 2003

V. Gutmann; The Donor Acceptor Approach to Molecular Interactions; Plenum, New York, 1978, Chapter 2

van Dam JEG, van den Oever MJA, Keijser, ERP, van der Putten J.C., Anayron C., Josol F., Peralta A.," Process for production of high density/high performance binderless boards from whole coconut husk - Part 2: Coconut husk morphology, composition and properties"; Industrial Crops and Products 24 (2006) 96–104

van Voorn B., Smit H., Sinke R., de Klerk B.; "Natural fibre reinforced sheet moulding compound" Compsosites: part A 32 (2001) 1271-1279

Vancso-Szmercsanyi I., Szilagyi A.; "Coordination polymers from polycondensates and metal oxides. II. Effect of water molecules on the reactions of polyesters with MgO and ZnO" J. Polymer Sci., vol 12, (1974) 2155-2163

Vázquez M.J., Garrote G., Alonso J.L., Domínguez H., Parajó J.C. Refining of autohydrolysis liquors for manufacturing xylooligosaccharides: evaluation of operational strategies, Bioresource Technology 96, (2005) 889-896

Ververis C, Georghiou K, Christodoulakis N, Santas P, Santas R., "Fiber dimensions, lignin and cellulose content of various plant materials and their suitability for paper production"; Ind Crop Product 19:245–254

Woodhams R.T., Thomas G.," Wood Fibers as Reinforcing Fillers for Polyorefins"; Polym. Eng. Sci. 24, (1984), 1166-1171

Yuan Q.P., Zhang H., Qian ZM, Yang XJ Pilot-plant production of xylo-oligosaccharides from corncob by steaming, enzymatic hydrolysis and nanofiltration, J. Chem. Technol. Biotechnol. 79, (2004) 1073-1079

BIOGRAPHY OF THE AUTHOR

Ryan Mills was born in Lewiston, Maine and raised in West Paris, Maine. He is a high school graduate of Oxford Hills High School and graduate of the University of Maine, (dual B.S. 1994) and the Institute of Paper Science and Technology, (M.S. 1996). He was raised in a forestry family managing timberland for the local paper and lumber mills in western Maine learning to enjoy timber and land management. Ryan is a candidate for the Doctor of Philosophy degree in Forest Resources from the University of Maine May, 2009.